Orographic gravity waves: Lessons learnt from the DEEPWAVE field campaign

Andreas Dörnbrack
DLR Oberpfaffenhofen

Photo: Sonja Gisinger

Photo: Petr Horalek

universität innsbruck

NCAR
NATIONAL CENTER FOR ATMOSPHERIC RESEARCH

GATS

DLR

UNITED STATES NAVY NAVAL RESEARCH LABORATORY

JOHANNES GUTENBERG UNIVERSITÄT MAINZ JG|U

Yale UNIVERSITY

NIWA Taihoro Nukurangi

LMU

UtahState University

1. **Motivation**

2. **DEEPWAVE Field Campaign**

3. **GW propagation from the Troposphere to the Stratosphere**
   Radiosonde analyses

4. **GW propagation from the Stratosphere to the Mesosphere**
   Ground-based Lidar observations

5. **Conclusions**

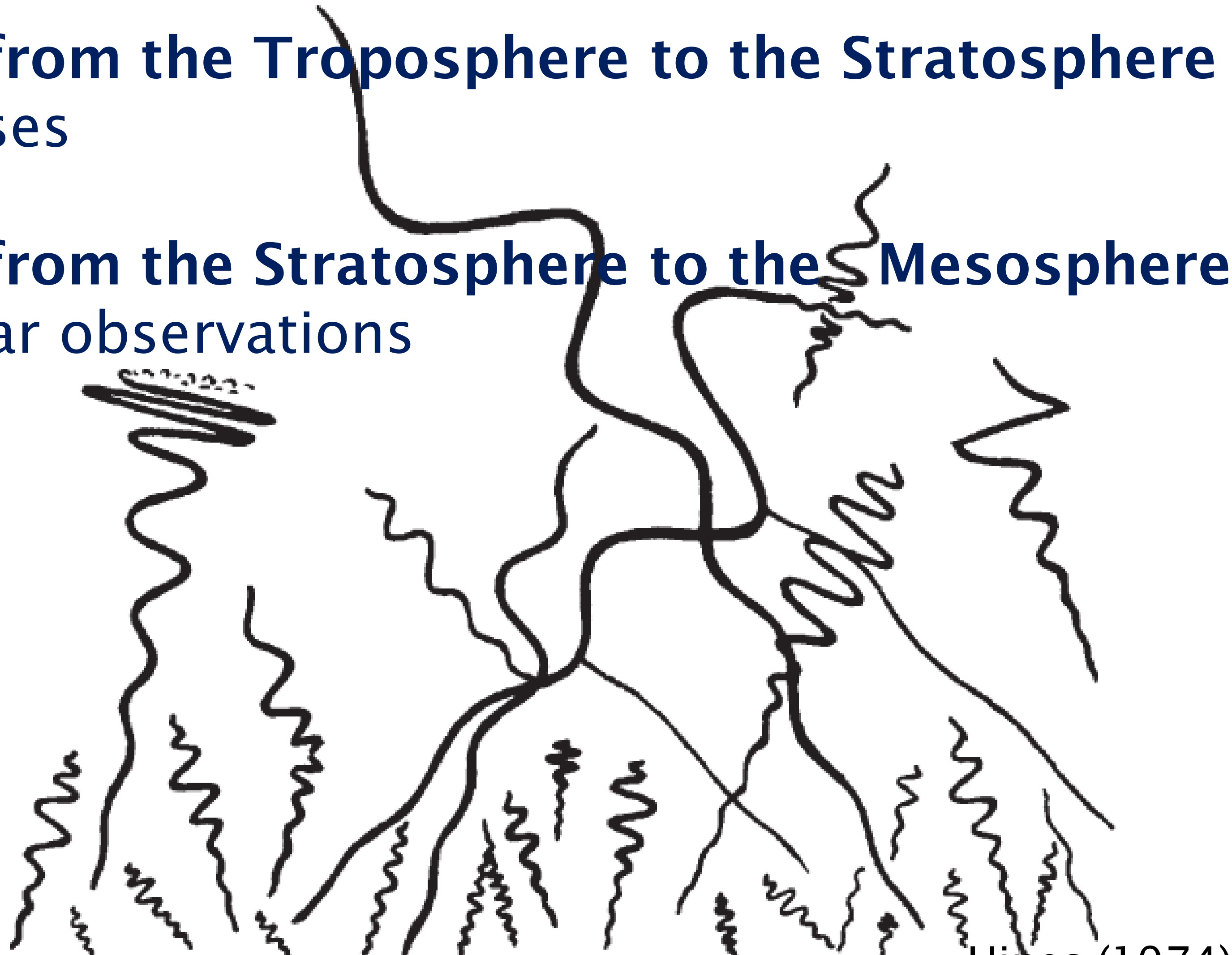

Hines (1974)

1. Motivation

- **Internal gravity waves**

  appear nearly everywhere in the atmosphere

  are often poorly represented in NWP and climate models

Atmospheric Gravity Waves

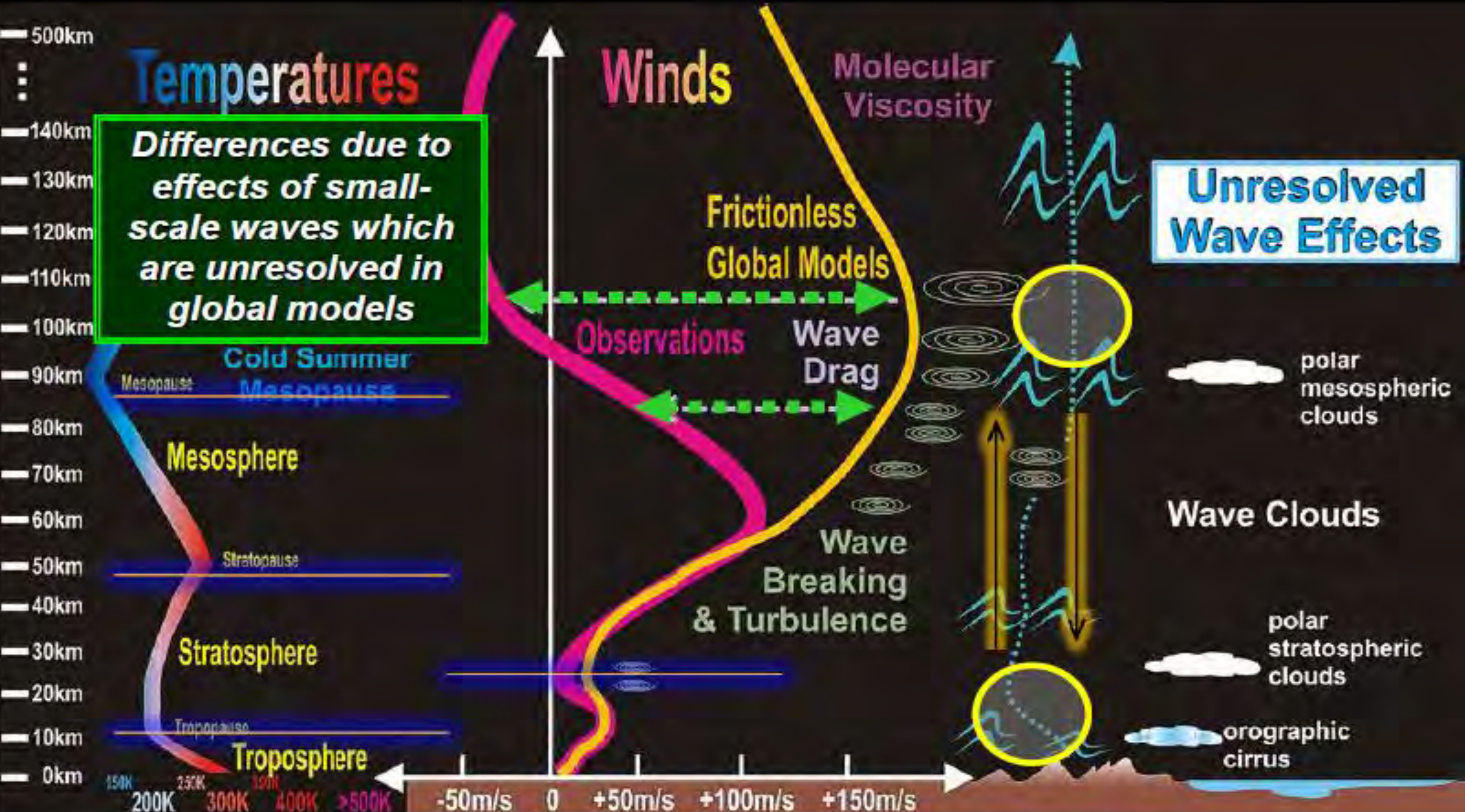

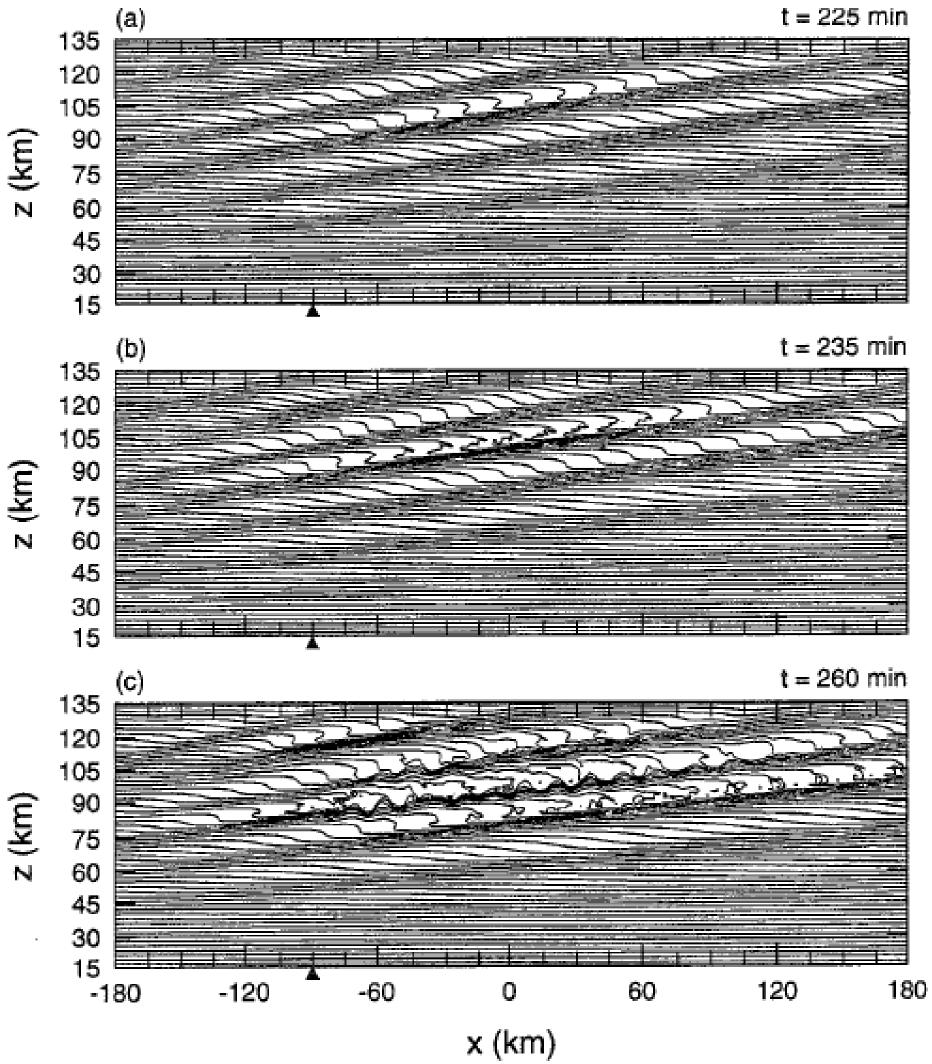

Prusa J. M., Smolarkiewicz P. K., Garcia R. R., 1996: On the propagation and breaking at high altitudes of gravity waves excited by tropospheric forcing. *J. Atmos. Sci.*, **53**, 2186–2216.

Atmospheric Gravity Waves

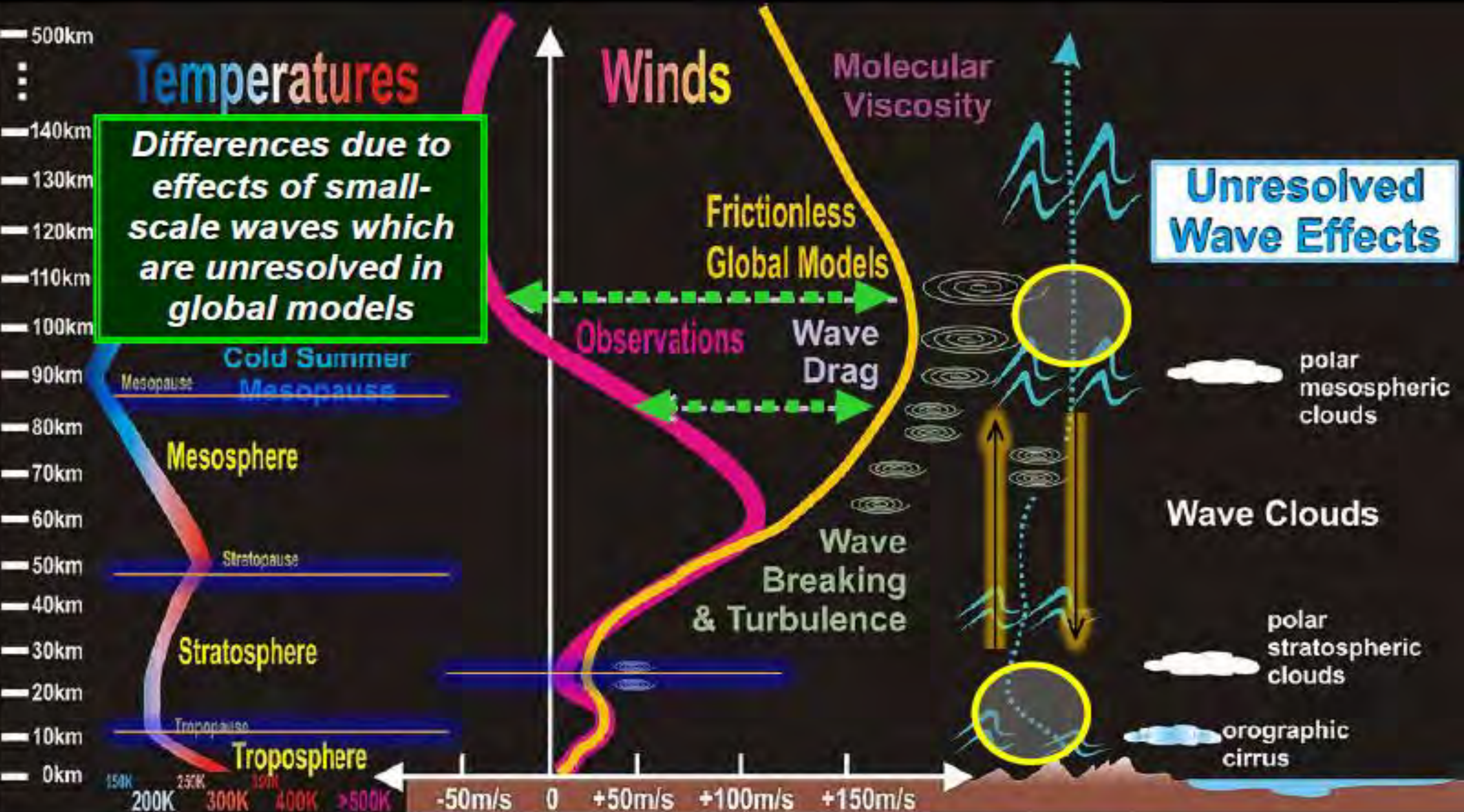

„Convective Waves“ above a single power plant, Northern Germany, 20 January 2015

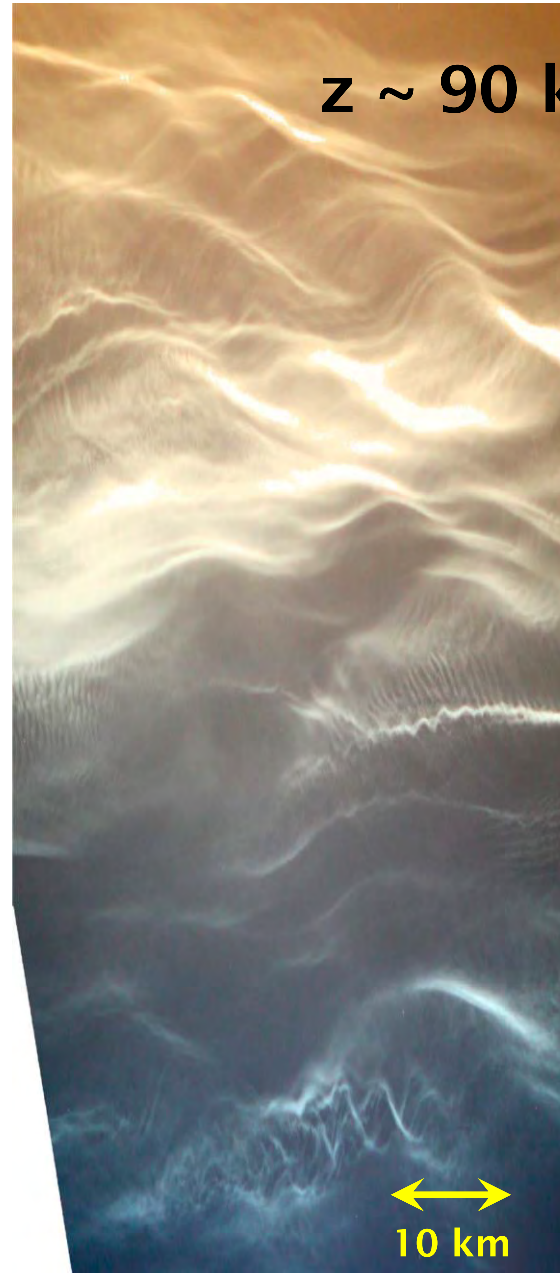

Baumgarten, G., and D. C. Fritts (2014), Quantifying Kelvin-Helmholtz instability dynamics observed in noctilucent clouds: 1. Methods and observations, J. Geophys. Res. Atmos., 119, 9324–9337, doi:10.1002/2014JD021832.

SPECIAL
Terrain-Induced Rotor Experiment (T-REX)
COLLECTION

An Intercomparison of T-REX Mountain-Wave Simulations and Implications for Mesoscale Predictability

JAMES D. DOYLE,[a] SAŠA GABERŠEK,[b] QINGFANG JIANG,[a] LIGIA BERNARDET,[c,l] JOHN M. BROWN,[c] ANDREAS DÖRNBRACK,[d] ELMAR FILAUS,[e] VANDA GRUBIŠIĆ,[f] DANIEL J. KIRSHBAUM,[g] OSWALD KNOTH,[e] STEVEN KOCH,[c,m] JUERG SCHMIDLI,[h] IVANA STIPERSKI,[i] SIMON VOSPER,[j] AND SHIYUAN ZHONG[k]

[a] *Naval Research Laboratory, Monterey, California*
[b] *UCAR, Monterey, California*
[c] *NOAA/Earth System Research Laboratory, Global Systems Division, Boulder, Colorado*
[d] *Institut für Physik der Atmosphäre, Deutsches Zentrum für Luft- und Raumfahrt, Oberpfaffenhofen, Germany*
[e] *Leibniz Institute for Tropospheric Research, Leipzig, Germany*
[f] *University of Vienna, Vienna, Austria*
[g] *University of Reading, Reading, United Kingdom*
[h] *Institute for Atmospheric and Climate Science, ETH, Zurich, Switzerland*
[i] *Meteorological and Hydrological Service, Zagreb, Croatia*
[j] *Met Office, Exeter, United Kingdom*
[k] *Michigan State University, East Lansing, Michigan*

Baseline: Θ (K) and w (ms^{-1})
h_m=100m, free slip (4h)

SEPTEMBER 2011 2817

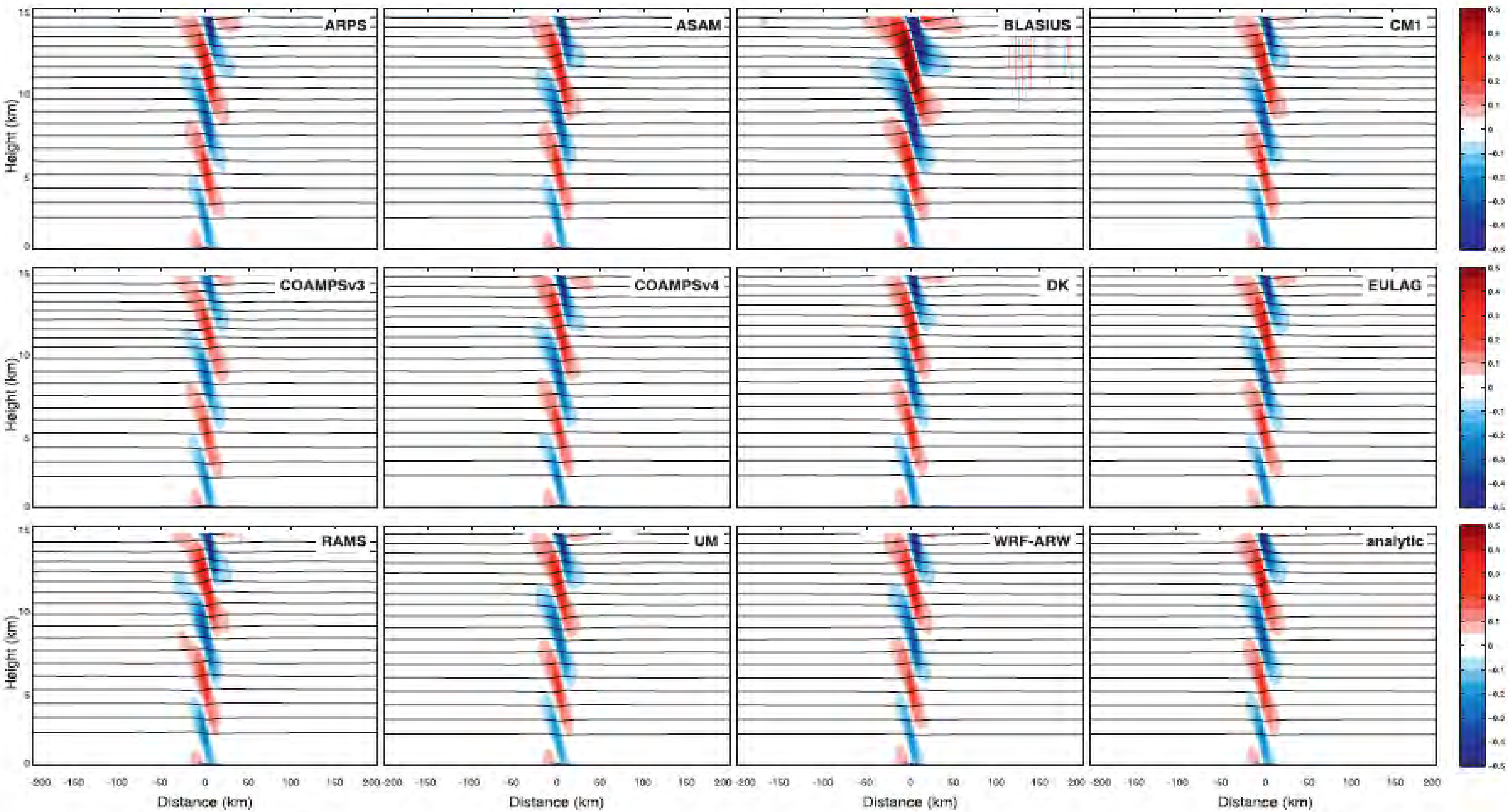

Nearly identical results for all models
(with exception of BLASIUS at upper levels due to anelastic assumptions)

Ex1000_fs: Θ (K) and w (ms^{-1})
h_m=1000 m, free slip (4h)

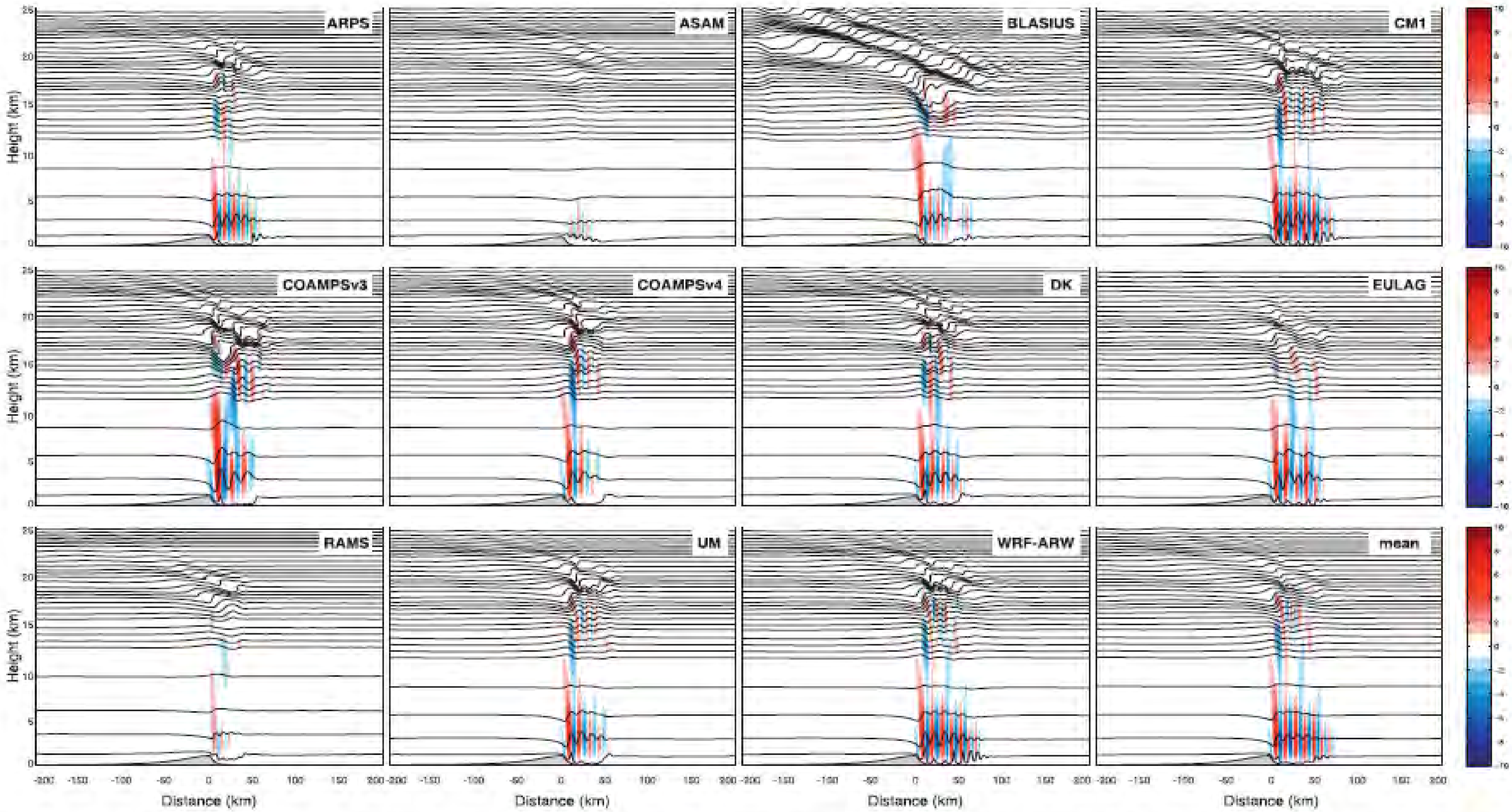

Most models exhibit trapped waves (variations in number of crests)
A few models show very weak vertical velocity (ASAM, RAMS…)

Ex2500_fs: Θ (K) and w (ms^{-1})
h_m=2500 m, free slip (4h)

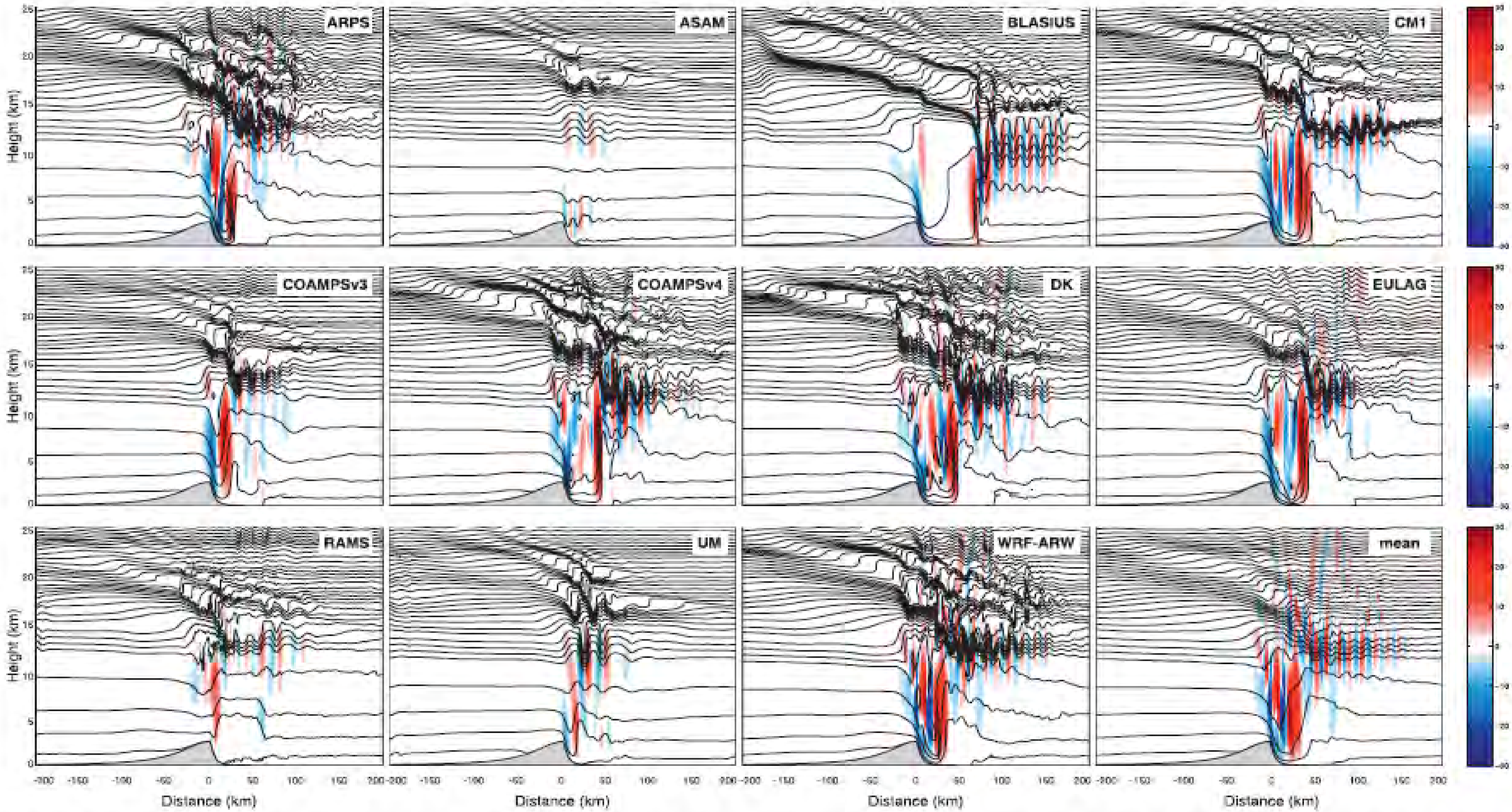

A subset of models with a very strong windstorm, breaking response
A few models show a much weaker response (ASAM, UM, RAMS)

nature geoscience

PERSPECTIVE

PUBLISHED ONLINE: 21 SEPTEMBER 2014 | DOI: 10.1038/NGEO2253

Atmospheric circulation as a source of uncertainty in climate change projections

Theodore G. Shepherd

"The most uncertain aspect of climate modelling lies in the representation of unresolved (subgrid scale) processes such as clouds, convection, and boundary-layer and **gravity-wave drag, and its sensitive interaction with large-scale dynamics**."

"The divergence of model projections that arises from model errors means that **it is essential to work towards reducing those errors, which are presumably associated with inadequate parameterizations of unresolved processes**."

2. DEEPWAVE Field Campaign

The Deep Propagating Gravity Wave Experiment (DEEPWAVE): An Airborne and Ground-Based Exploration of Gravity Wave Propagation and Effects from their Sources throughout the Lower and Middle Atmosphere

David C. Fritts[1], Ronald B. Smith[2], Michael J. Taylor[3], James D. Doyle[4], Stephen D. Eckermann[5], Andreas Dörnbrack[6], Markus Rapp[6], Bifford P. Williams[1], P.-Dominique Pautet[3], Katrina Bossert[1], Neal R. Criddle[3], Carolyn A. Reynolds[4], P. Alex Reinecke[4], Michael Uddstrom[7], Michael J. Revell[7], Richard Turner[7], Bernd Kaifler[6], Johannes S. Wagner[6], Tyler Mixa[1], Christopher G. Kruse[2], Alison D. Nugent[2], Campbell D. Watson[2], Sonja Gisinger[6], Steven M. Smith[8], Ruth S. Lieberman[1], Brian Laughman[1], James J. Moore[9], William O. Brown[9], Julie A. Haggerty[9], Alison Rockwell[9], Gregory J. Stossmeister[9], Steven F. Williams[9], Gonzalo Hernandez[10], Damian J. Murphy[11], Andrew R. Klekociuk[11], Iain M. Reid[12], and Jun Ma[13]

Bull. Am. Meteorol. Soc. (2015), in press

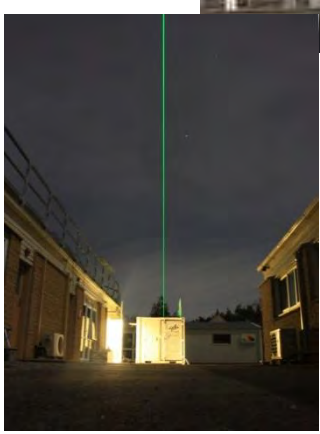

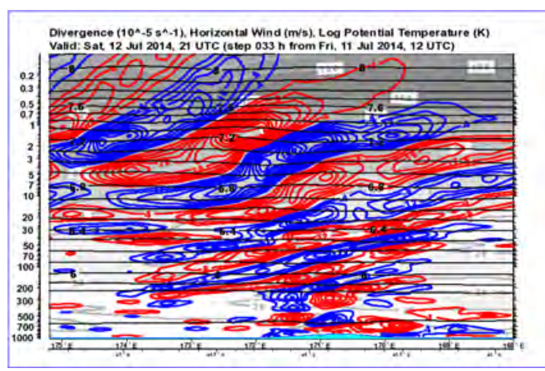

2. DEEPWAVE Field Campaign

OBJECTIVES:

- study **dynamical coupling processes** by gravity waves
  from the **troposphere into the stratosphere and mesosphere**
  by characterizing the complete life cycle of gravity waves:

  gravity wave excitation,

  propagation, and

  dissipation

  employing observational and modelling tools

- improve GW parameterizations for use in general circulation models

BMBF Research Initiative: ROMIC (Role of the Middle atmosphere In Climate)
2014 -2017

DFG Research Group: MSGwaves (Multiscale Dynamics of Gravity Waves)
2014-2020

Stratospheric GW hotspots

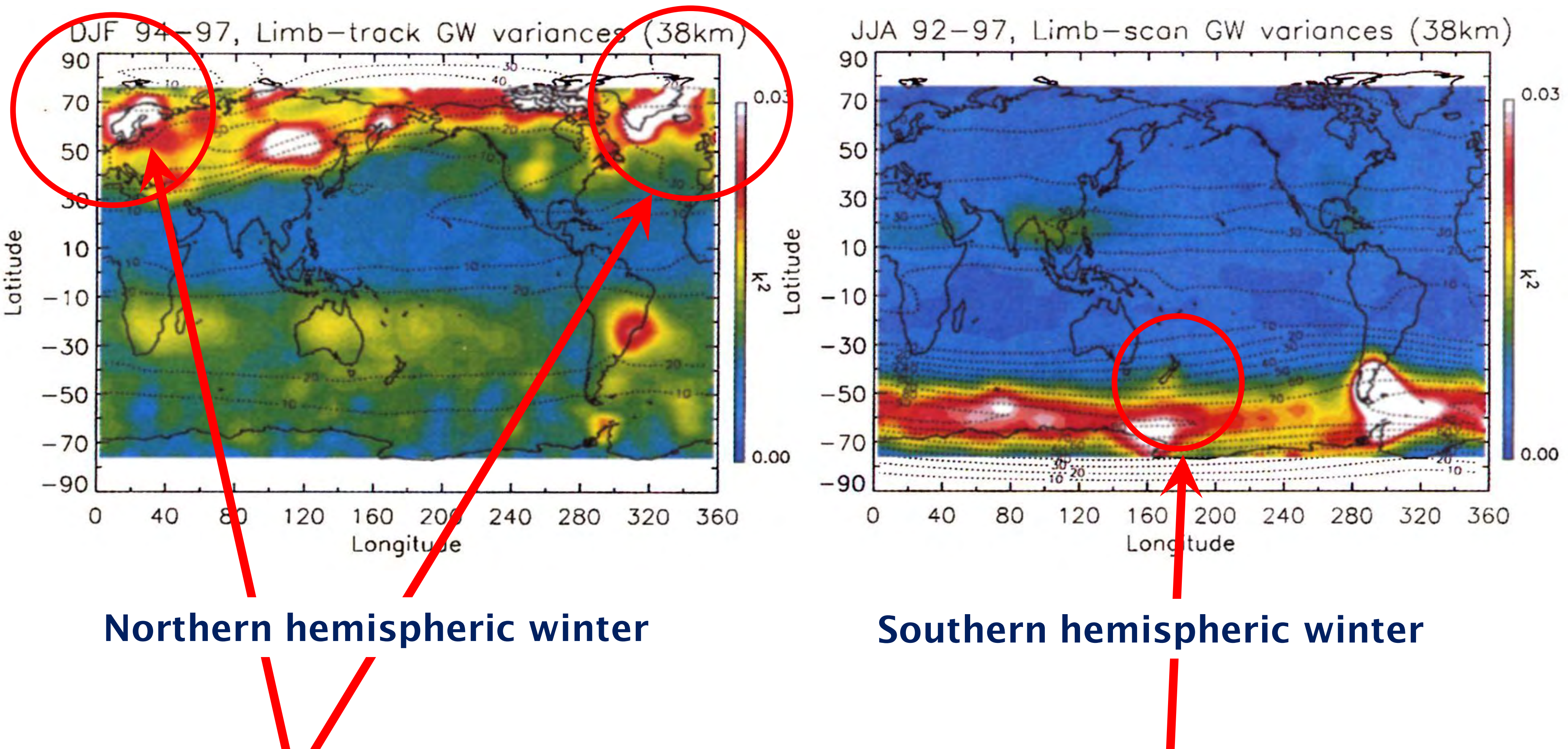

Focus of GW-LCYCLE
2013, 2015/16

US funded NFS project DEEPWAVE
(moved from South America)

Jiang et al., 2003

New Zealand: Gravity Wave Hot Spot in SH winter

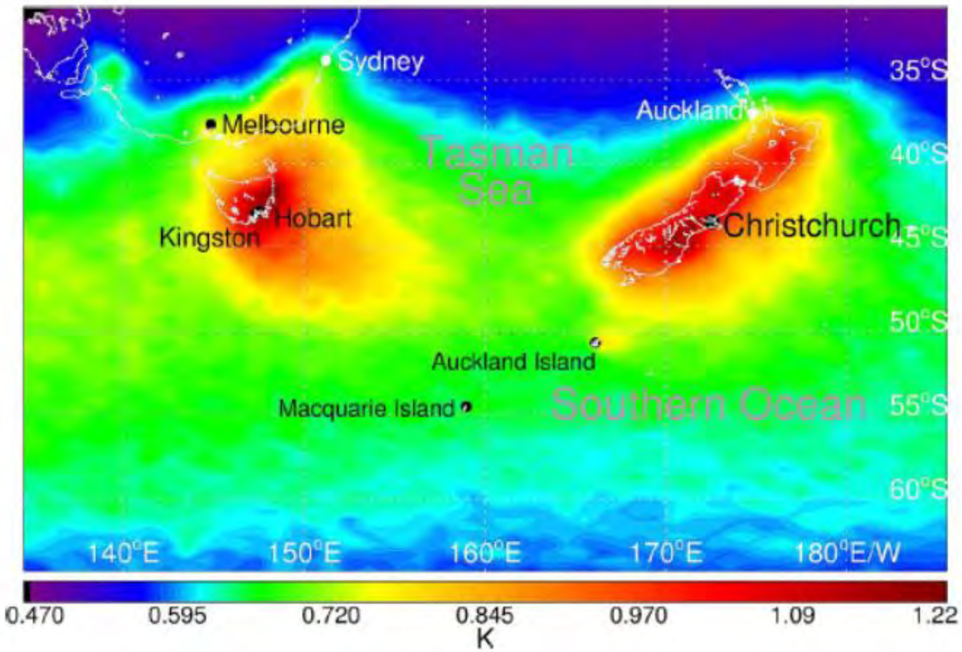

AIRS RMS Temperature
at 2.5 hPa for June/July 2001-2013

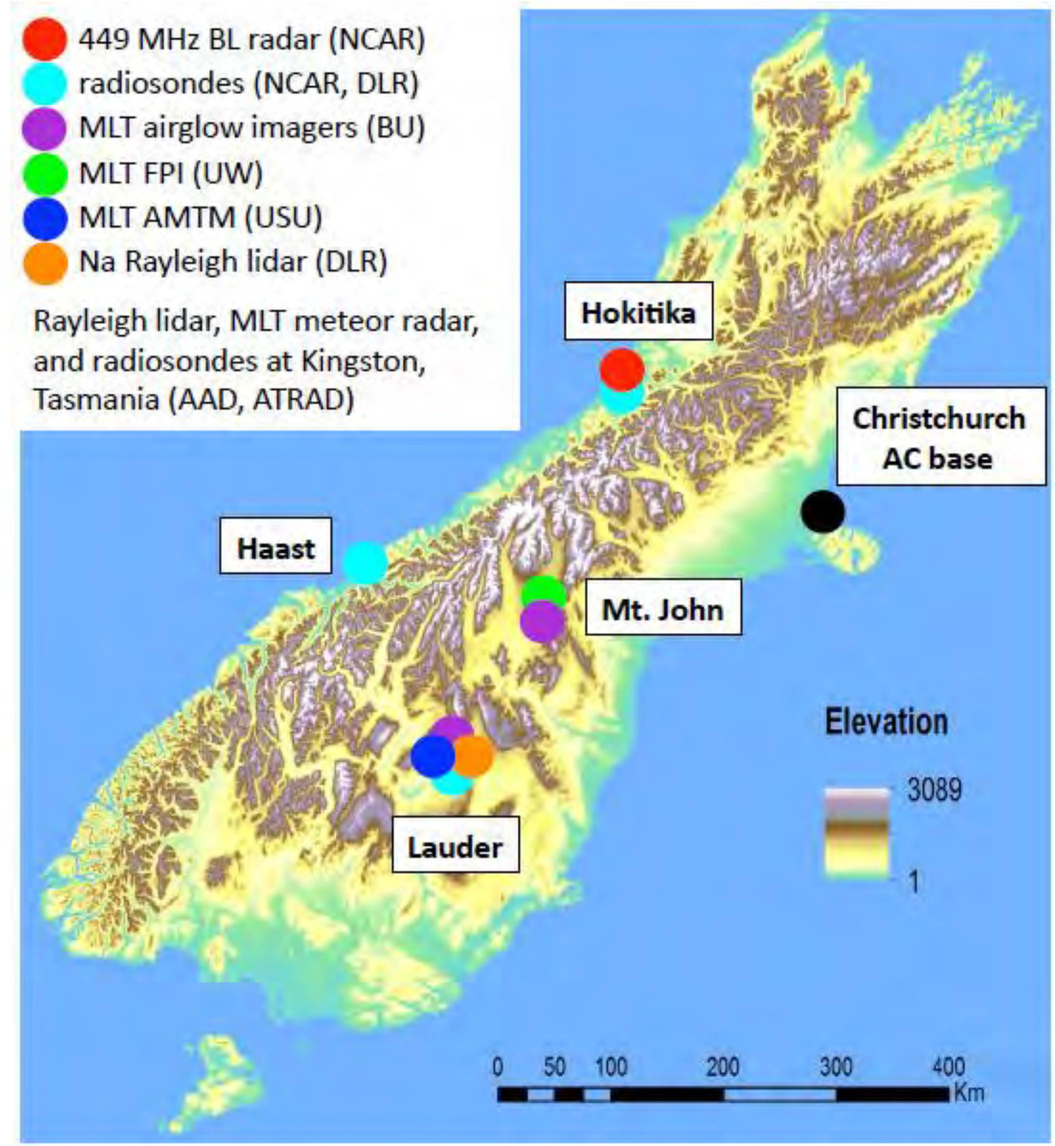

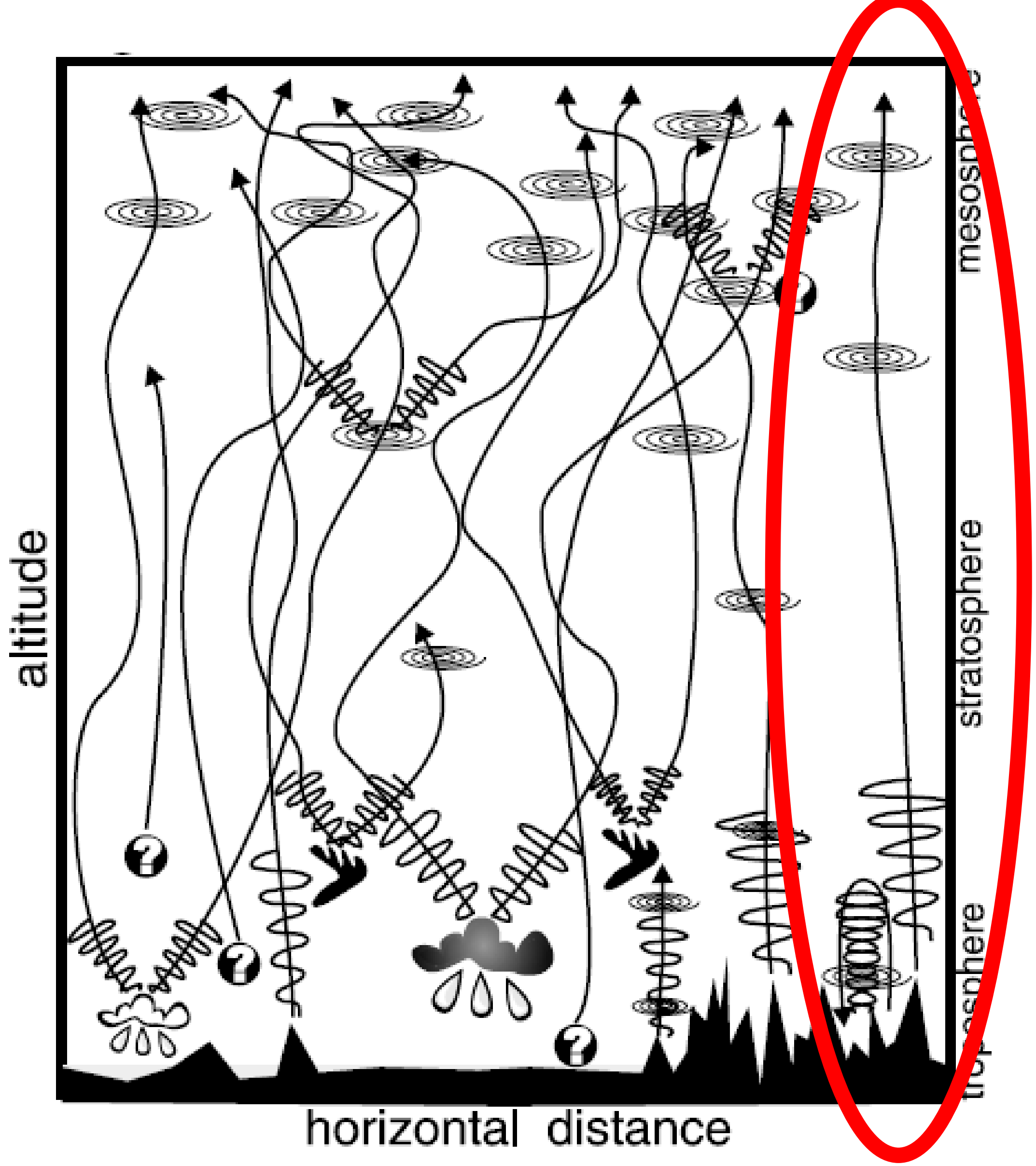

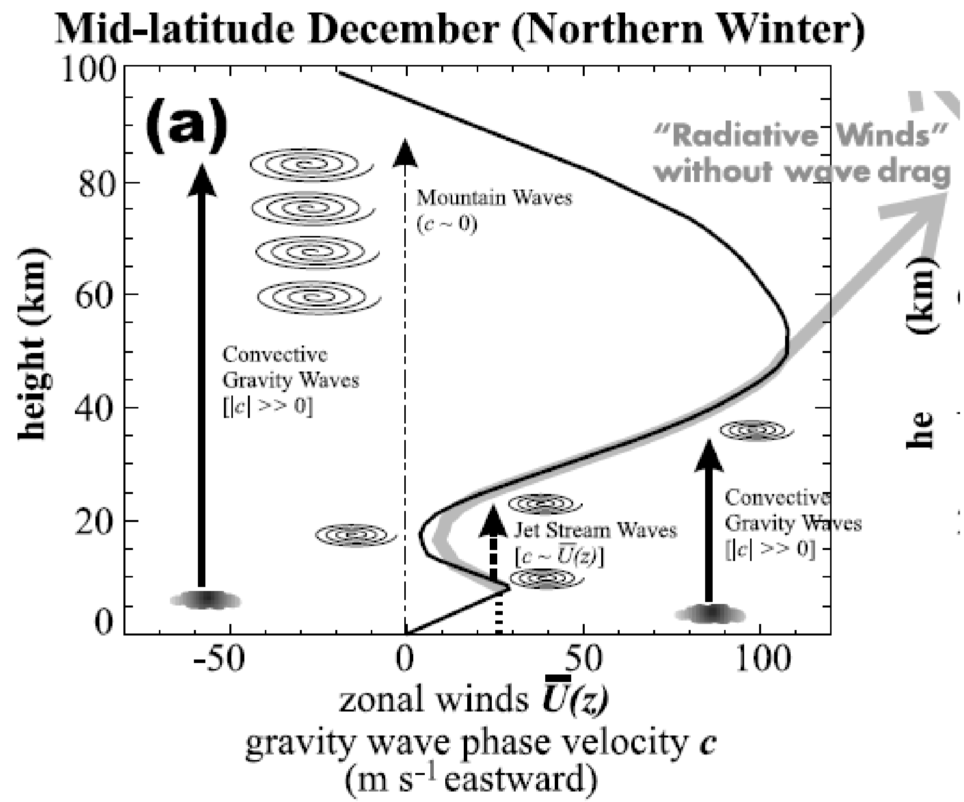

Kim et al., 2003

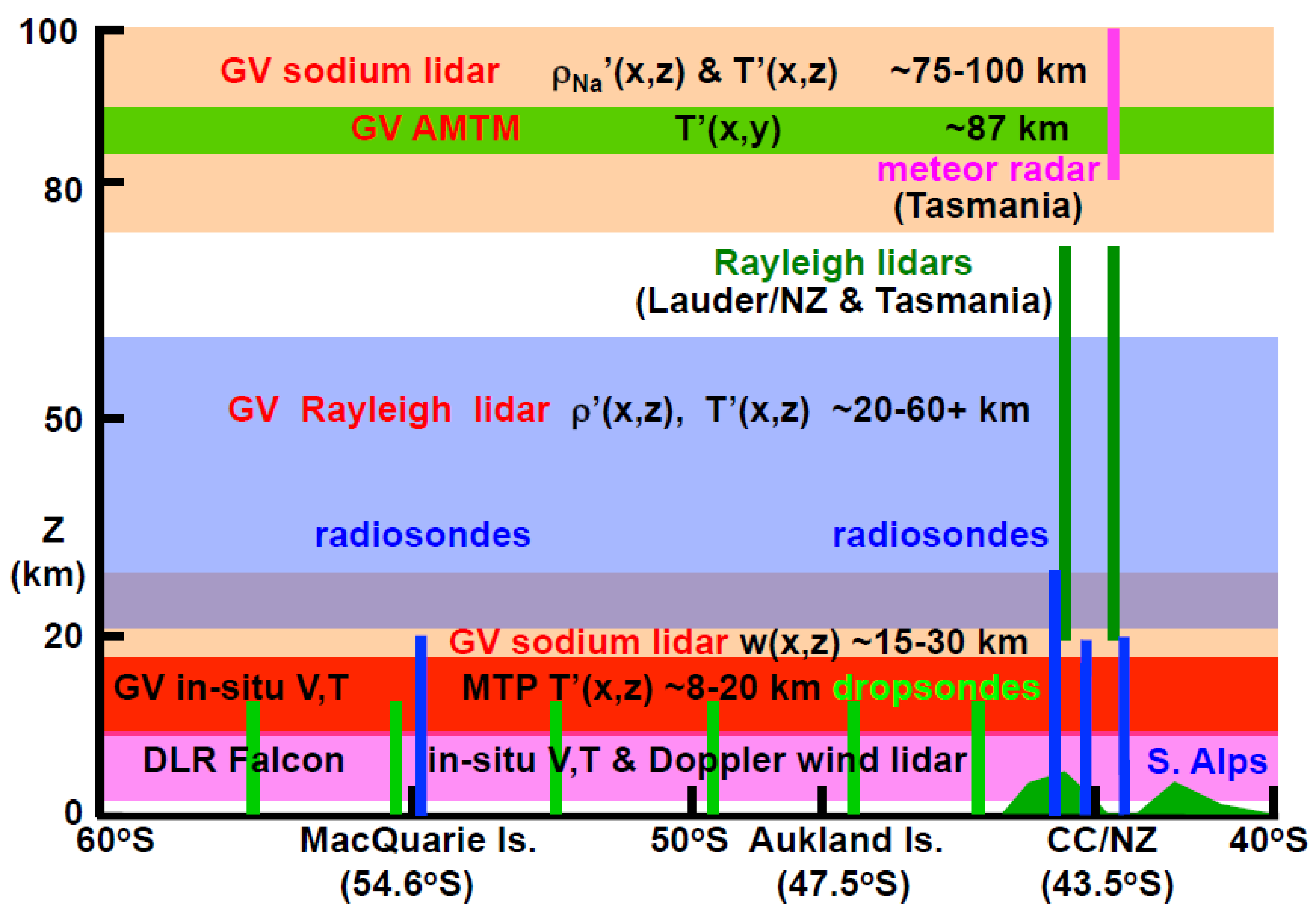

GV sodium lidar
ρ_{Na}'(x,z) & T'(x,z)
~75-100 km
GV AMTM
T'(x,y)
~87 km
meteor radar
(Tasmania)
Rayleigh lidars
(Lauder/NZ & Tasmania)
GV Rayleigh lidar
ρ'(x,z), T'(x,z)
~20-60+ km
radiosondes
radiosondes
GV sodium lidar w(x,z) ~15-30 km
GV in-situ V,T
MTP T'(x,z) ~8-20 km
dropsondes
DLR Falcon
in-situ V,T & Doppler wind lidar
S. Alps
100
80
50
Z
(km)
20
0
60°S
MacQuarie Is.
(54.6°S)
50°S
Aukland Is.
(47.5°S)
CC/NZ
(43.5°S)
40°S

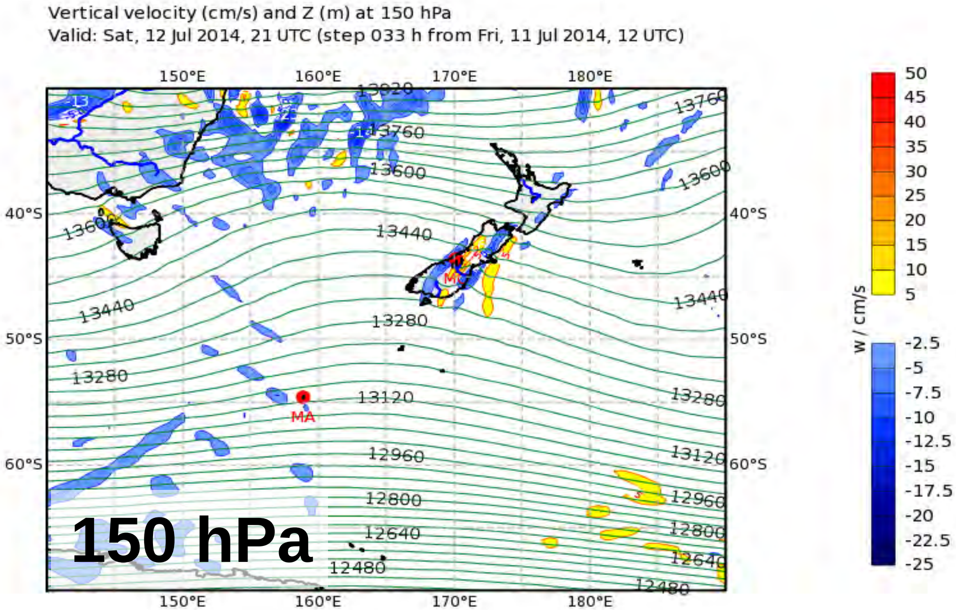

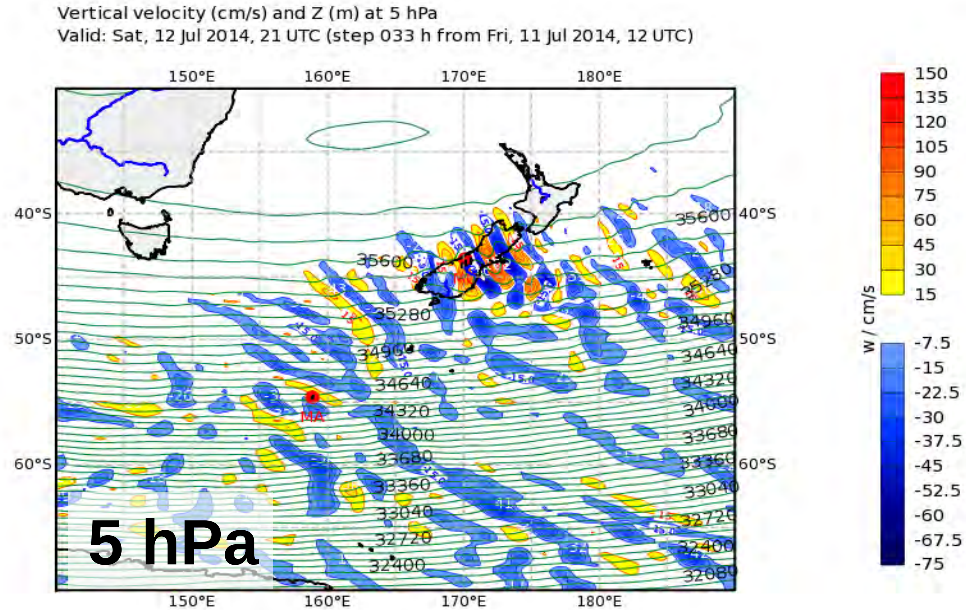

12 July 2014 21 UTC

13 July 09 NZST

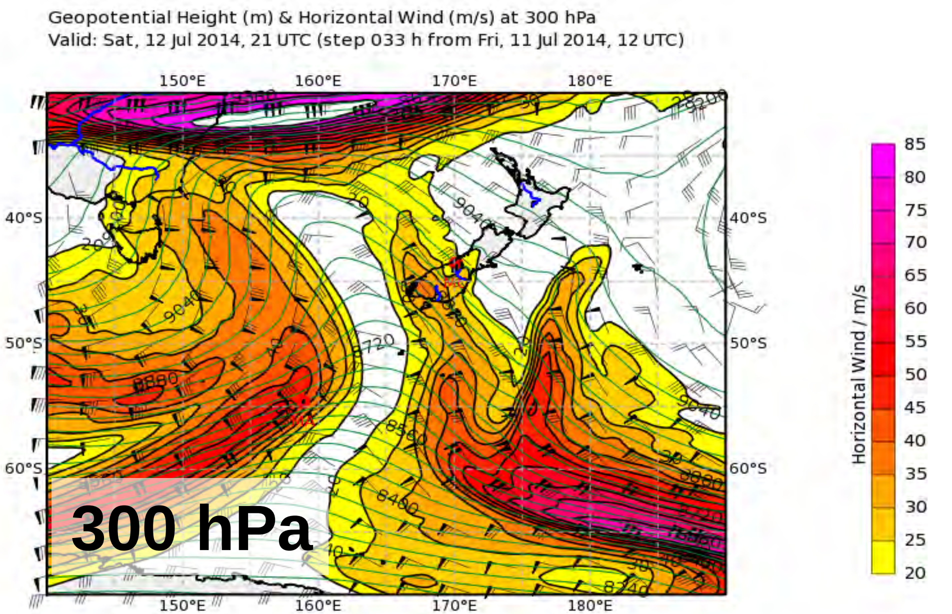

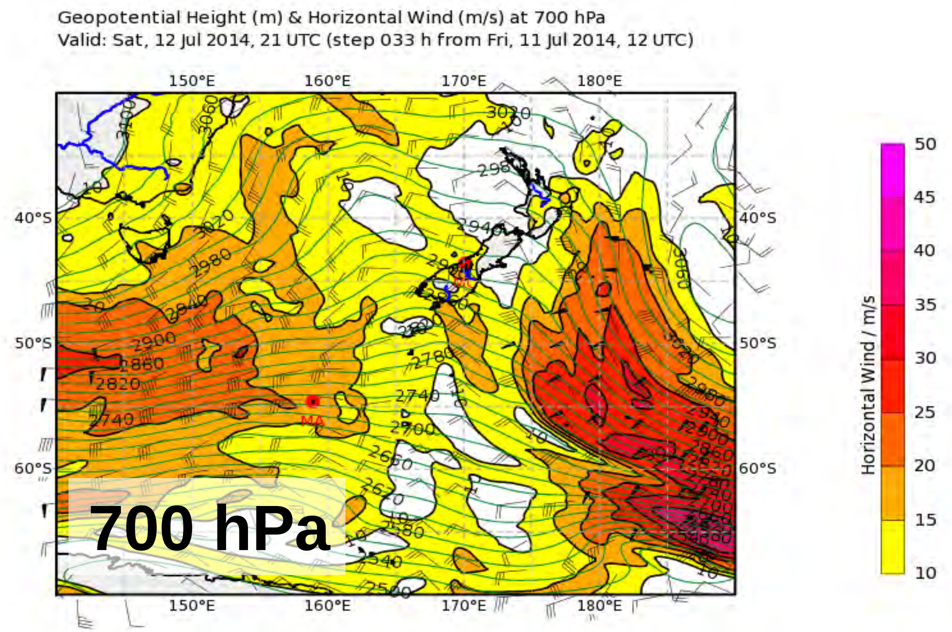

RF-09 12-Jul 21 UTC
09 local

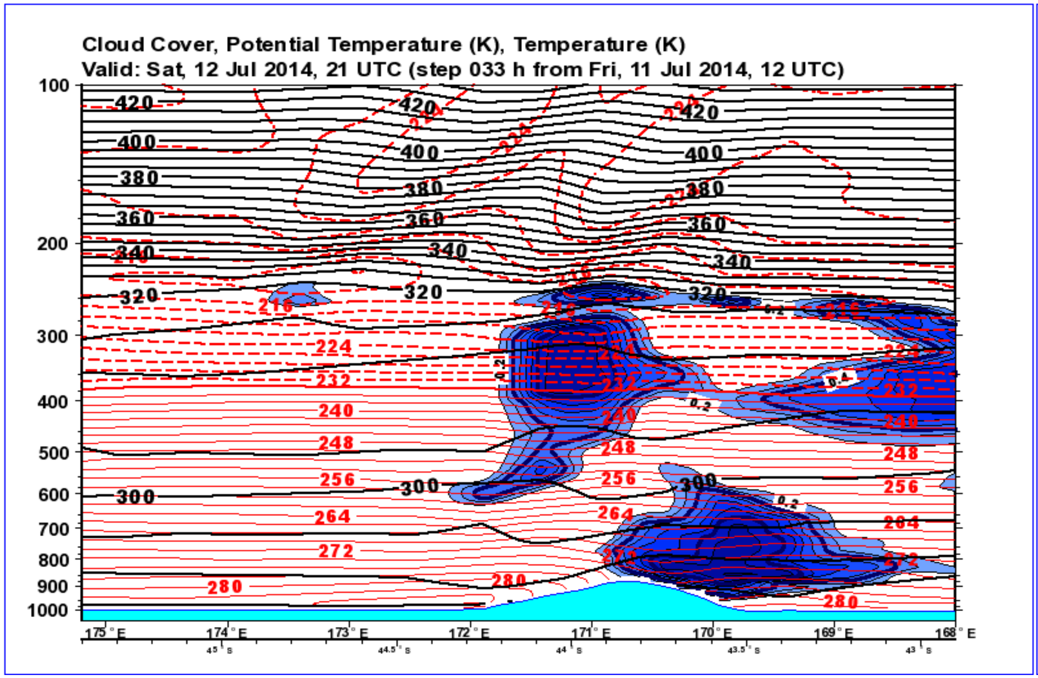

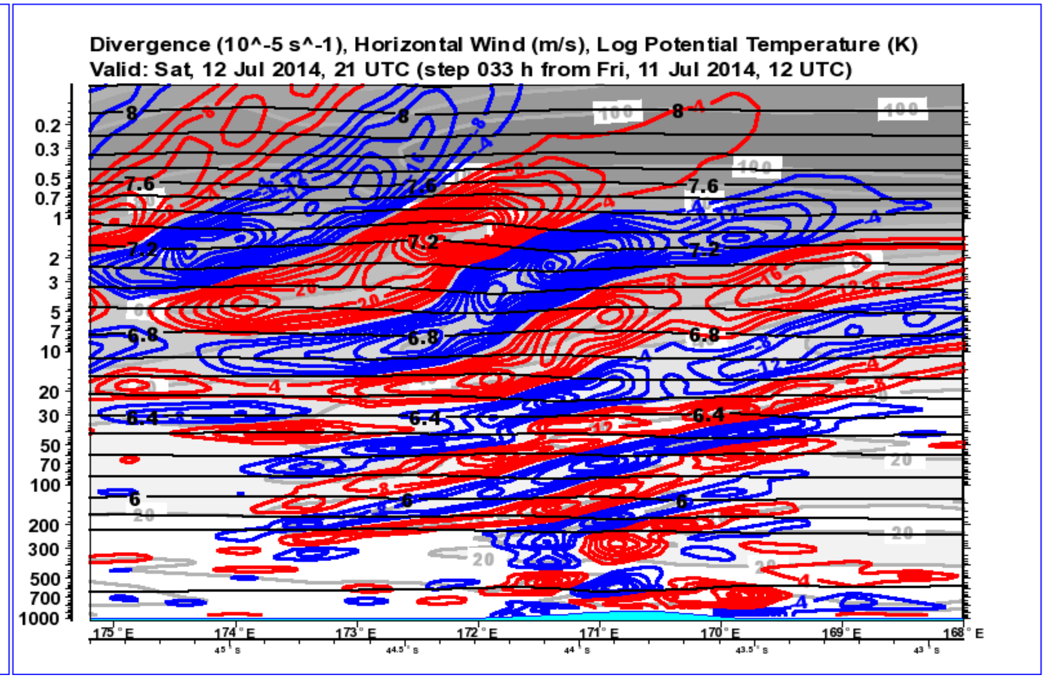

Horizontal average of horizontal wind over the South Island/NZ

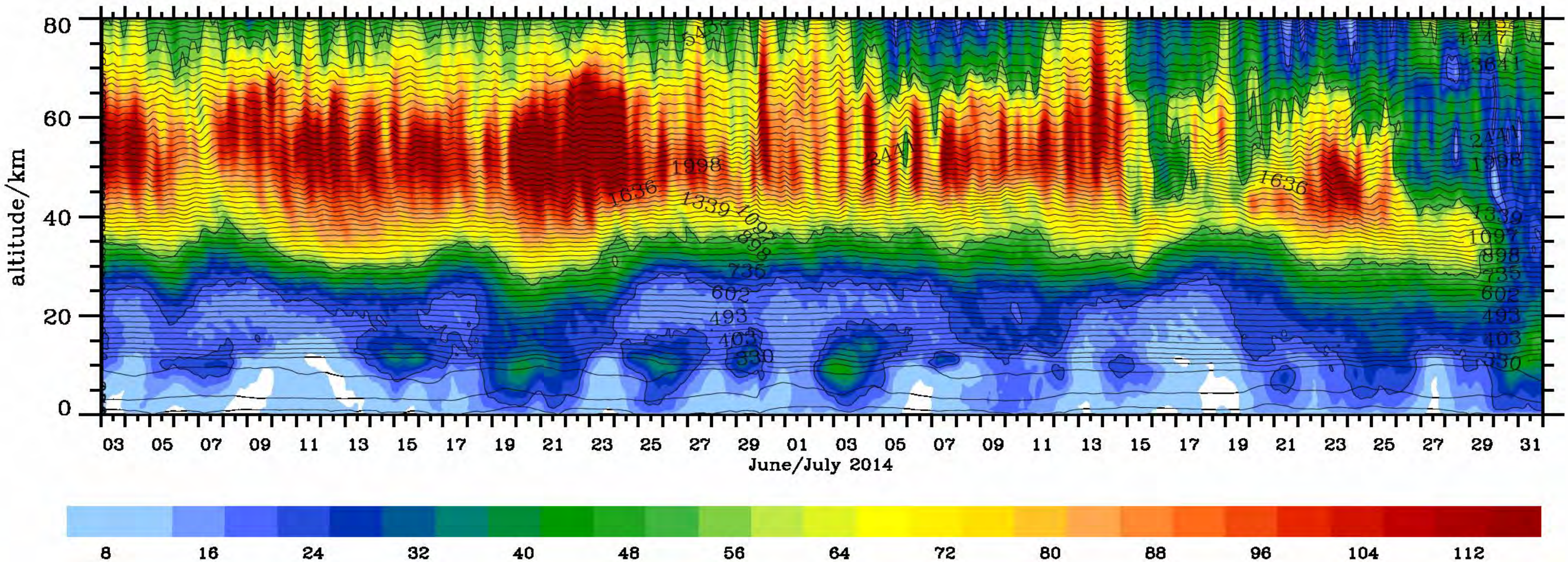

V_{HOR}/ms^{-1}

ECMWF T1279/L137 operational analyses (6 h)
and 1 hourly high-resolution IFS predictions

Horizontal average of horizontal wind over the South Island/NZ

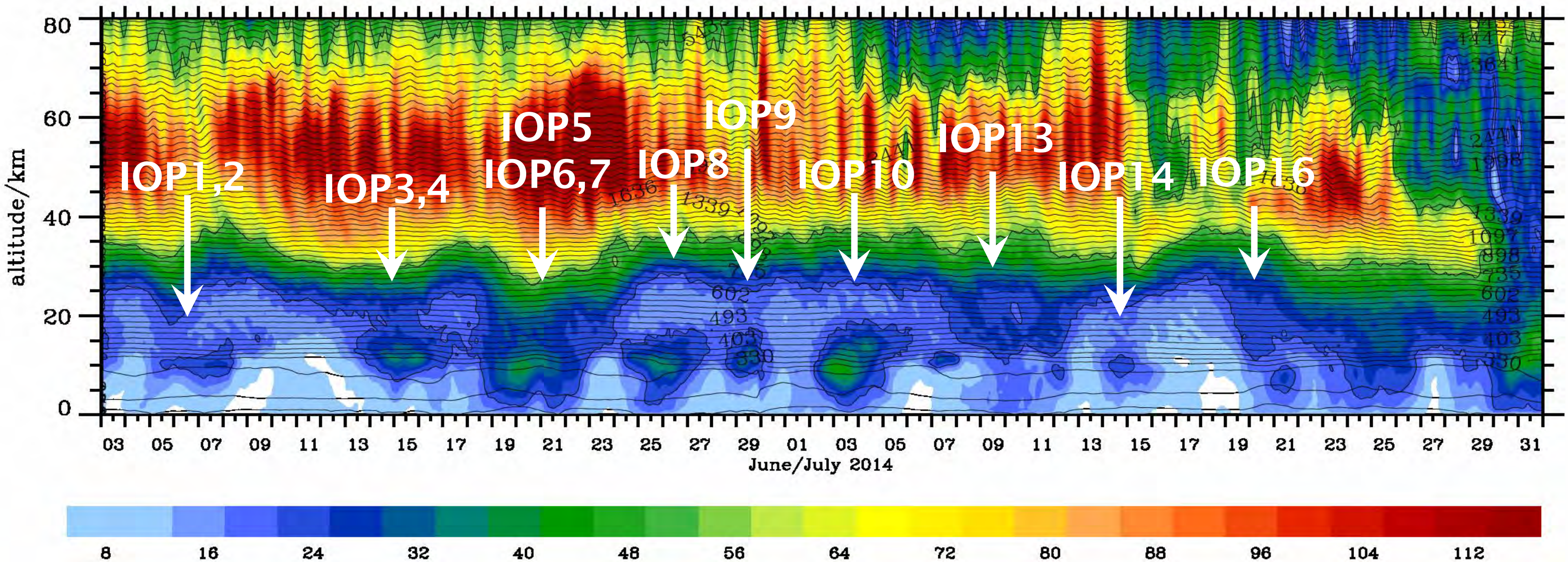

V_{HOR}/ms^{-1}

ECMWF T1279/L137 operational analyses (6 h)
and 1 hourly high-resolution IFS predictions

3. From the Troposphere to the Stratosphere

Radiosonde analyses from Lauder/NZ (45˚S, 169˚E)

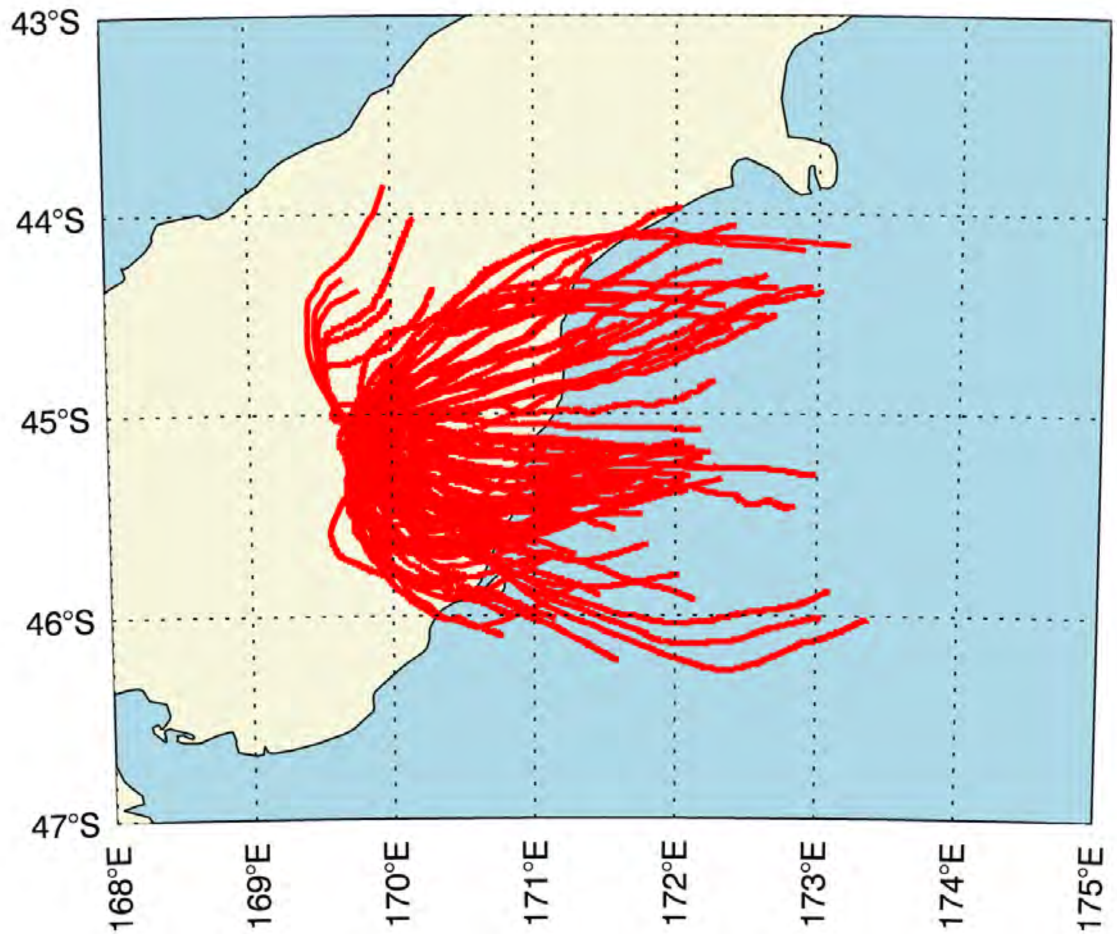

- 98 soundings in total
- mean height reached: 31.1 km
- maximum height reached: 36.6 km

Sonja Gisinger, DLR

3 hourly radiosonde profiles

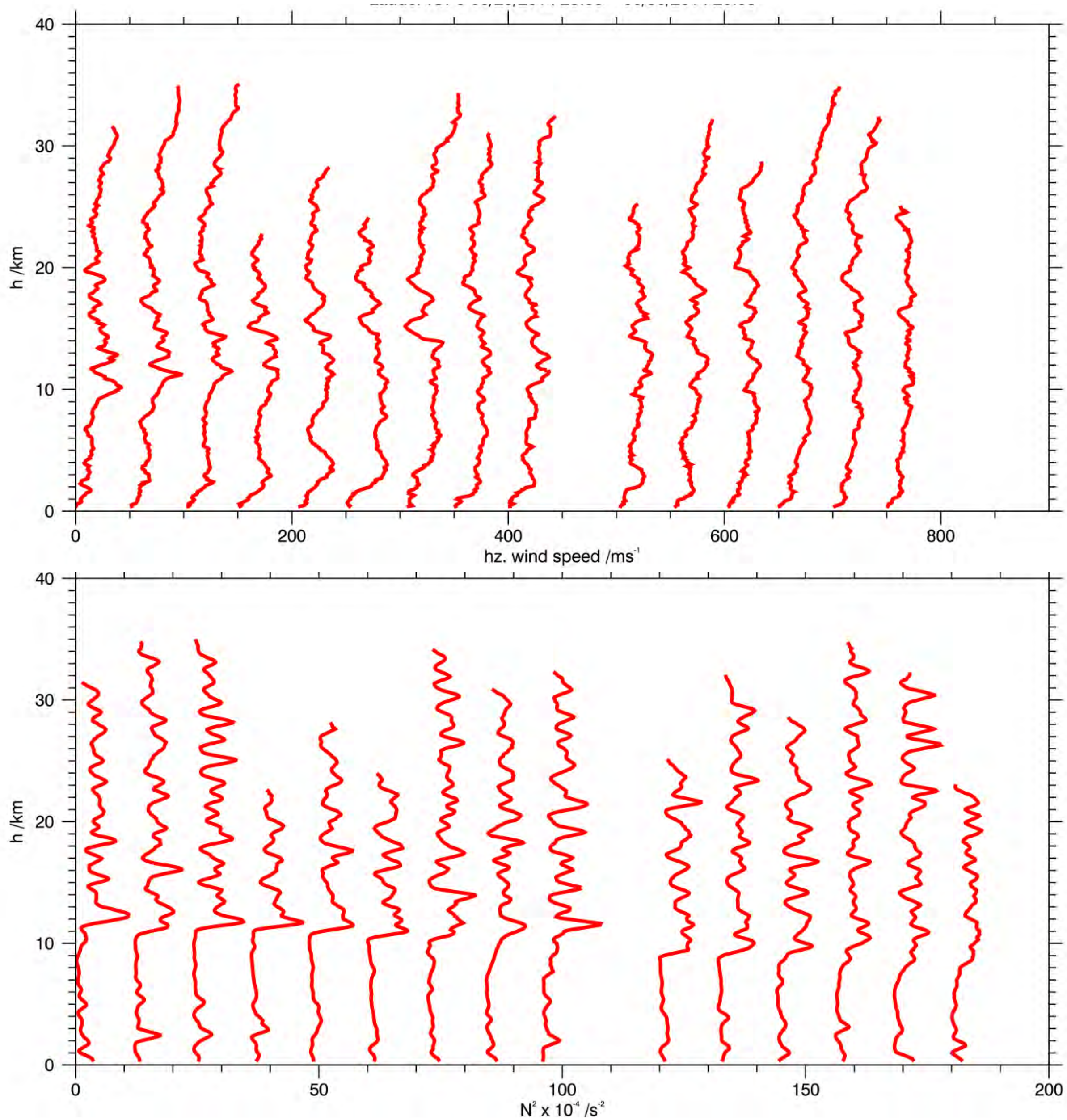

V_{HOR}/ms^{-1}

N^2/s^{-2}

Sonja Gisinger, DLR

Brunt-Väisälä Frequency N^2 and Tropopause Height above Lauder/NZ

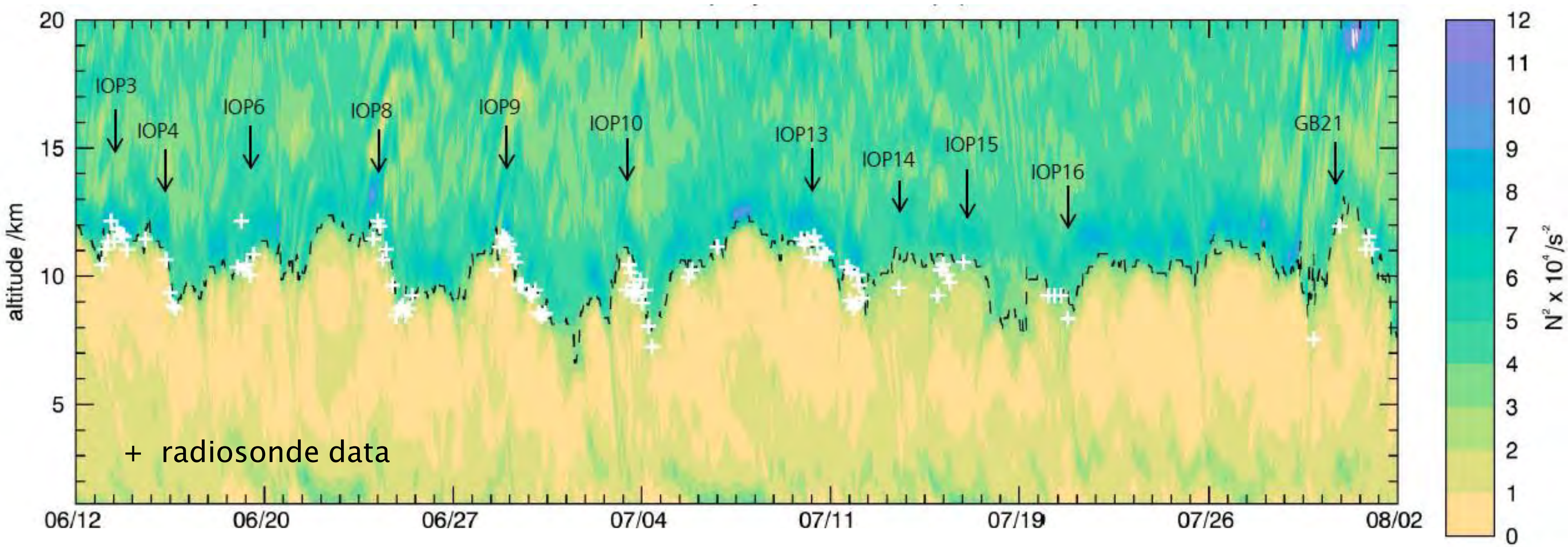

ECMWF T1279/L137 operational analyses (6 h) and 1 hourly high-resolution IFS predictions

Sonja Gisinger, DLR

Estimation of Gravity Wave Parameters

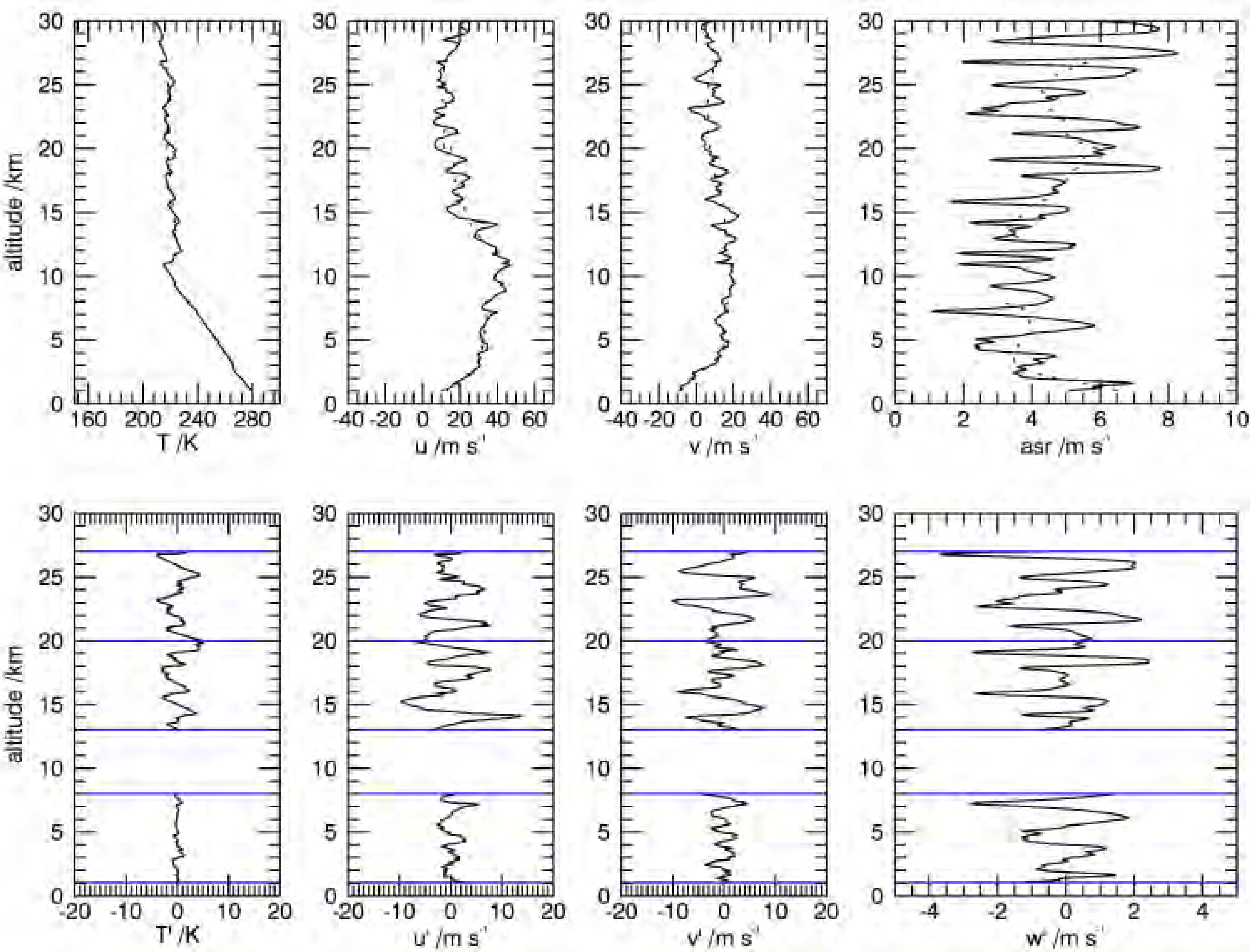

solid lines:
RS profiles

dashed lines:
background profiles

Perturbations

mstrato:
mid stratosphere

lstrato:
low stratosphere

tropo:
troposphere

Mean magnitude of horizontal wind perturbations: 6 … 8 m/s
Mean magnitude of vertical wind perturbations: 1 … 2 m/s

Gravity wave energies (Geller and Gong 2010)

- kinetic energy: $\langle KE_{volume} \rangle = \frac{1}{2}[\langle \rho u'^2 \rangle + \langle \rho v'^2 \rangle]$
- potential energy: $\langle PE_{volume} \rangle = \frac{1}{2}\frac{g^2}{N^2}\left\langle \rho \frac{T'^2}{T_b{}^2} \right\rangle$
- vertical energy: $\langle VE_{volume} \rangle = \frac{1}{2}\langle \rho w'^2 \rangle$

Energies sensitive to different parts of the GW spectrum

KE: sensitive to low frequency waves/inertial gravity waves
VE: sensitive to high frequency gravity waves
PE: mixed

Gravity Wave Energies

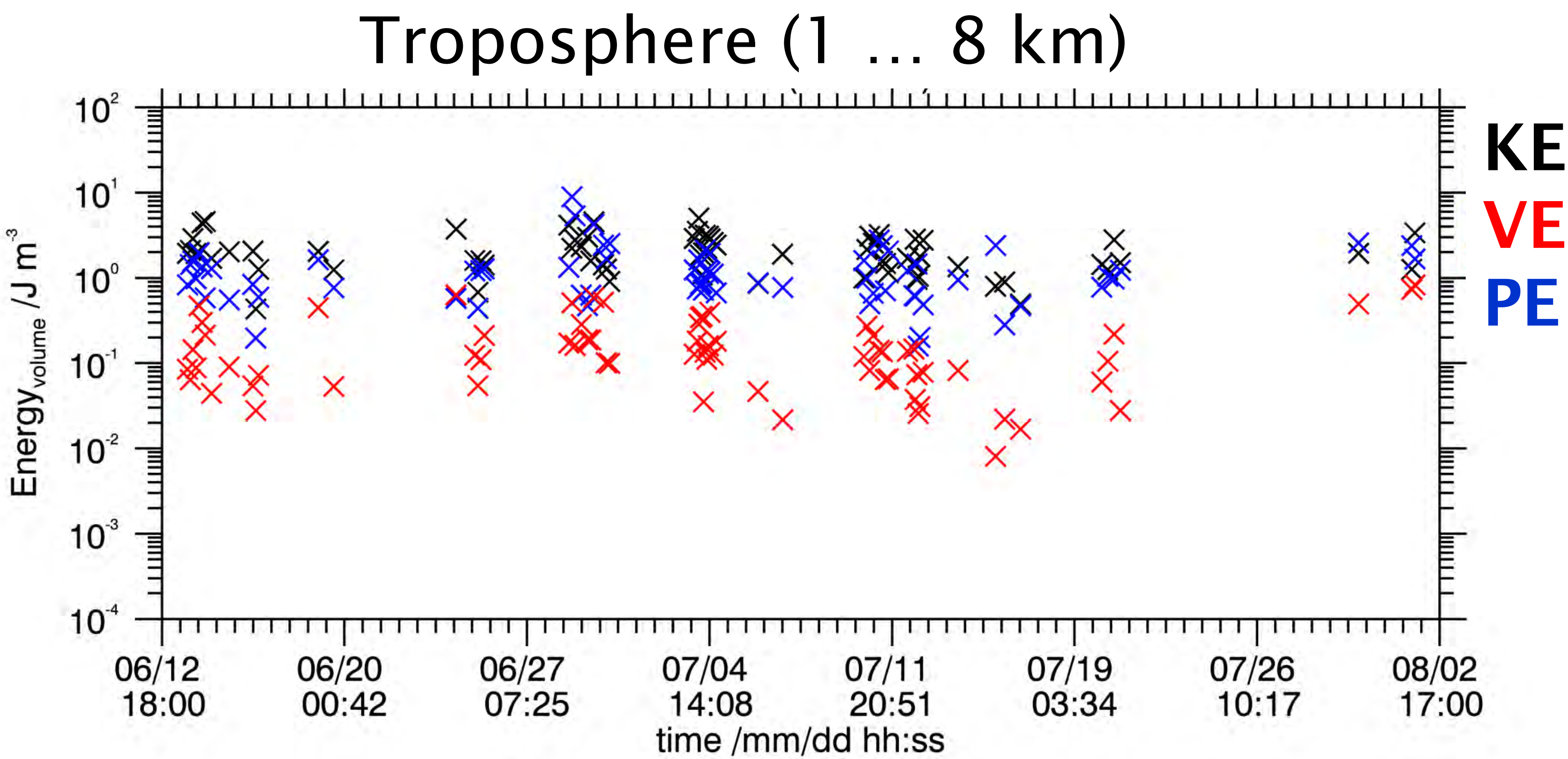

Sonja Gisinger, DLR

Gravity Wave Energies

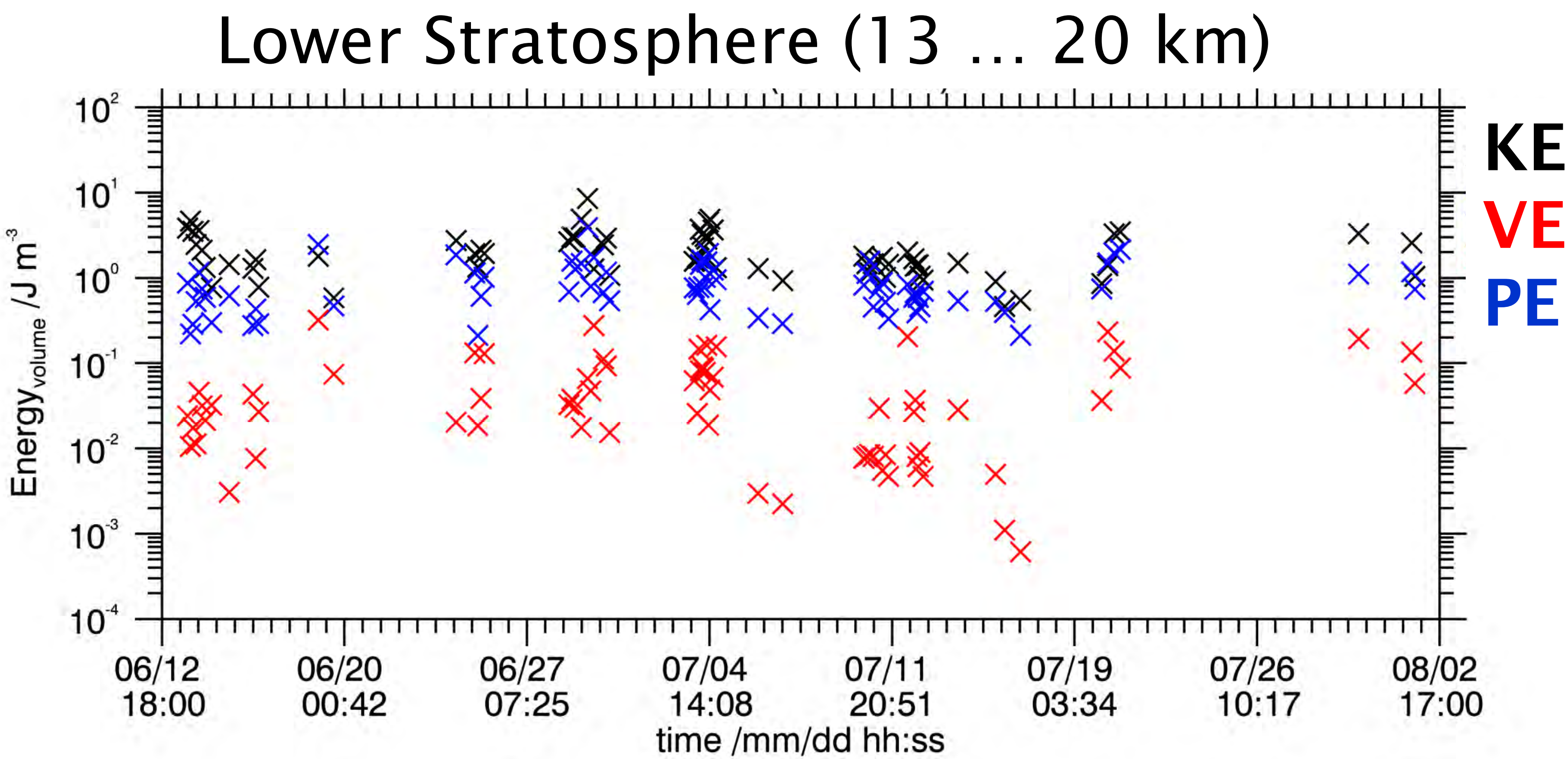

Sonja Gisinger, DLR

Gravity Wave Energies

Mid Stratosphere (20 … 27 km)

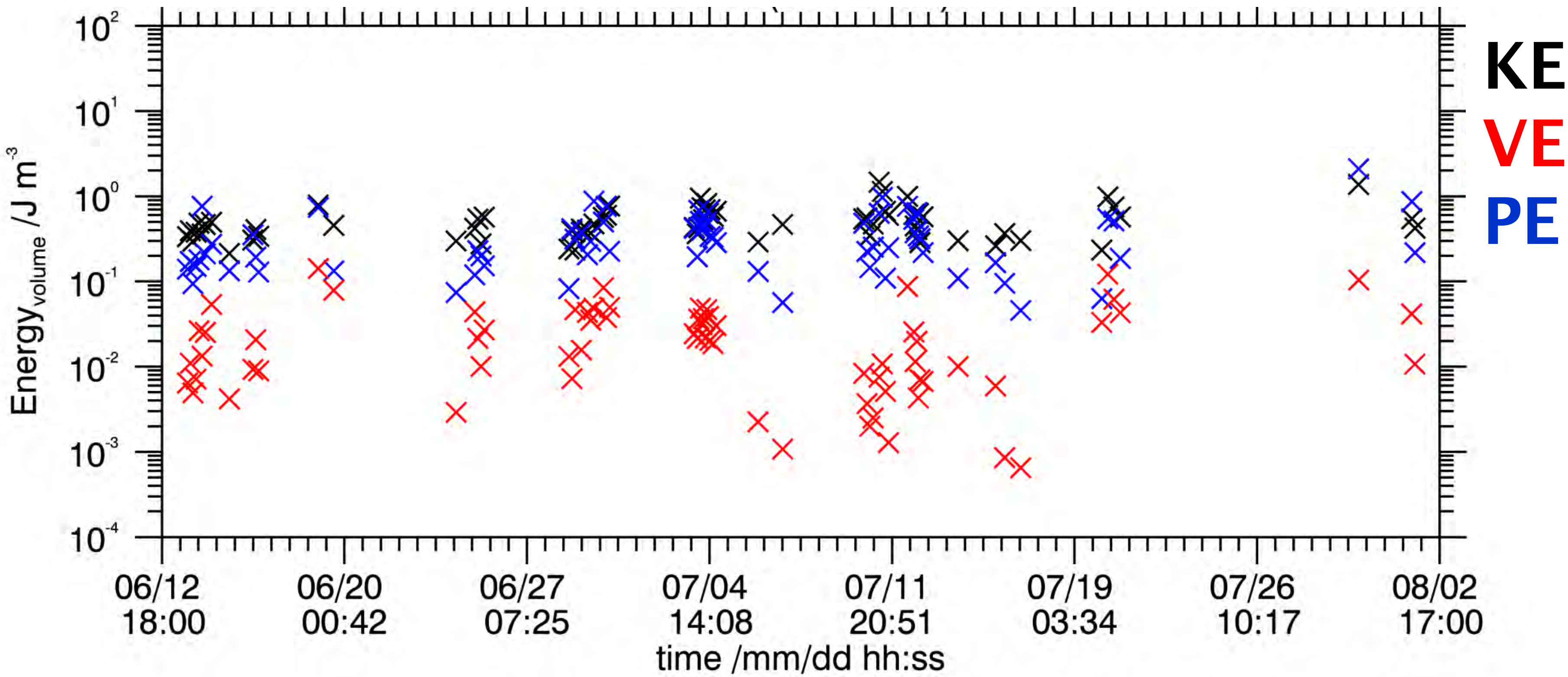

Sonja Gisinger, DLR

Vertical Energy (VE) Ratios

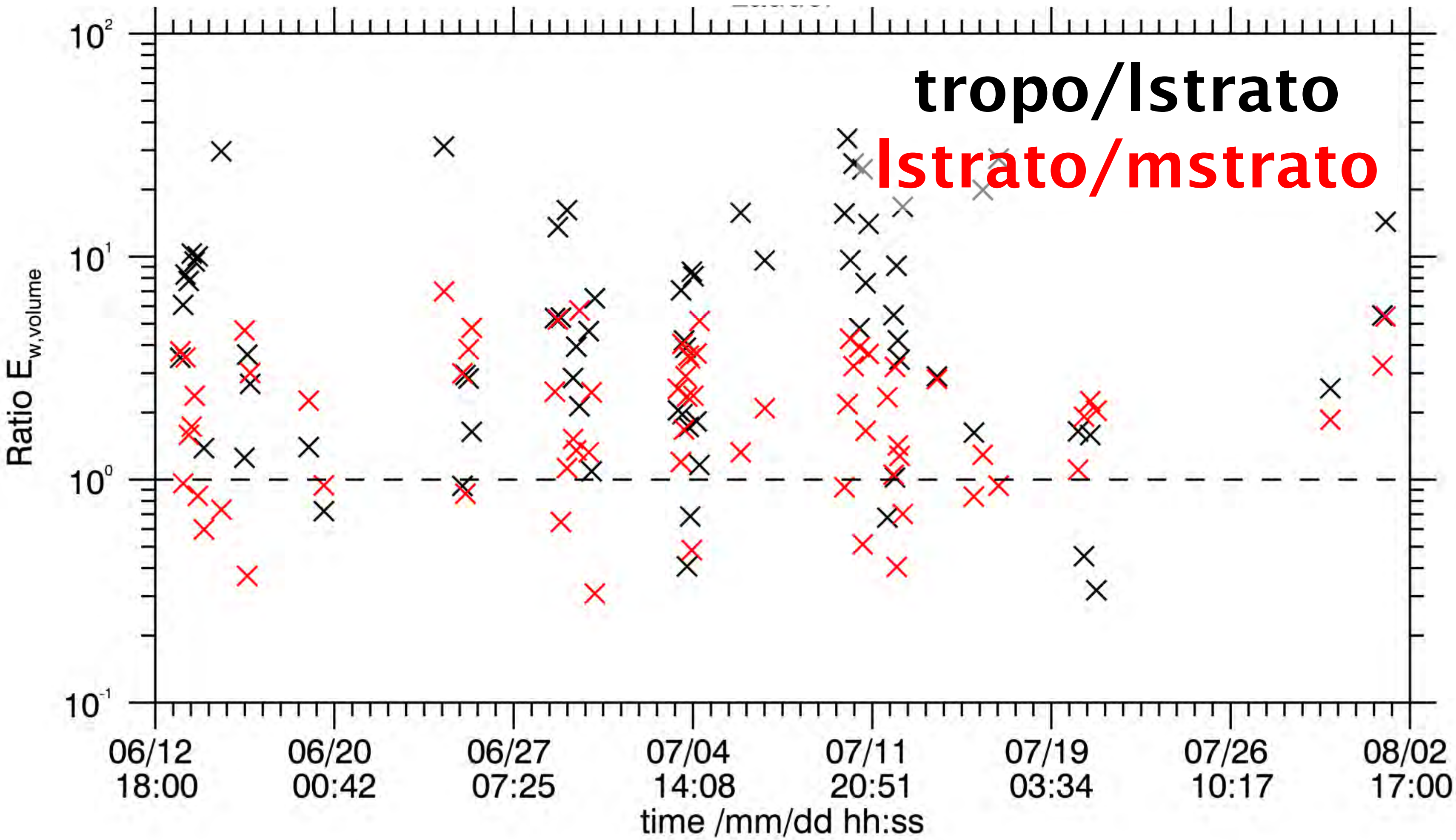

Ratio < 1: VE higher in upper layer – input of GW energy in upper layer

Ratio > 1: VE lower in upper layer – GW dissipation, no conservative propagation

Sonja Gisinger, DLR

Kinetic Energy (KE) Ratios

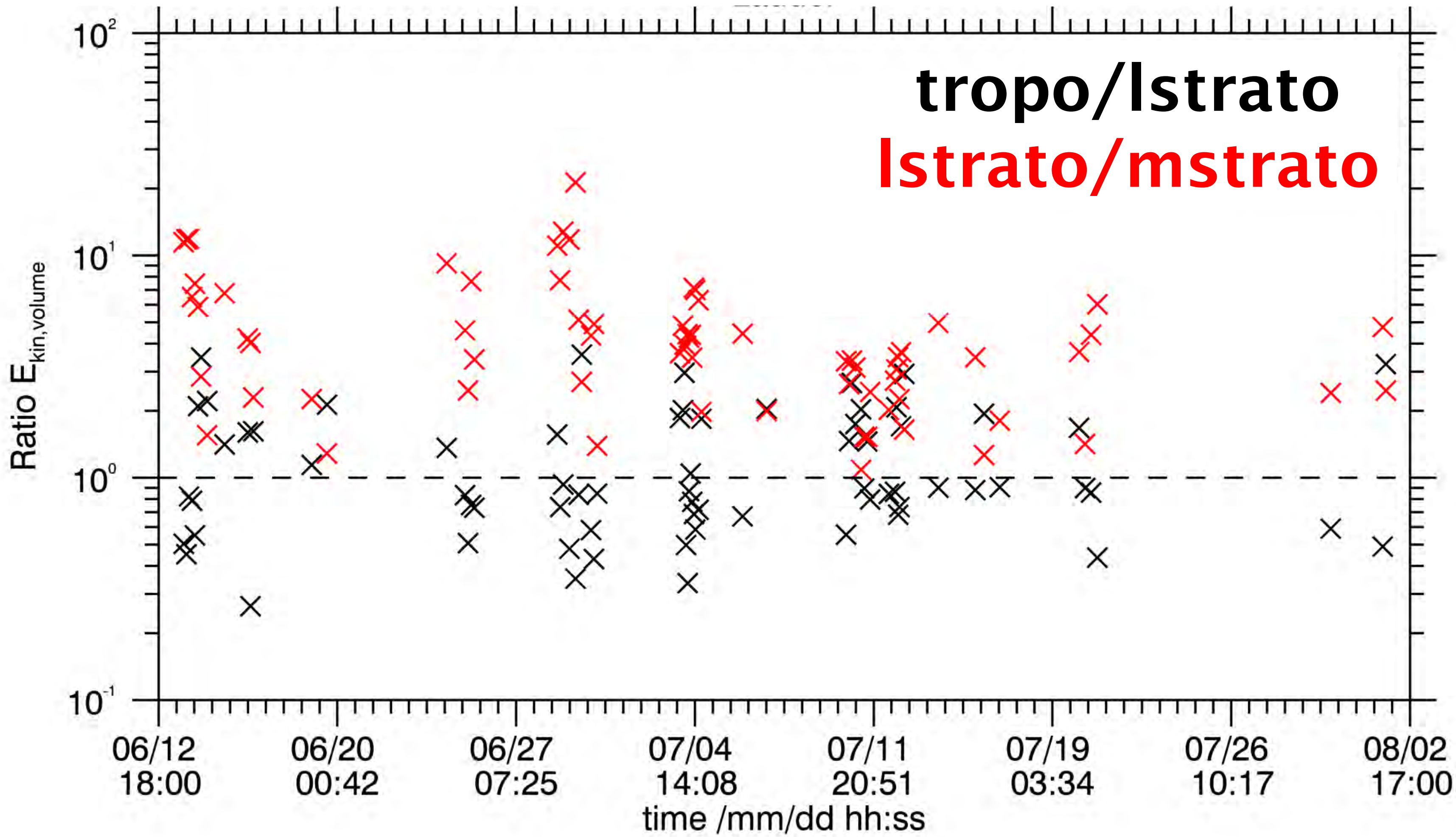

Ratio < 1: KE higher in upper layer – input of GW energy in upper layer

Ratio > 1: KE lower in upper layer – GW dissipation, no conservative propagation

Sonja Gisinger, DLR

Results: completely different behaviour of VE and KE :

> tropopause regions seems to be a source/an amplifier of low frequency gravity waves (KE) and a filter for high-frequency waves

- Correlations with wind speed

Surface wind (1-3 km)	tropo	lstrato
KE	0.27	0.22
VE	0.62	0.46

TP-Jet region (8-13 km)	tropo	lstrato
KE	0.42	0.35
VE	0.46	0.30

+ (KE: tropo, surface wind → TP-Jet region)

- (VE: tropo, surface wind → TP-Jet region)

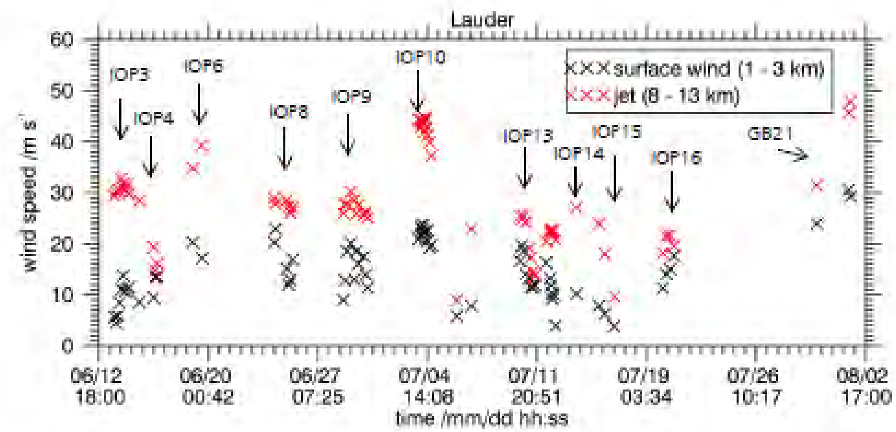

- Correlations with PE

	tropo	lstrato	mstrato
KE,PE	0.14	0.62	0.65
VE,PE	0.41	0.47	0.52

- for $\Omega \rightarrow f$: good correlation for KE,PE
- for $\Omega \rightarrow N$: good correlation for VE,PE

Sonja Gisinger, DLR

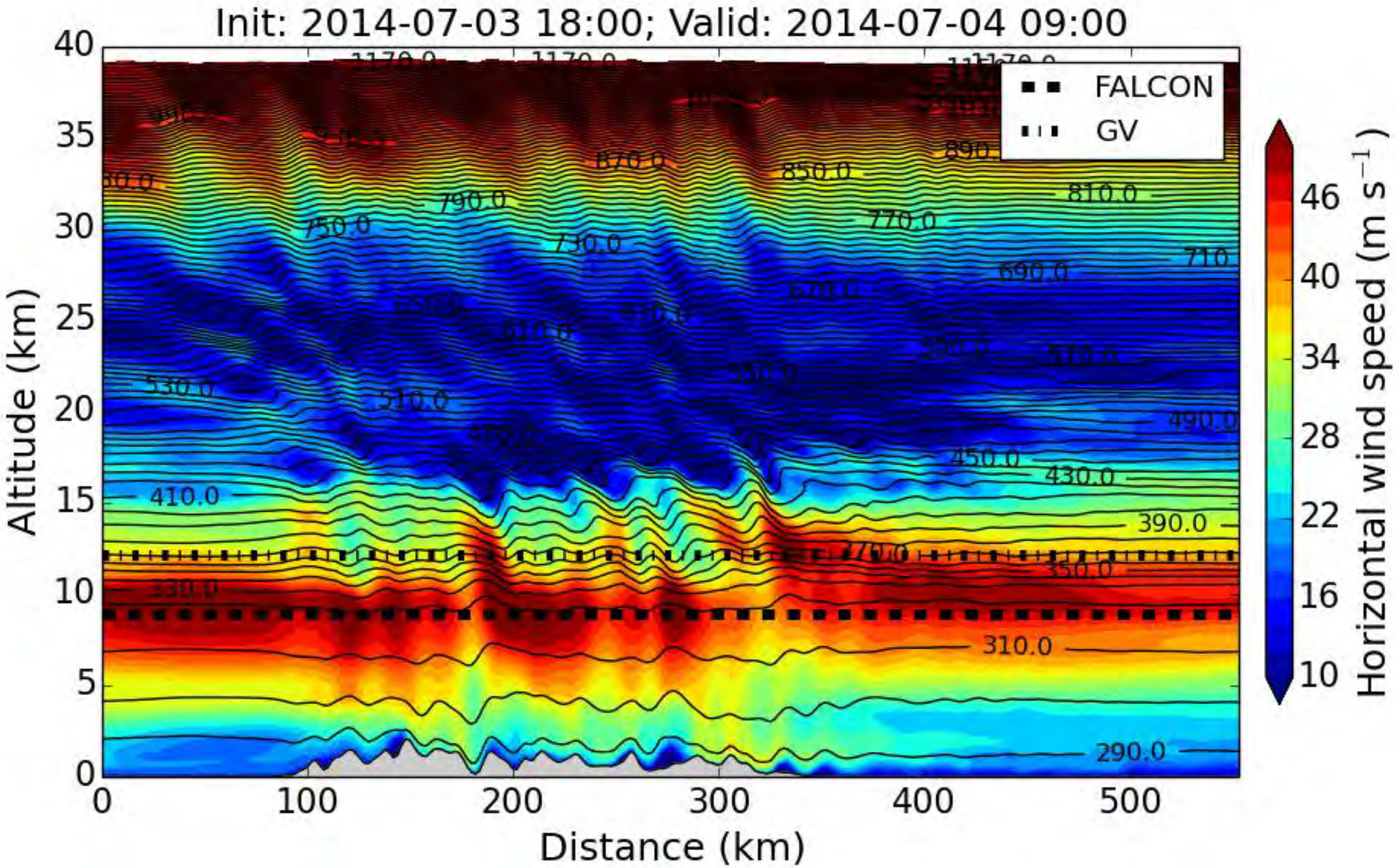

Johannes Wagner, DLR

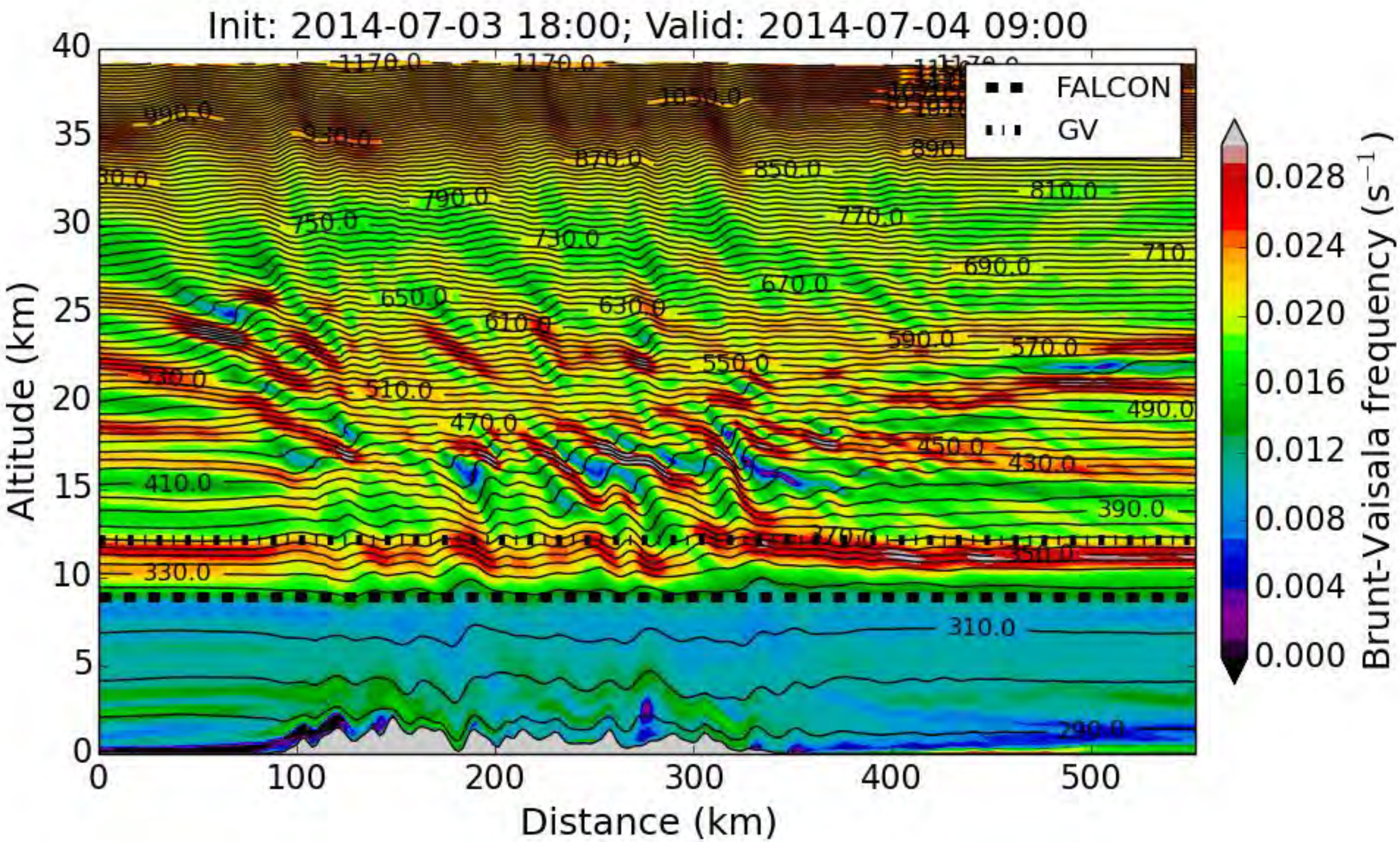

Johannes Wagner, DLR

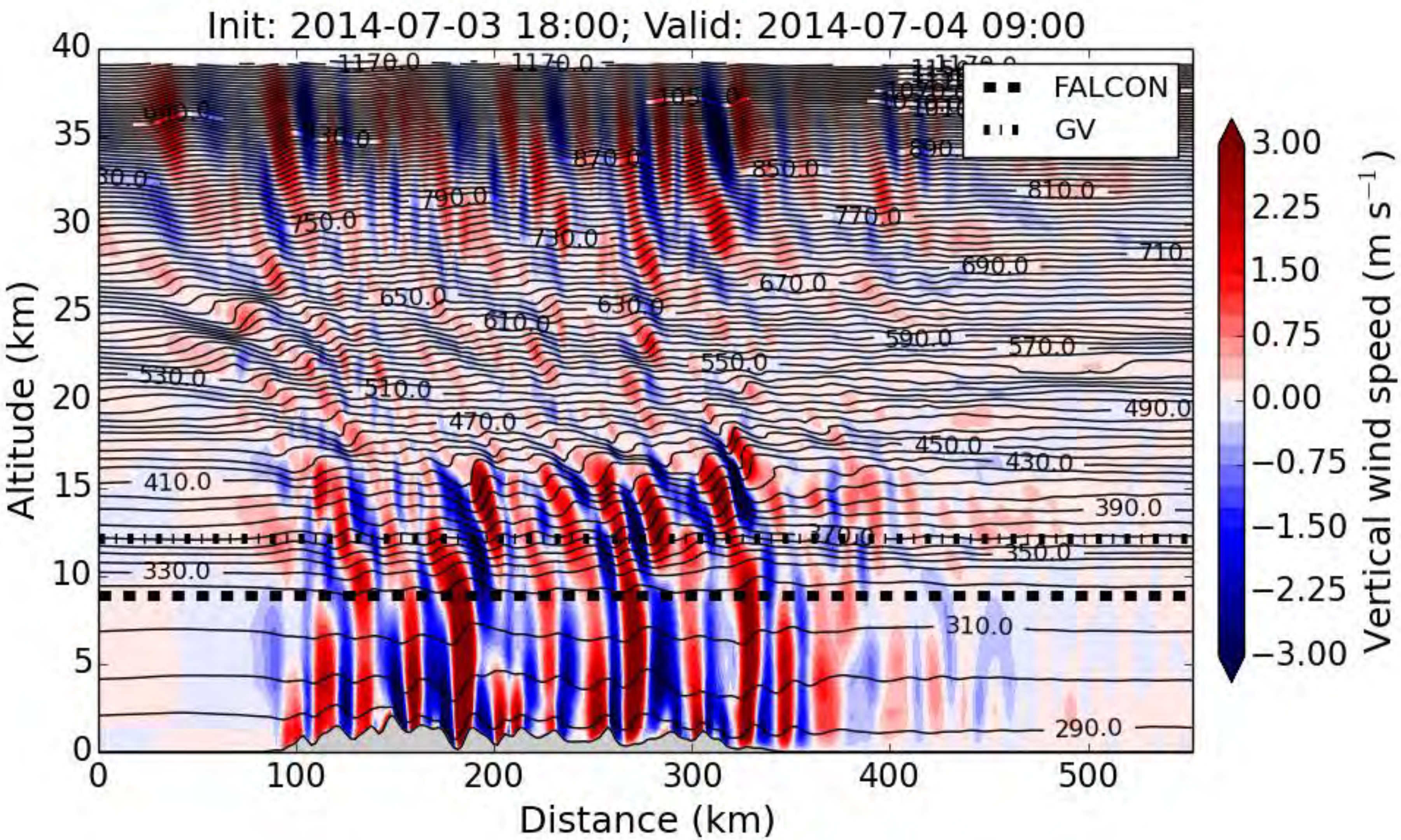

Johannes Wagner, DLR

4. From the Stratosphere to the Mesosphere
Ground-based Lidar observations

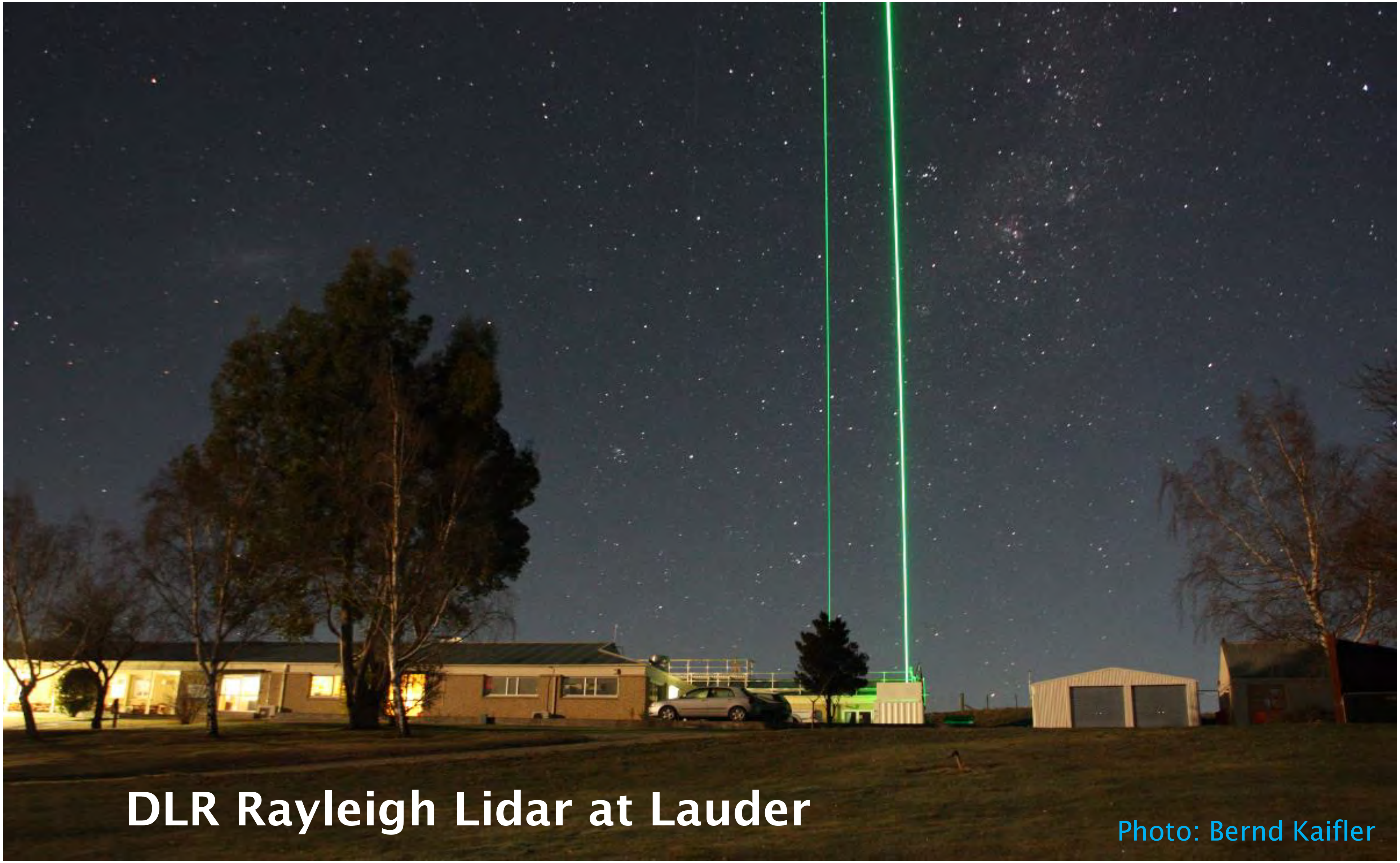

DLR Rayleigh Lidar at Lauder

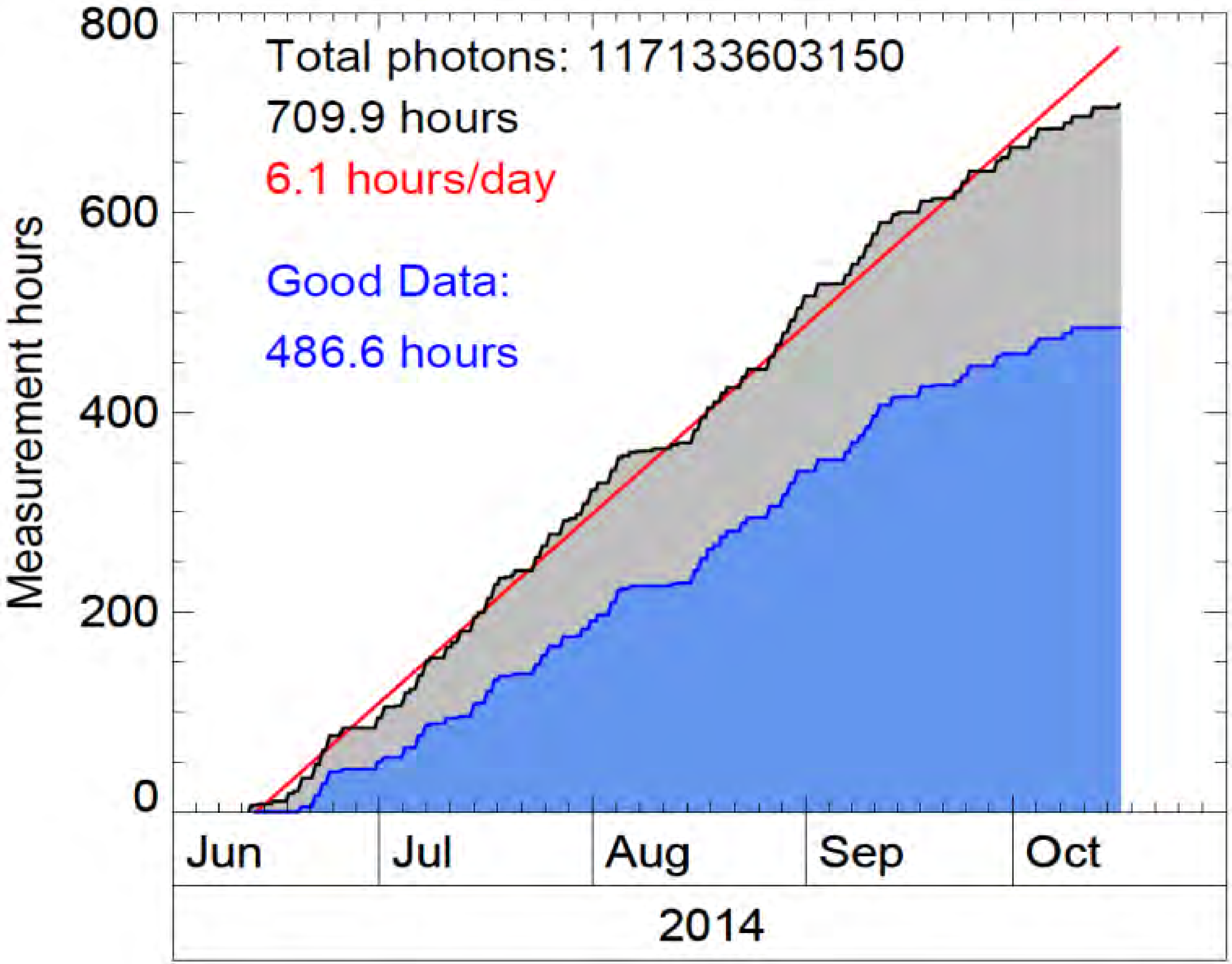

Resolutions

Raw profiles

$\Delta z = 10$ m
$\Delta t = 10$ ms

Bernd & Natalie Kaifler,
Benedikt Ehard, DLR

Rayleigh lidar and radiosonde daily mean temperature at Lauder, NZ

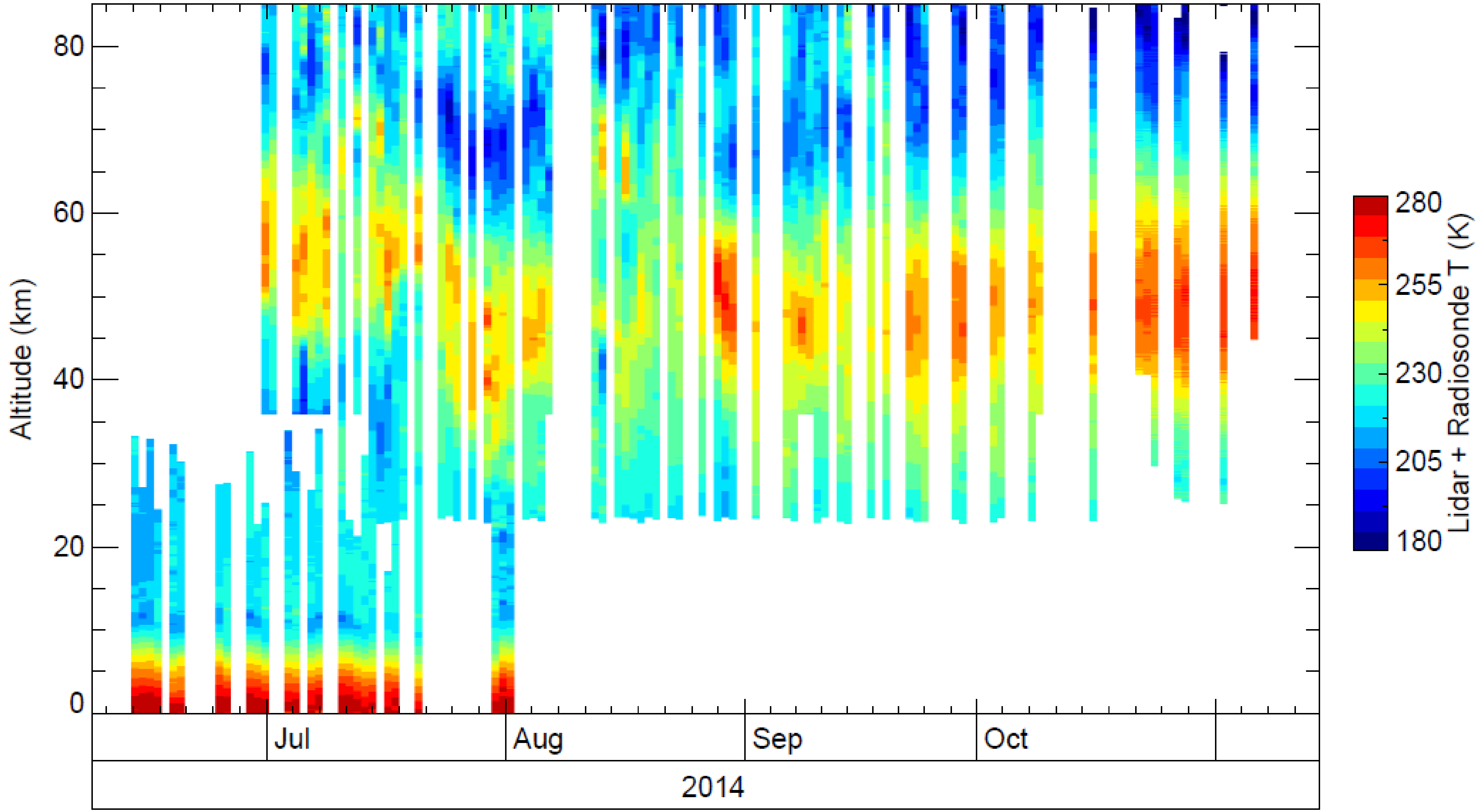

Bernd & Natalie Kaifler,
Benedikt Ehard, DLR

Questions

- How can we detect mountain waves in lidar data?
- What conditions are needed for deep gravity wave propagation?

Derivation of T' and E_p from temperature profiles

Temperature T

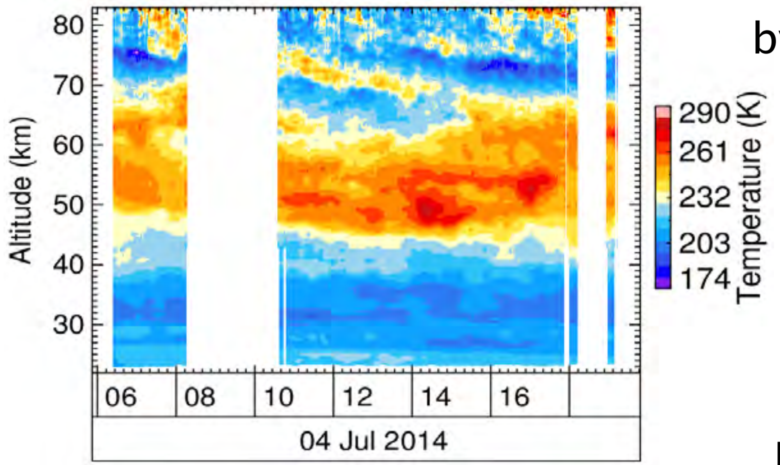

Removal of background temperature T_0 by polynomial fitting method

Temperature perturbation T'

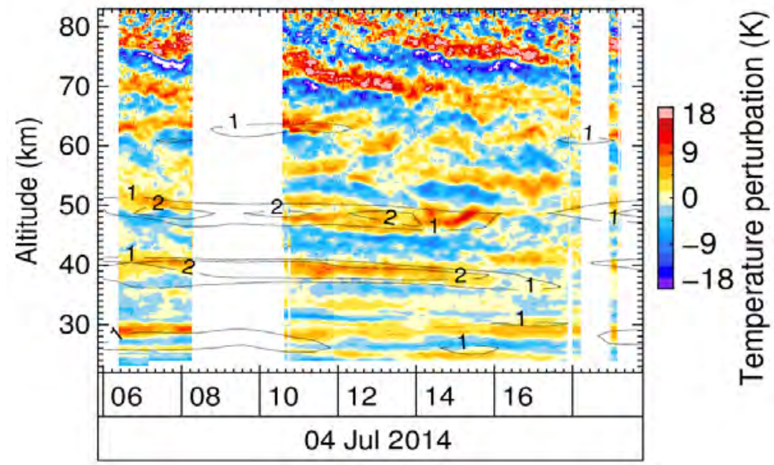

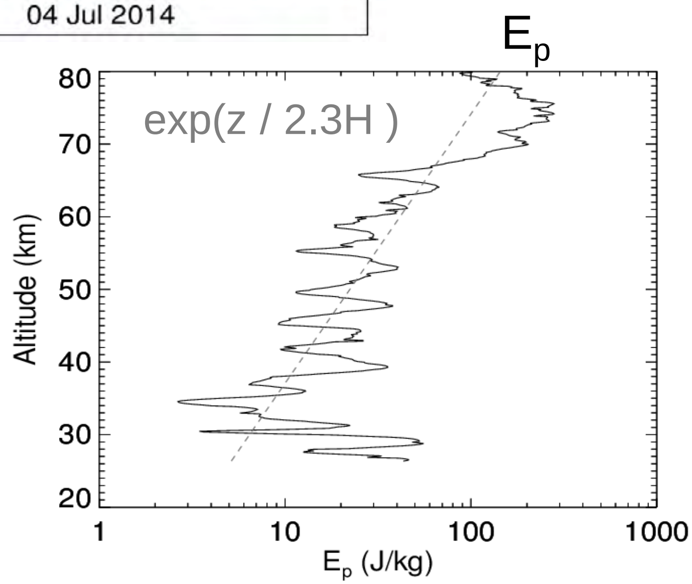

Gravity wave potential energy density:

$$E_p(z) = \frac{1}{2}\frac{g^2}{N^2(z,t)}\overline{\left(\frac{T'(z,t)}{T_0(z,t)}\right)^2}$$

Bernd & Natalie Kaifler, Benedikt Ehard, DLR

Gravity wave potential energy density

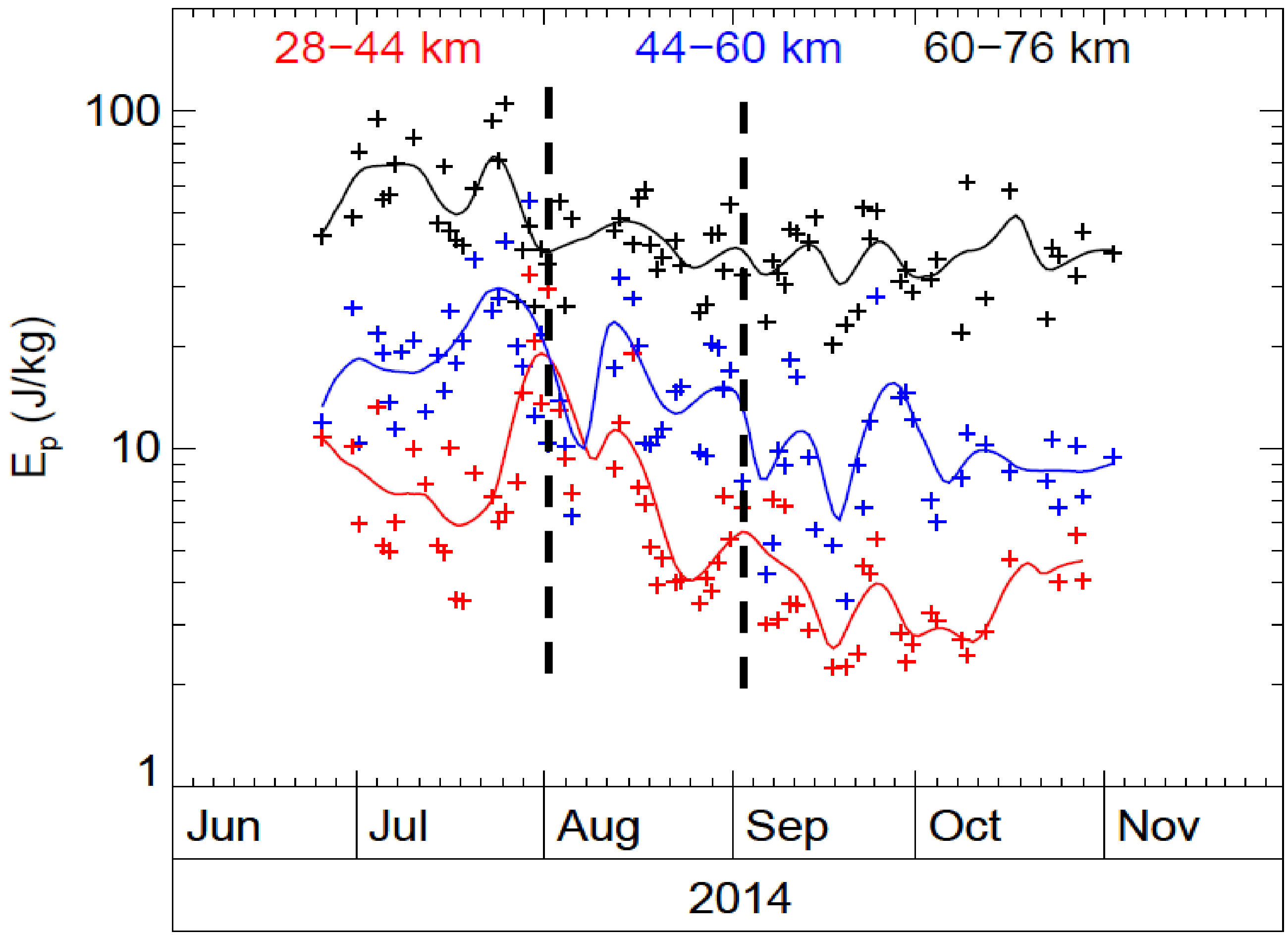

large variability

modulation with a period of 1-3 weeks

no „deep propagation“ of large-amplitude mountain waves

Bernd & Natalie Kaifler,
Benedikt Ehard, DLR

Mountain Waves on 1 August 2014
(GB21)

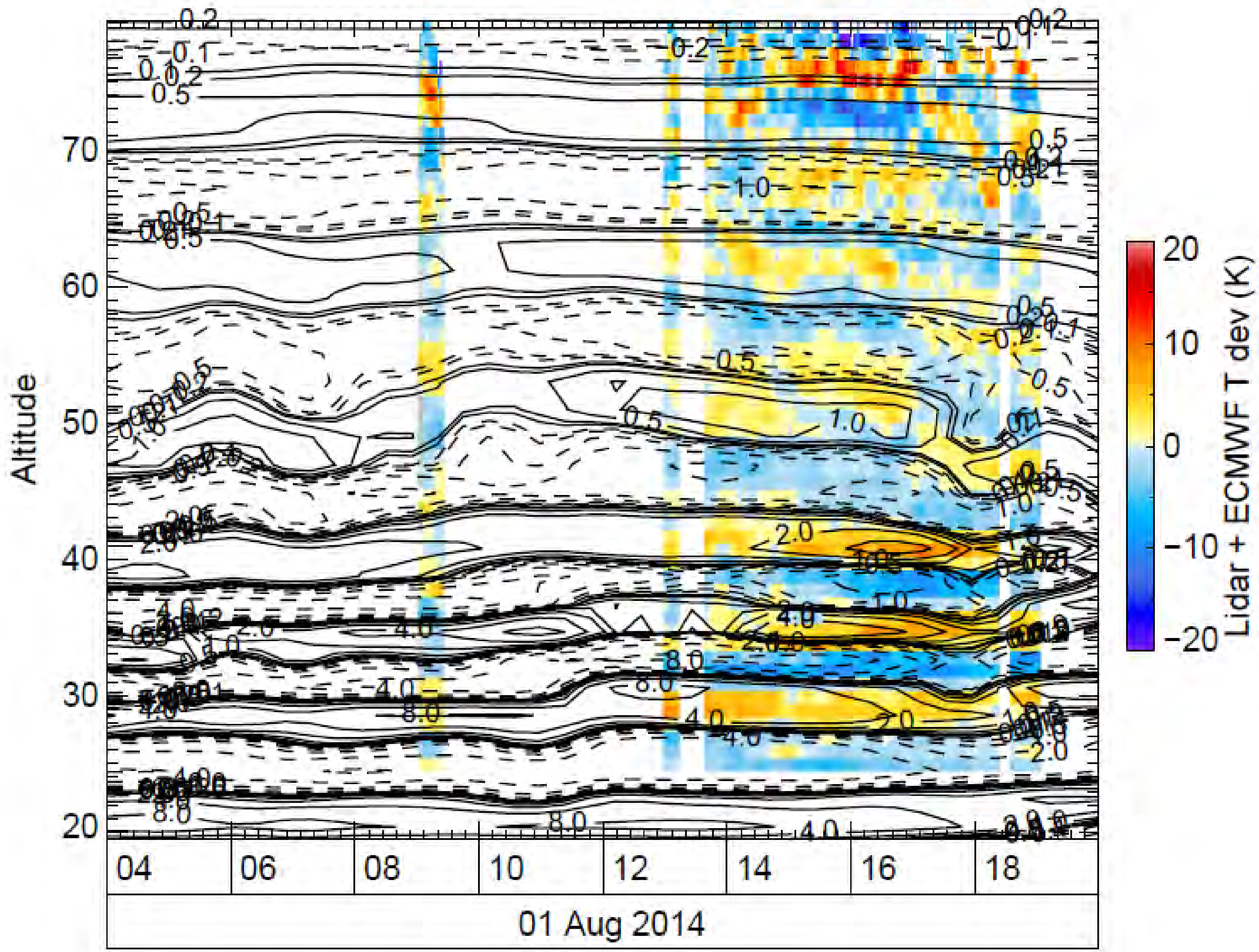

Bernd & Natalie Kaifler,
Benedikt Ehard, DLR

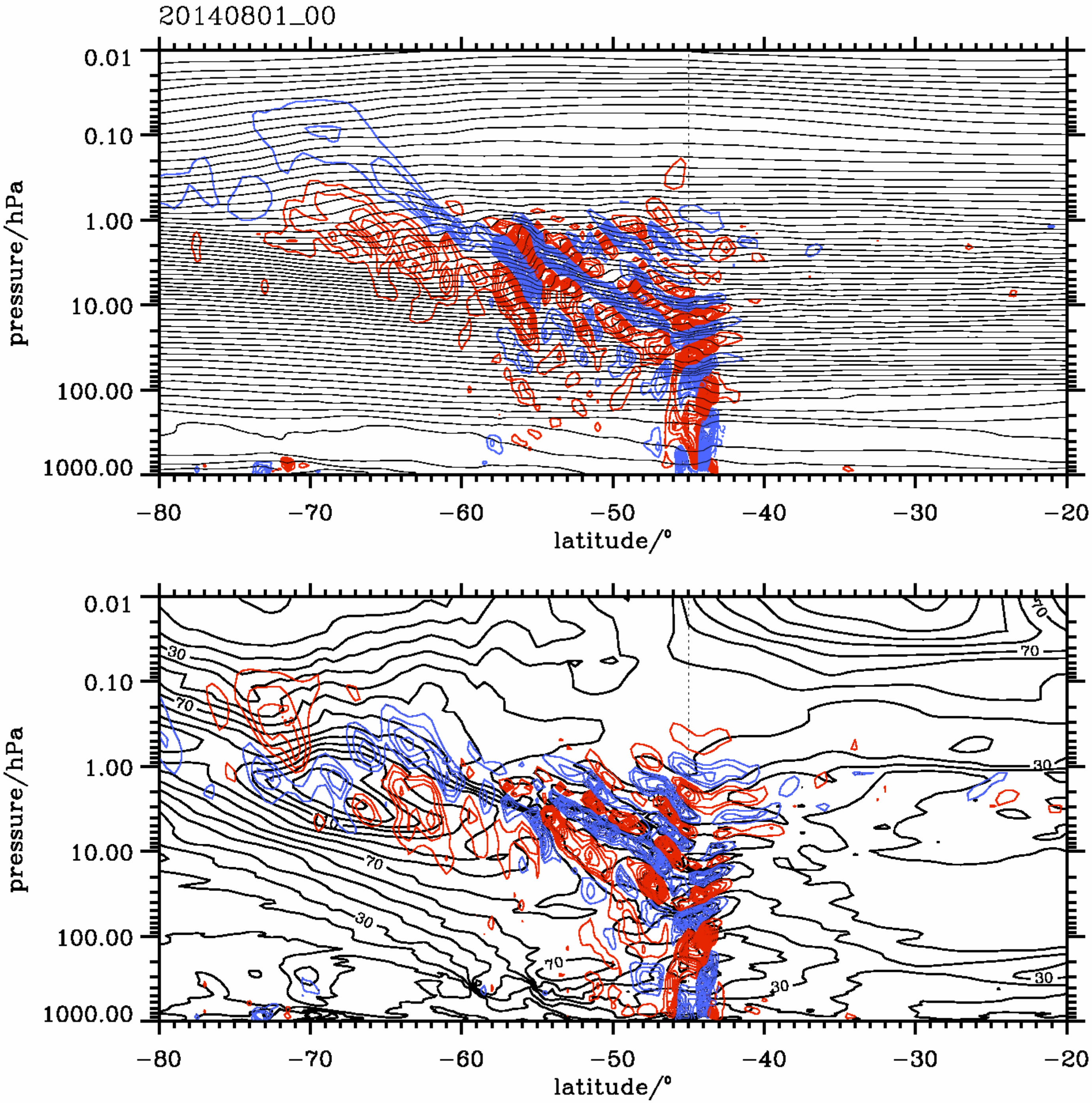

20140801_00
0.01
0.10
1.00
10.00
100.00
1000.00
pressure/hPa
−80
−70
−60
−50
−40
−30
−20
latitude/°
30
70
30
70
30
70
30
30
30
70

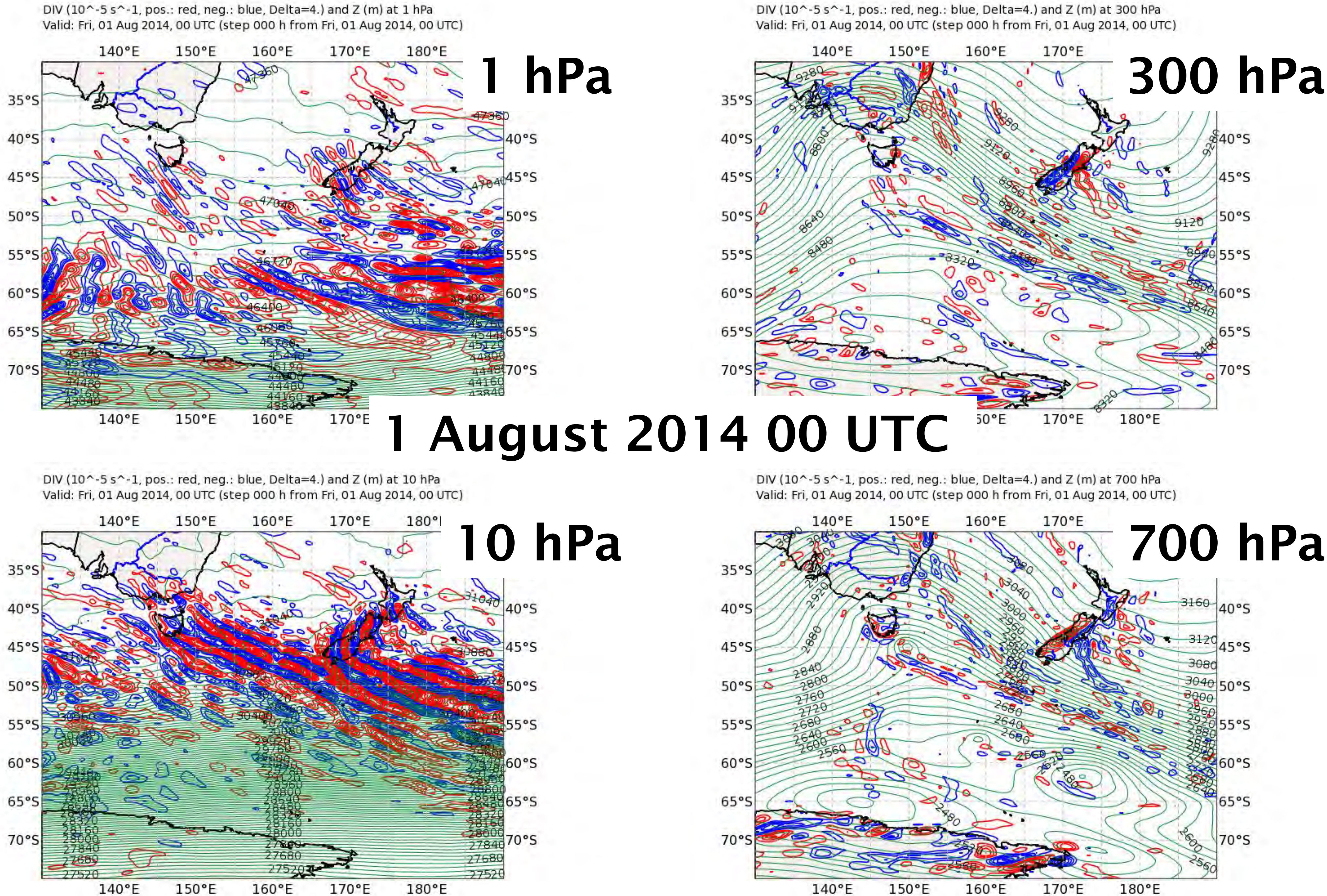

DIV (10^-5 s^-1, pos.: red, neg.: blue, Delta=4.) and Z (m) at 1 hPa
Valid: Fri, 01 Aug 2014, 00 UTC (step 000 h from Fri, 01 Aug 2014, 00 UTC)
1 hPa
DIV (10^-5 s^-1, pos.: red, neg.: blue, Delta=4.) and Z (m) at 300 hPa
Valid: Fri, 01 Aug 2014, 00 UTC (step 000 h from Fri, 01 Aug 2014, 00 UTC)
300 hPa
1 August 2014 00 UTC
DIV (10^-5 s^-1, pos.: red, neg.: blue, Delta=4.) and Z (m) at 10 hPa
Valid: Fri, 01 Aug 2014, 00 UTC (step 000 h from Fri, 01 Aug 2014, 00 UTC)
10 hPa
DIV (10^-5 s^-1, pos.: red, neg.: blue, Delta=4.) and Z (m) at 700 hPa
Valid: Fri, 01 Aug 2014, 00 UTC (step 000 h from Fri, 01 Aug 2014, 00 UTC)
700 hPa

Mountain Waves on 1 August 2014 (GB21)

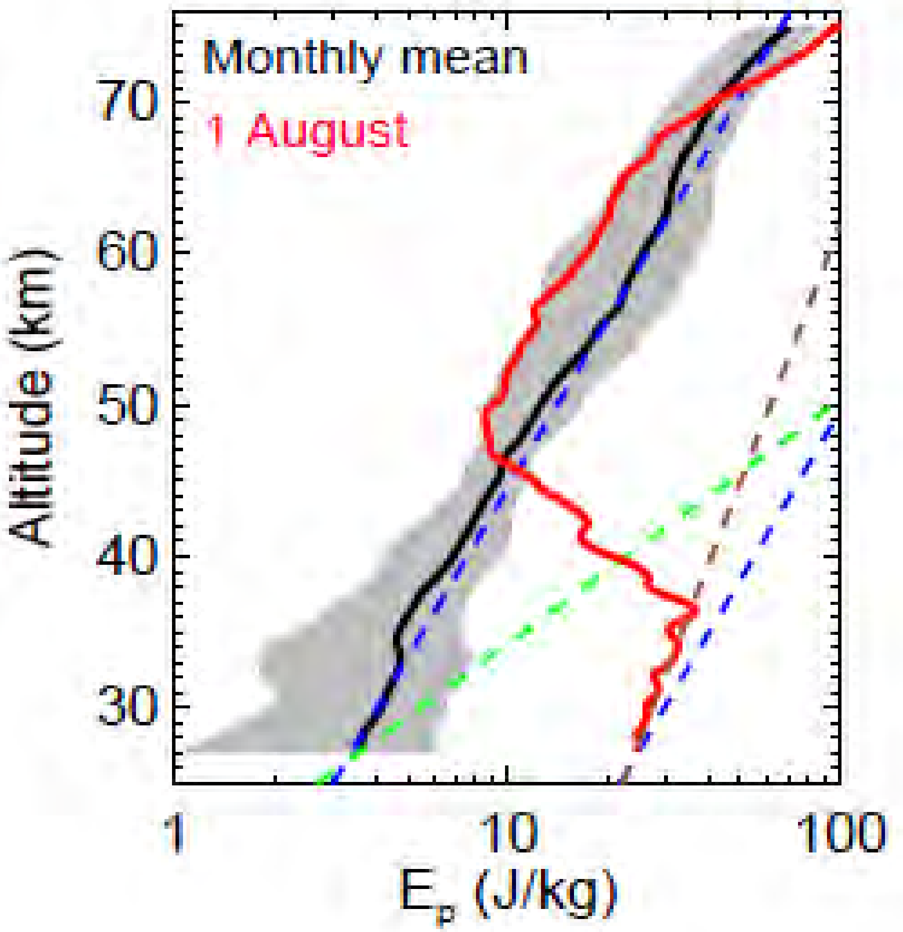

- High tropospheric wind speed
- Enhanced stratospheric E_p
- Stationary waves with short vertical wavelength (~ 6 km)

Bernd & Natalie Kaifler,
Benedikt Ehard, DLR

Mountain Waves on 1 August 2014 (GB21)

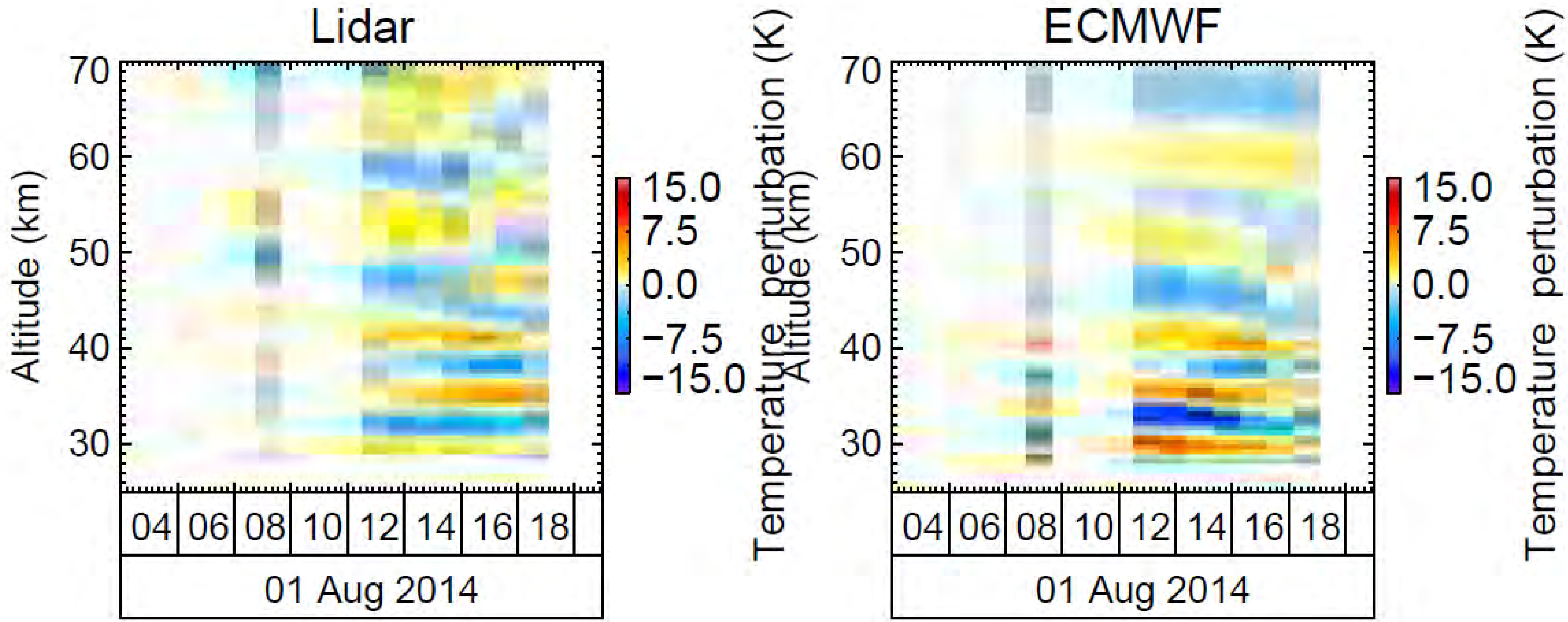

Benedikt Ehard, DLR

Mountain Waves on 1 August 2014
(GB21)

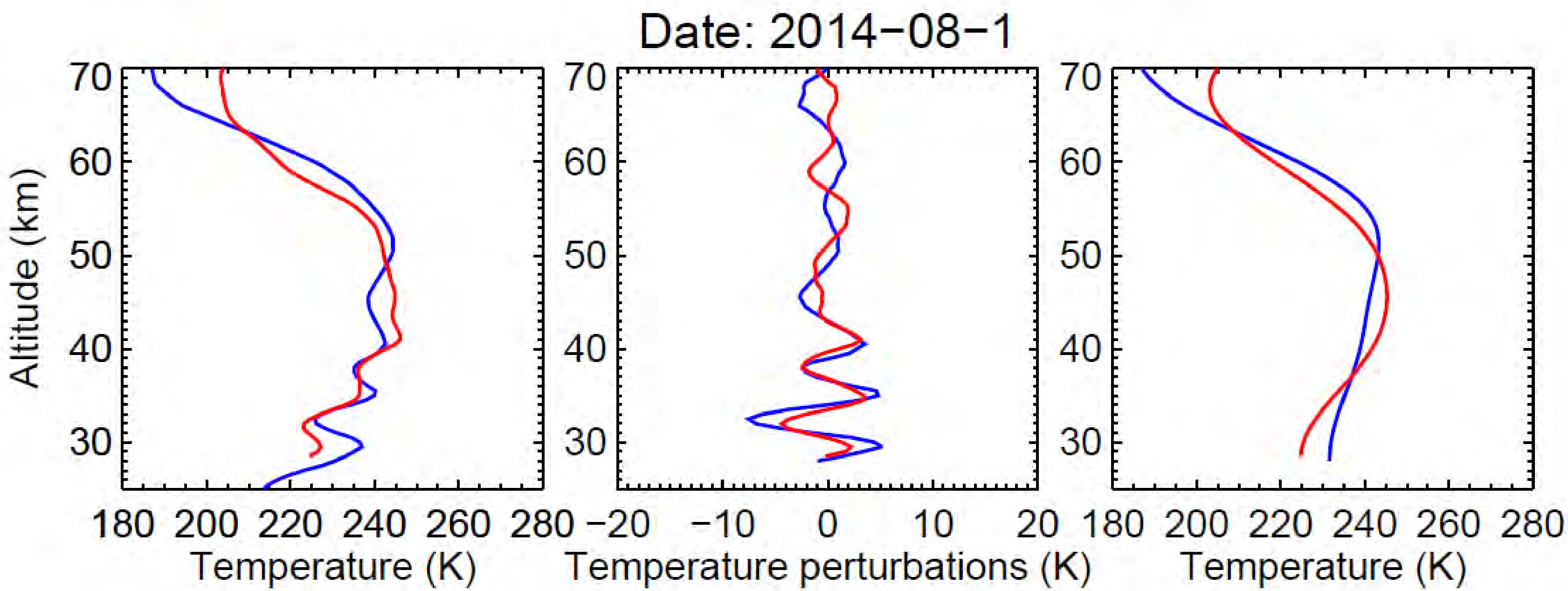

Daily mean Temperature

Background Temperature

LIDAR **ECMWF**

Benedikt Ehard, DLR

Mountain Waves on 1 August 2014
(GB21)

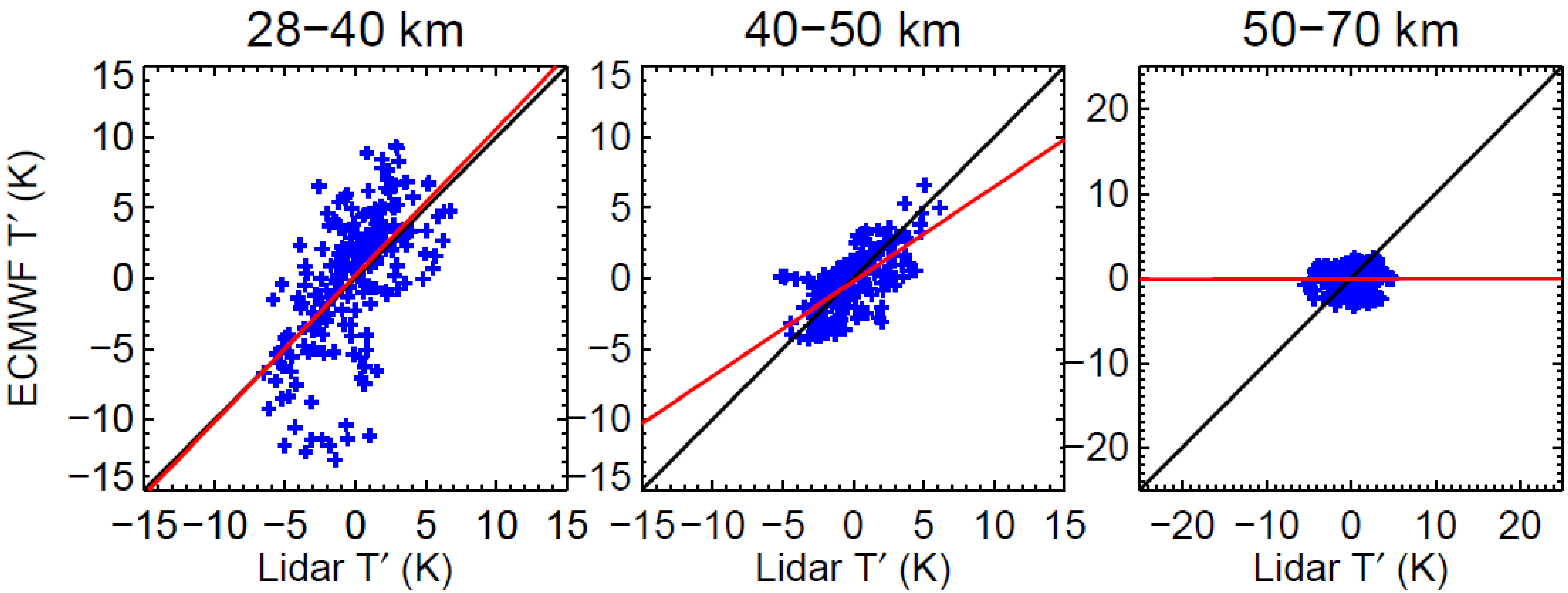

y = 1.038x +0.207
r = 0.604

y = 0.671x −0.226
r = 0.688

y = 0.001x −0.077
r = 0.001

Benedikt Ehard, DLR

Mountain Waves (?) on 4 July 2014
(IOP 10)

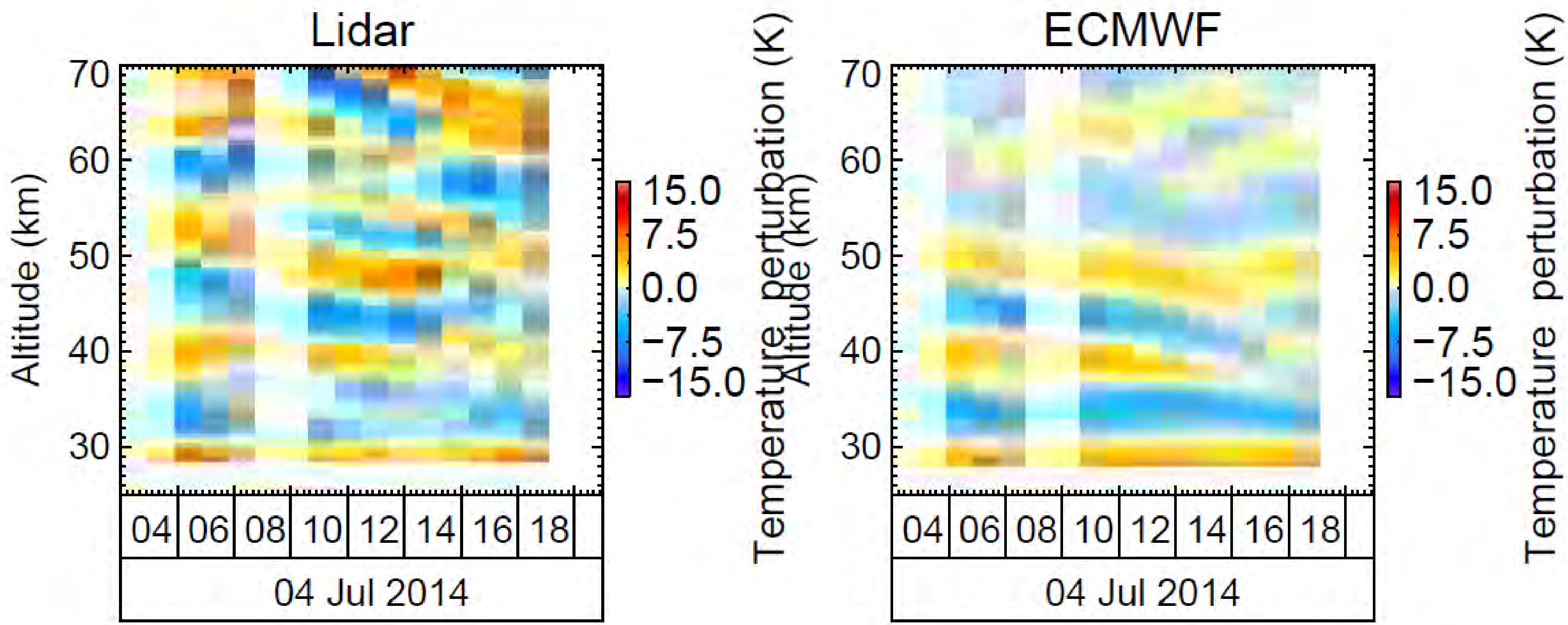

Benedikt Ehard, DLR

Mountain Waves (?) on 4 July 2014
(IOP 10)

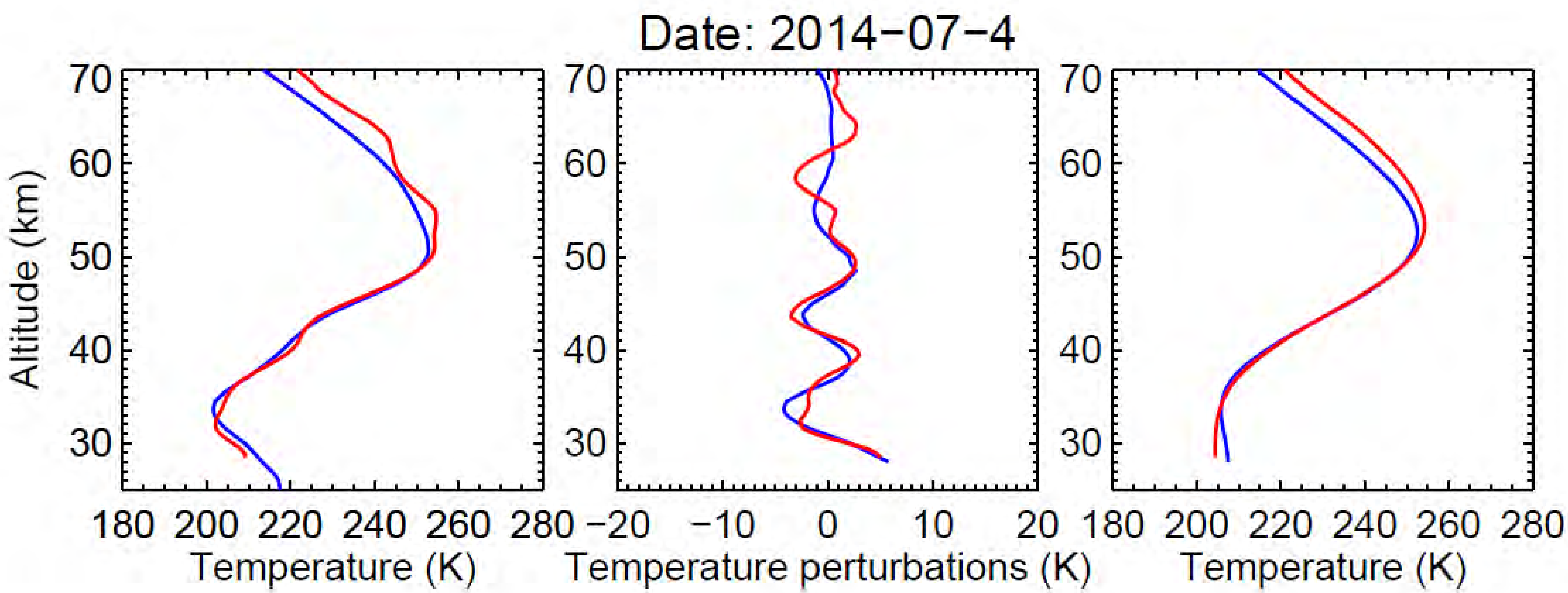

Daily mean Temperature **Background Temperature**

LIDAR **ECMWF**

Benedikt Ehard, DLR

Mountain Waves (?) on 4 July 2014
(IOP 10)

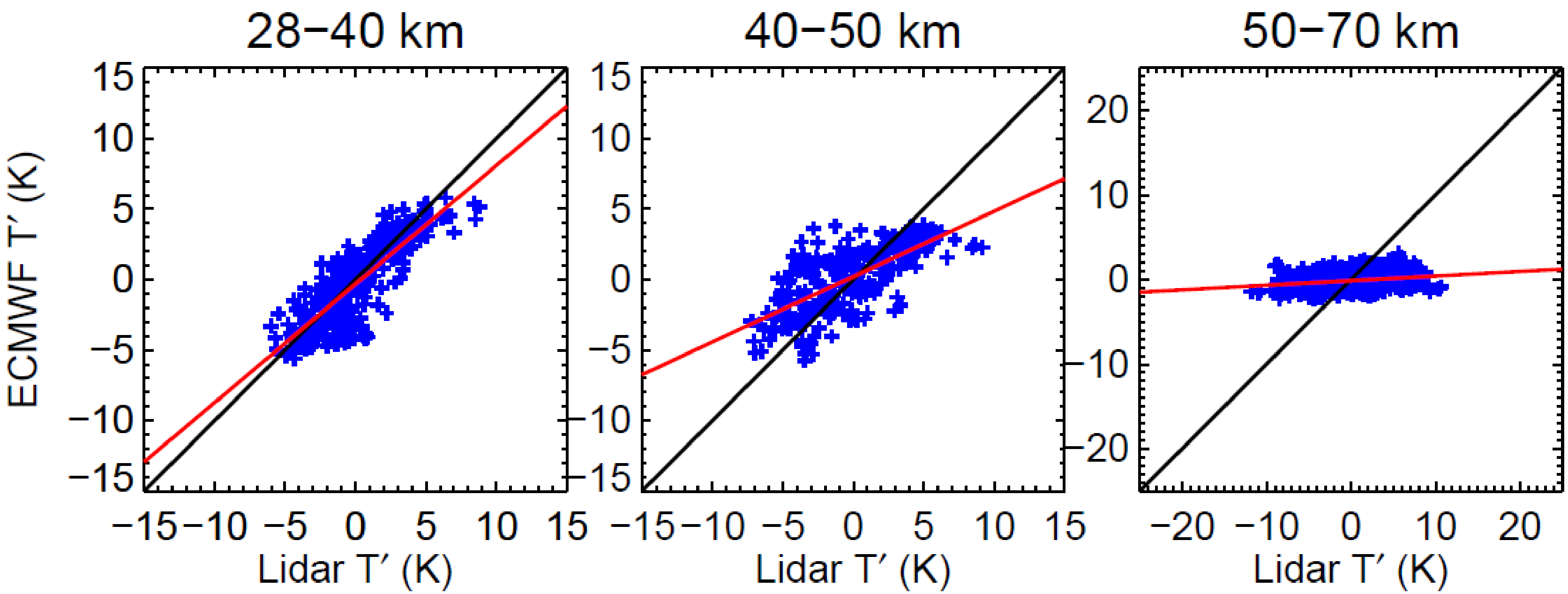

y = 0.840x −0.317
r = 0.820

y = 0.463x +0.210
r = 0.711

y = 0.055x −0.124
r = 0.224

Benedikt Ehard, DLR

Distinction between GW types using 2d wavelets (I)

Temperature perturbation (K)

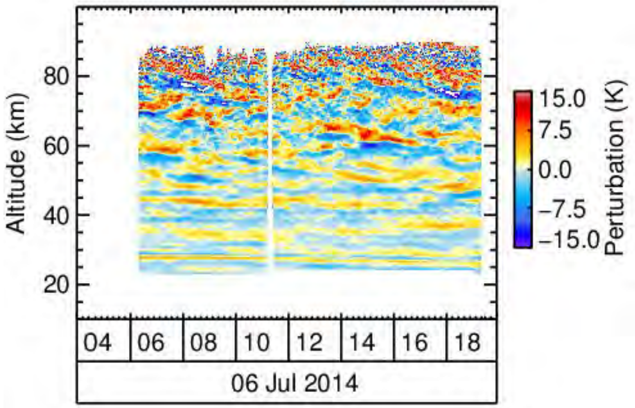

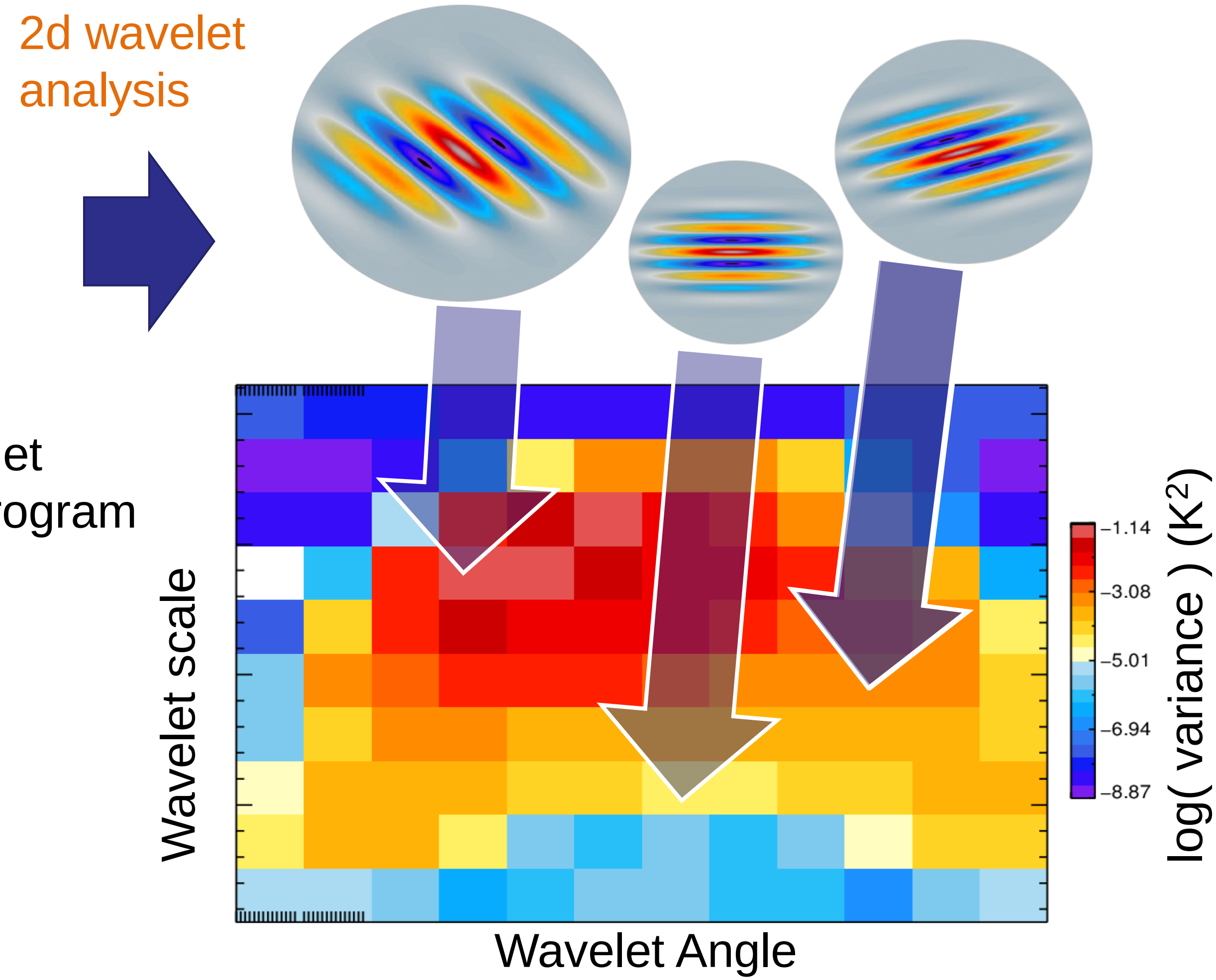

Kaifler, B., N. Kaifler, B. Ehard, A. Dörnbrack, M. Rapp, D. C. Fritts, 2015: Influences of source conditions on mountain wave penetration into the stratosphere and mesosphere, Geoph. Res. Letters, submitted

Distinction between GW types using 2d wavelets (I)

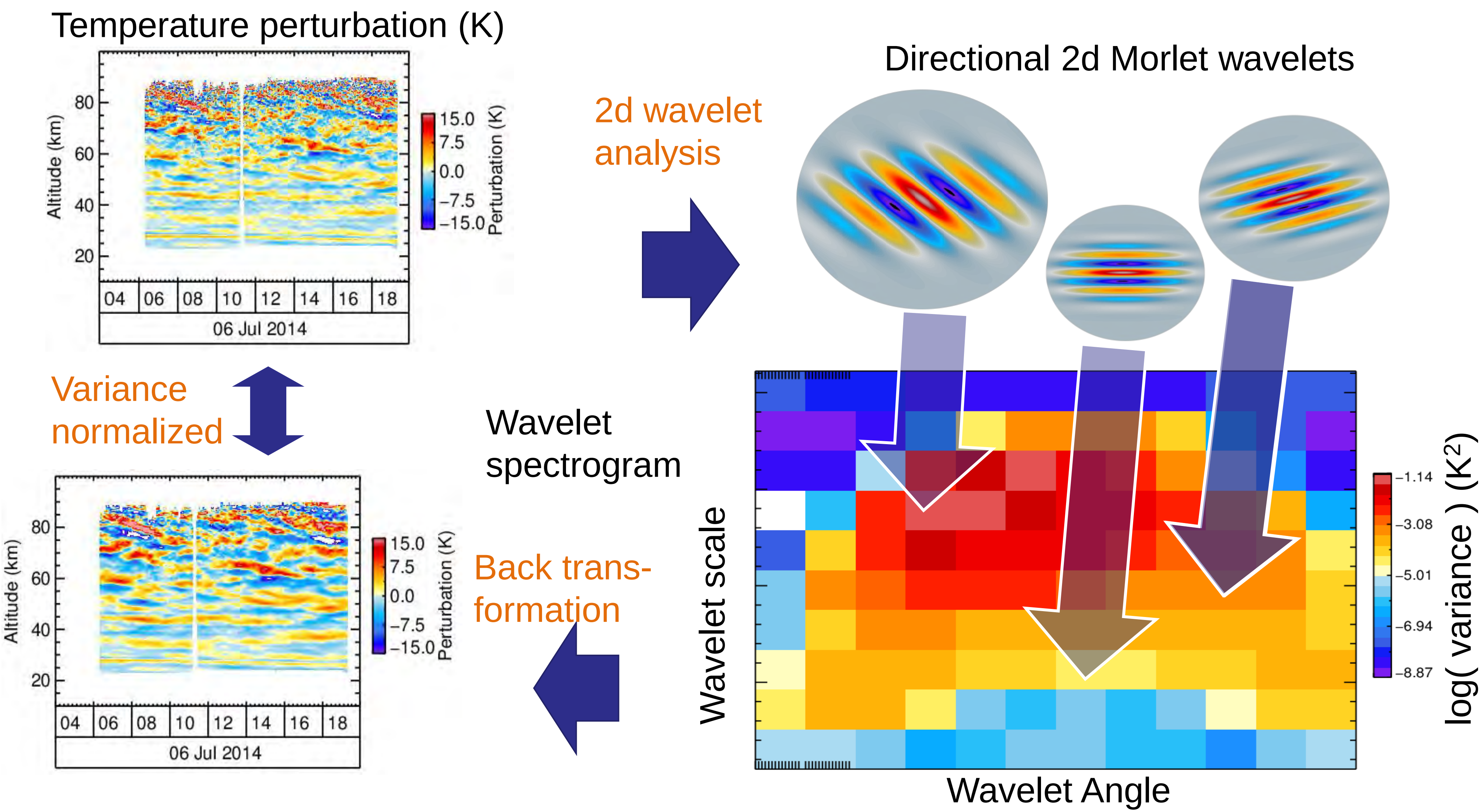

Kaifler, B., N. Kaifler, B. Ehard, A. Dörnbrack, M. Rapp, D. C. Fritts, 2015: Influences of source conditions on mountain wave penetration into the stratosphere and mesosphere, Geoph. Res. Letters, submitted

Distinction between GW types using 2d wavelets (II)

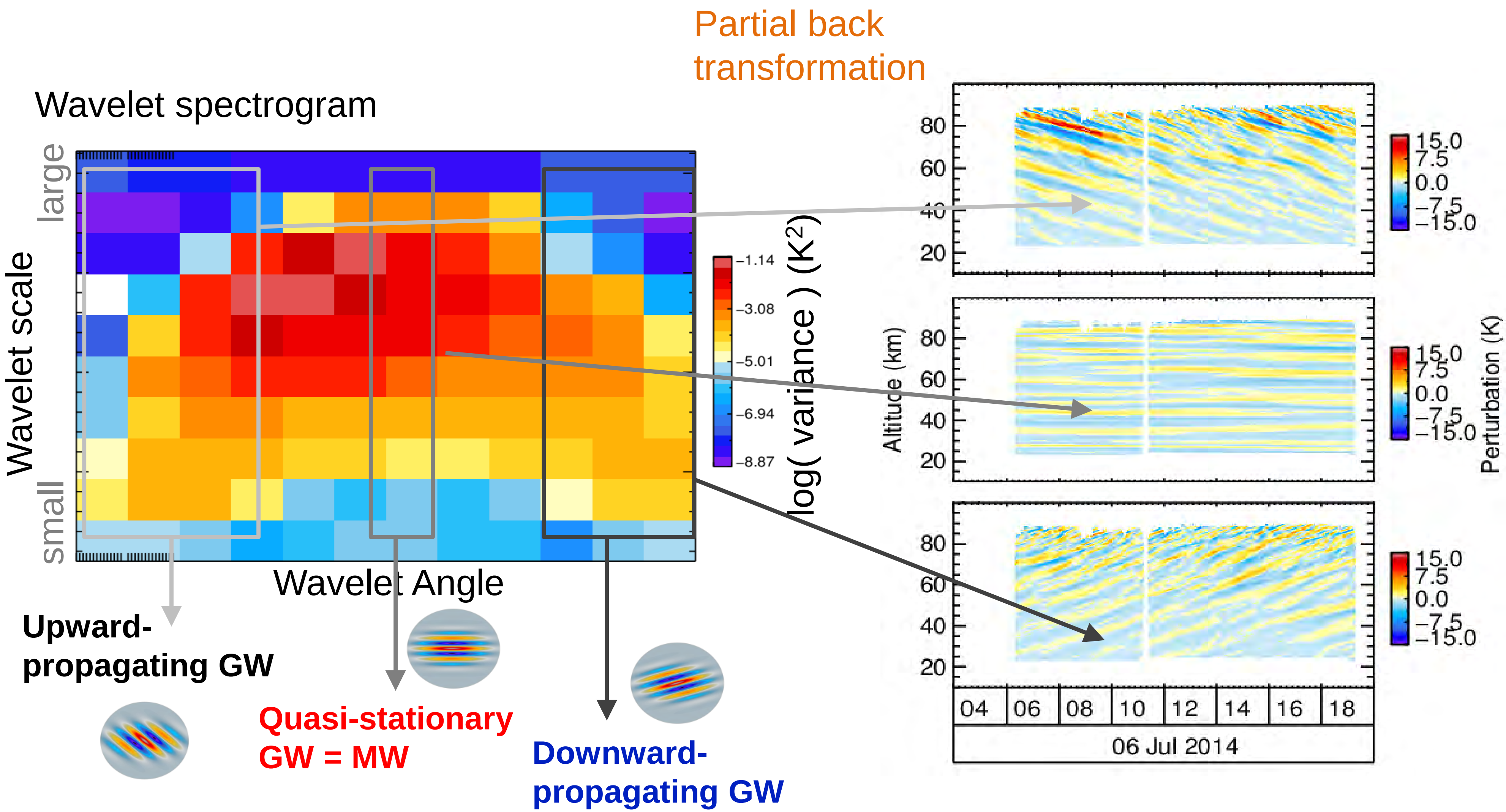

Kaifler, B., N. Kaifler, B. Ehard, A. Dörnbrack, M. Rapp, D. C. Fritts, 2015: Influences of source conditions on mountain wave penetration into the stratosphere and mesosphere, Geoph. Res. Letters, submitted

Distinction between GW types using 2d wavelets (III)

Upward-propagating GW

Quasi-stationary GW = MW

Downward-propagating GW

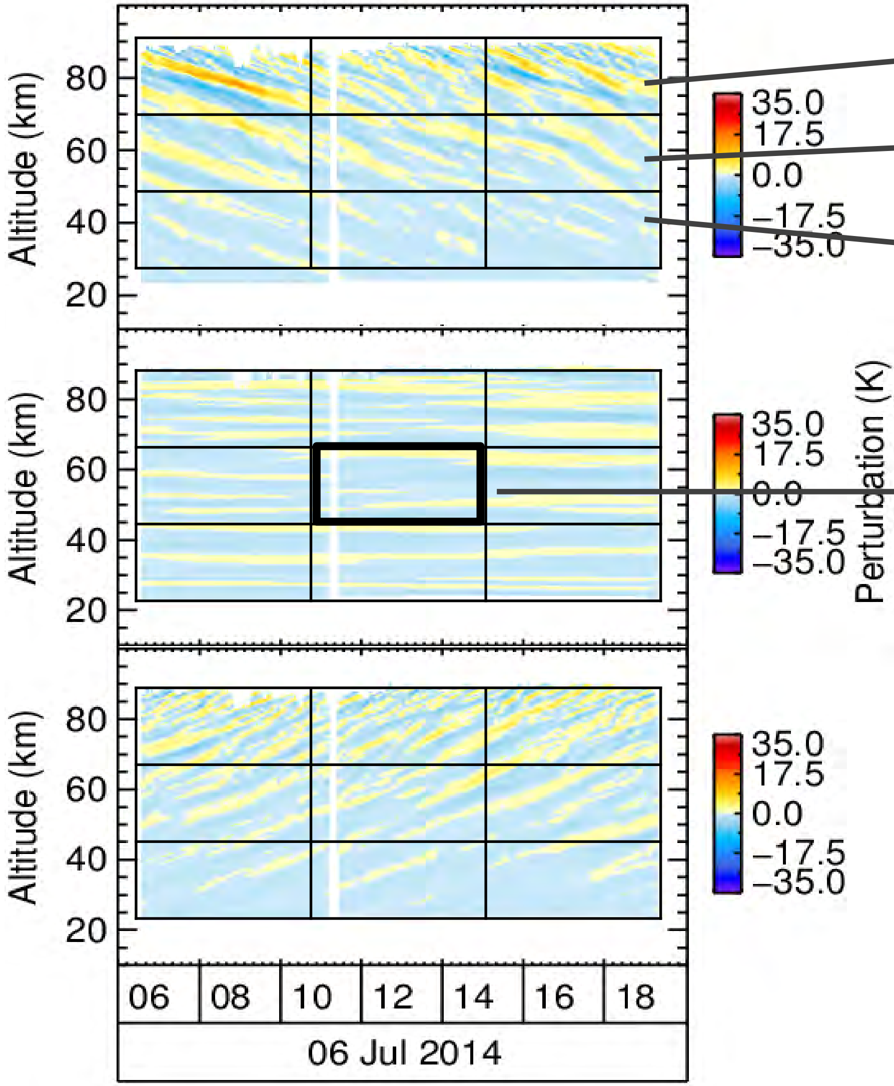

mesosphere

stratopause

stratosphere

E_p

Estimate of EP for
- MW, upward and downward propagating GW
- every 3 h
- 3 altitude ranges

Kaifler, B., N. Kaifler, B. Ehard, A. Dörnbrack, M. Rapp, D. C. Fritts, 2015: Influences of source conditions on mountain wave penetration into the stratosphere and mesosphere, Geoph. Res. Letters, submitted

Lauder GW statistics

Quasi-stationary GW = MW
Upward-propagating GW
Downward-propagating GW

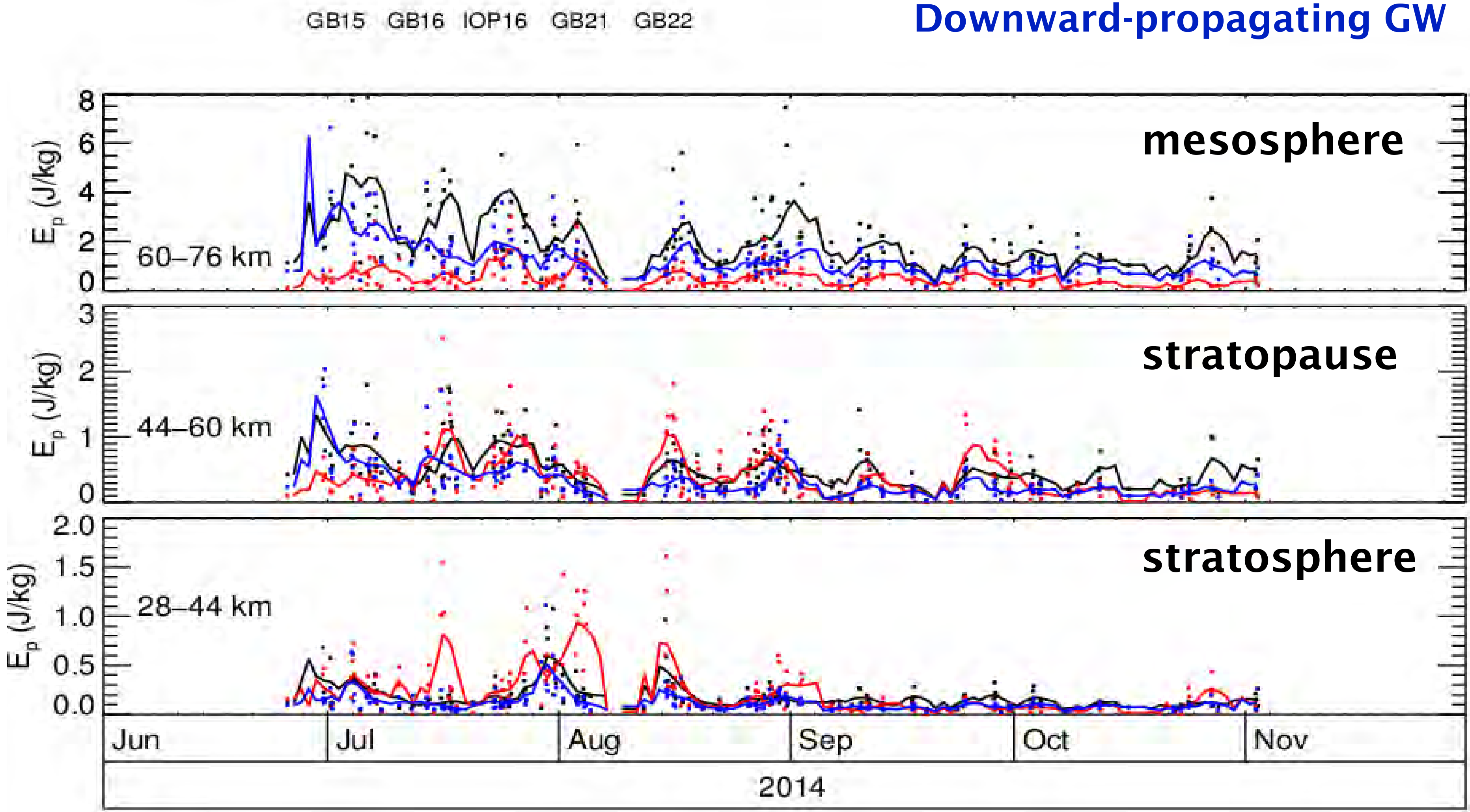

Kaifler, B., N. Kaifler, B. Ehard, A. Dörnbrack, M. Rapp, D. C. Fritts, 2015: Influences of source conditions on mountain wave penetration into the stratosphere and mesosphere, Geoph. Res. Letters, submitted

Correlation between stratospheric mountain wave E_p and tropospheric forcing

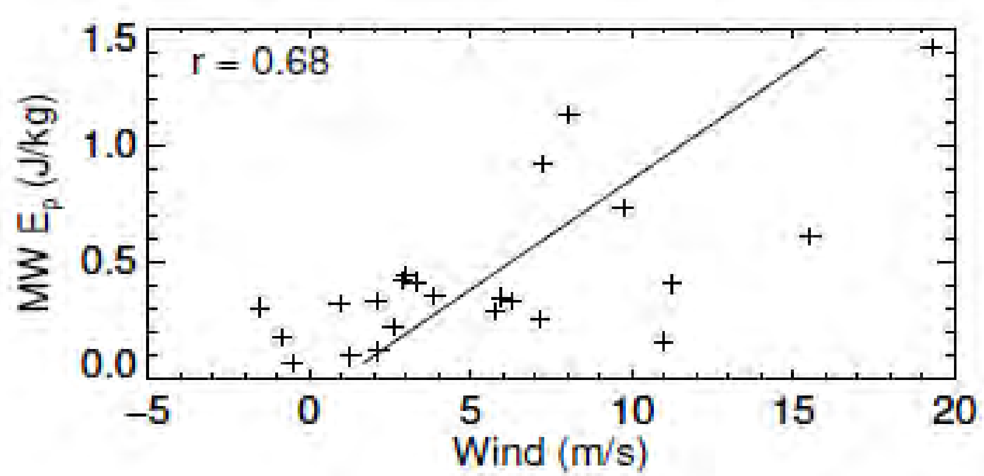

Cross-mountain flow at 1 km level

Simple relationship:

The stronger the forcing, the larger mountain waves energies in the stratosphere

Kaifler, B., N. Kaifler, B. Ehard, A. Dörnbrack, M. Rapp, D. C. Fritts, 2015: Influences of source conditions on mountain wave penetration into the stratosphere and mesosphere, Geoph. Res. Letters, submitted

Correlation between mesospheric mountain wave E_p and tropospheric forcing

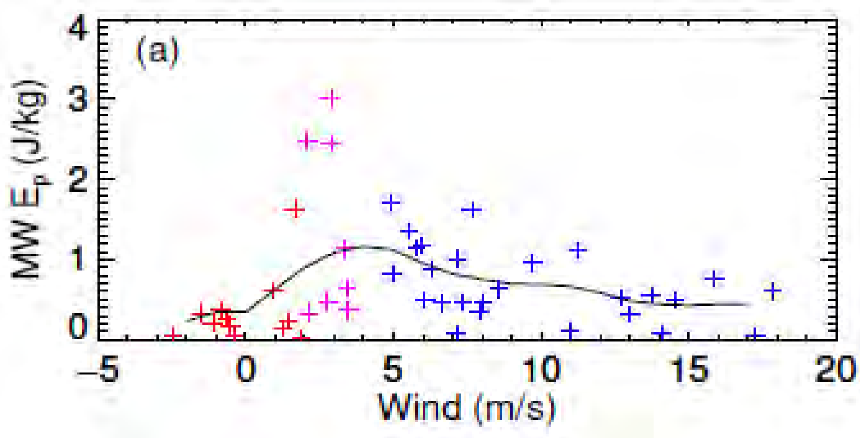

Cross-mountain flow at 1 km level

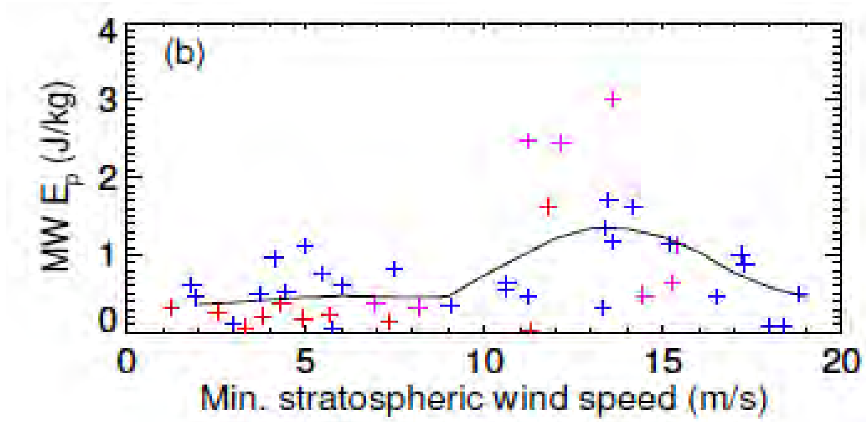

Cross-mountain flow 15-40 km

Deep MW propagation occurs under condition of

- **weak to moderate forcing** and
- **sufficiently stronger stratospheric winds**

Kaifler, B., N. Kaifler, B. Ehard, A. Dörnbrack, M. Rapp, D. C. Fritts, 2015: Influences of source conditions on mountain wave penetration into the stratosphere and mesosphere, Geoph. Res. Letters, submitted

5. Summary

- surprisingly good agreement of observed gravity waves with ECMWF‘s IFS

- deep vertical propagation of gravity waves depends critically on the magnitude of the stratospheric flow in an altitude range between 25 and 40 km

- large-amplitude mountain waves in the stratosphere during strong tropospheric forcing

- weak to moderate forcing and sufficiently stronger stratospheric winds needed for deep GW propagation

- other sources not yet considered in NWP models:

  - GW-tide interaction may be an efficient secondary source for GWs
  - non-orographic GWs excited by polar night jet

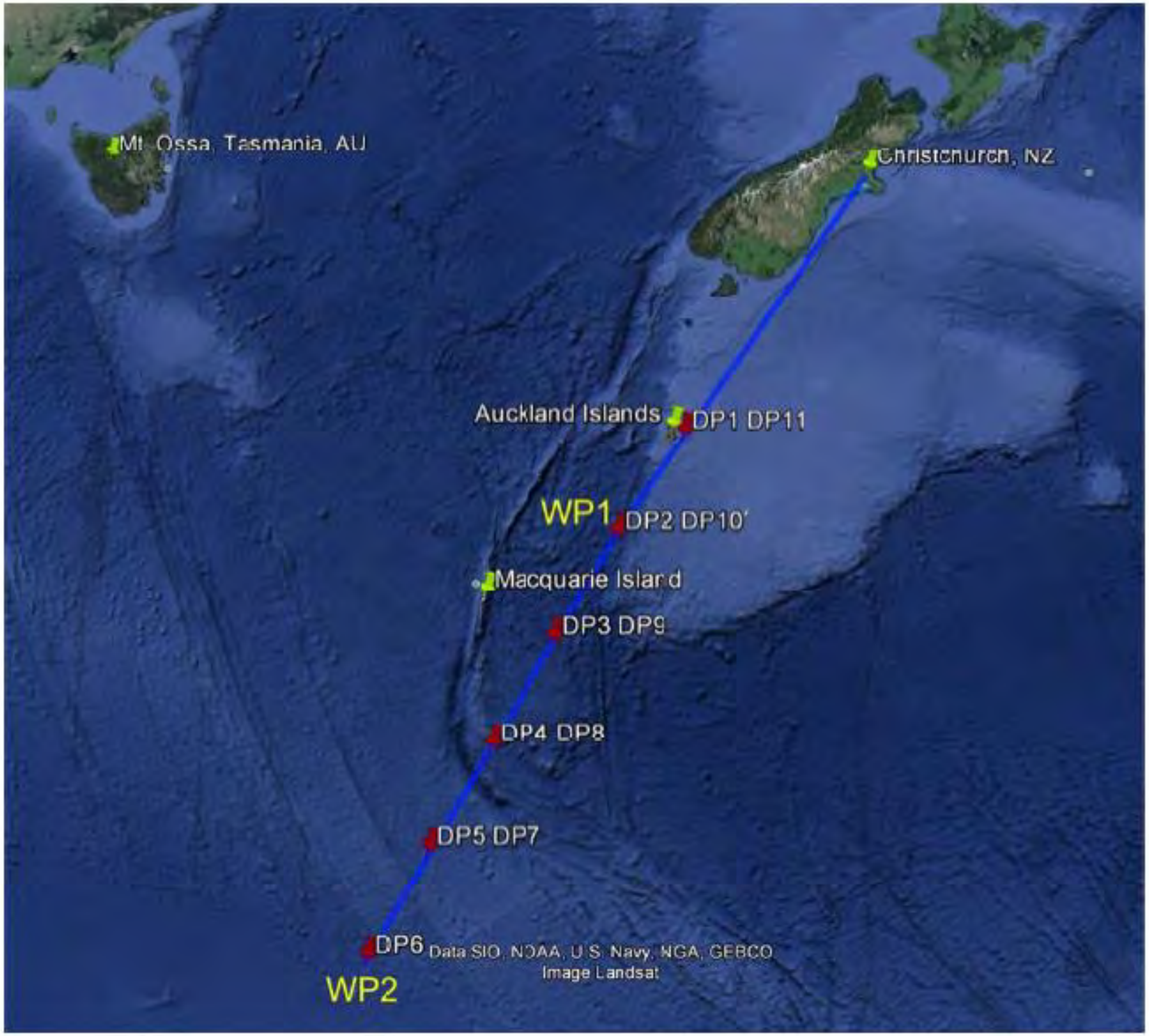
Mt. Ossa, Tasmania, AU
Christchurch, NZ
Auckland Islands
DP1 DP11
WP1
DP2 DP10
Macquarie Island
DP3 DP9
DP4 DP8
DP5 DP7
DP6
Data SIO, NOAA, U.S. Navy, NGA, GEBCO
Image Landsat
WP2

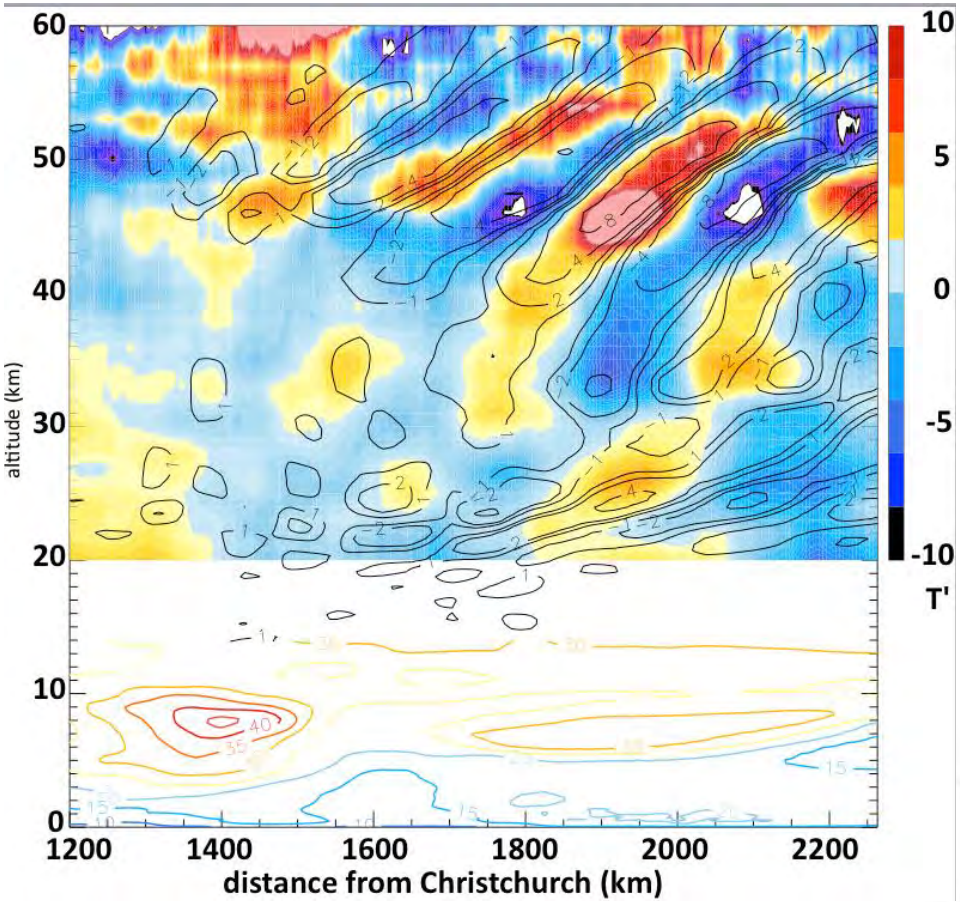

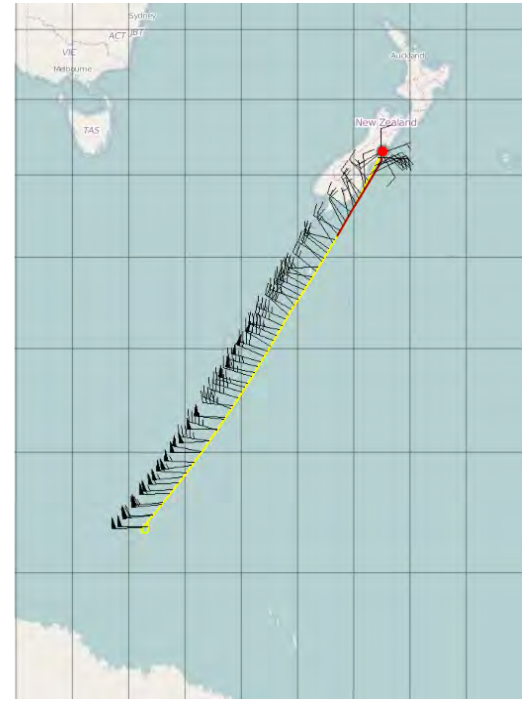

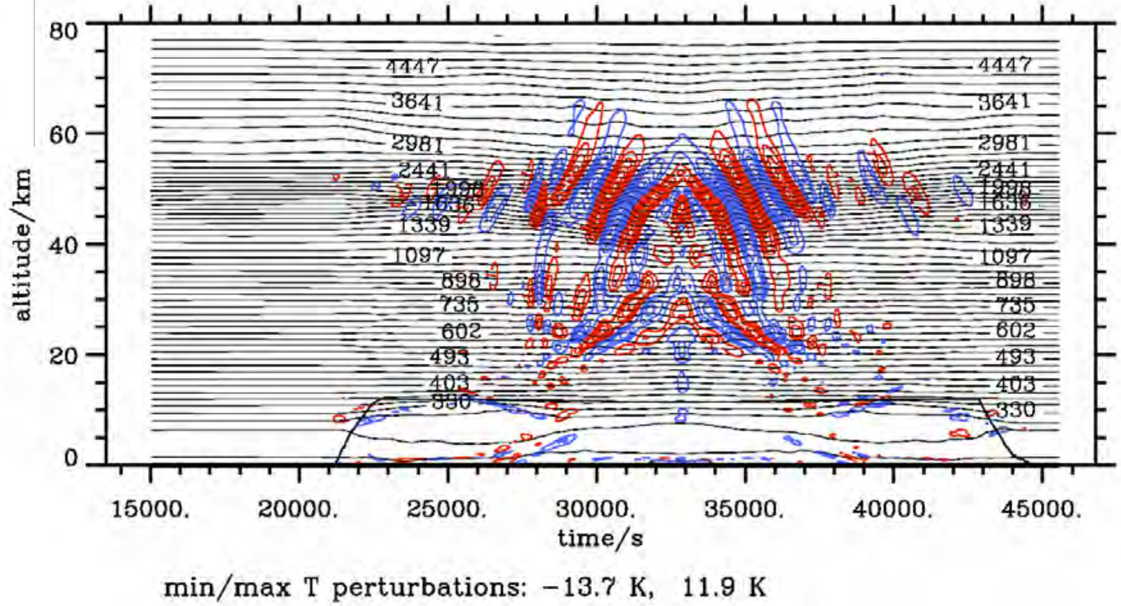

Biff Williams & Dave Fritts, GATS

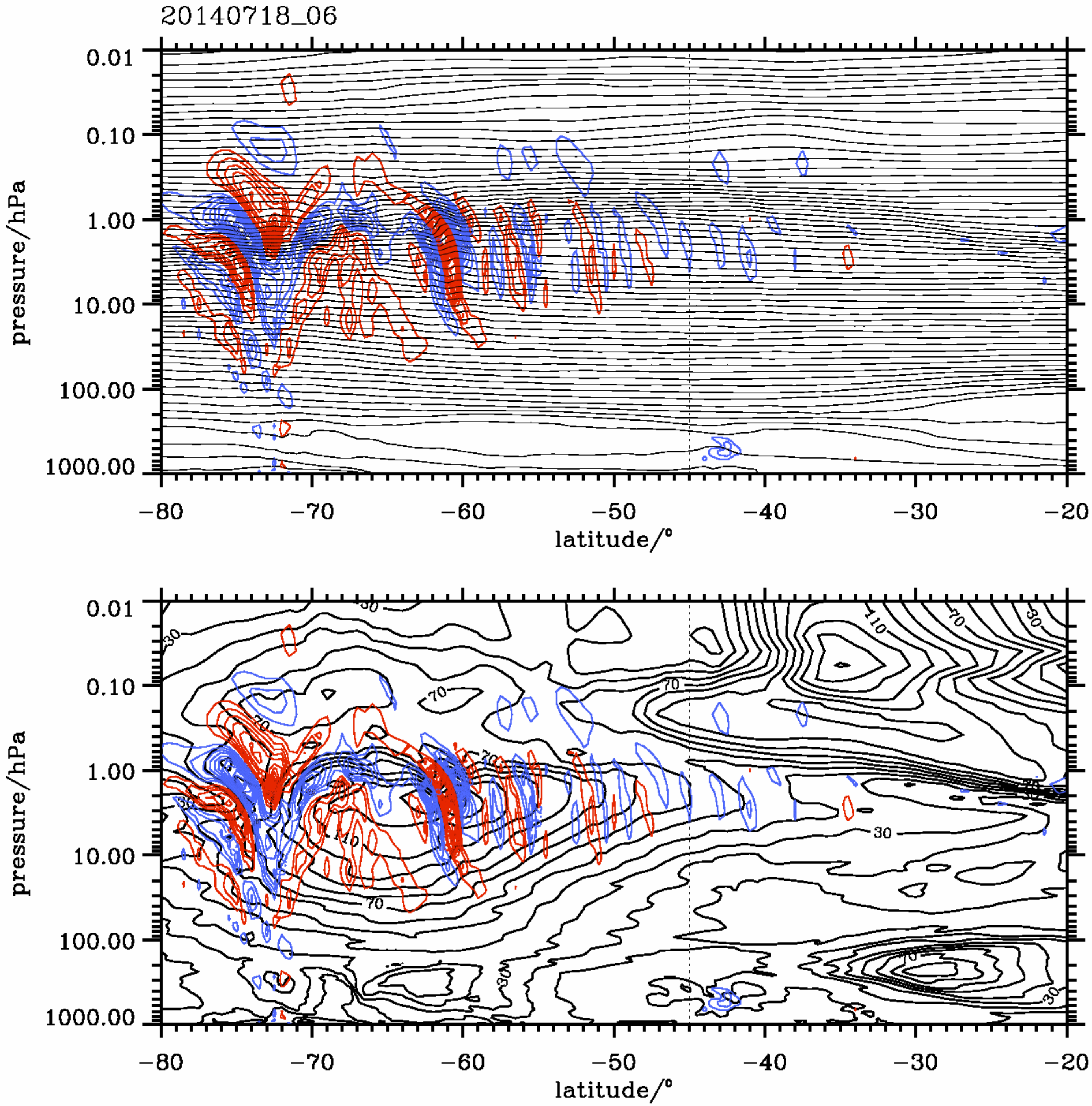
20140718_06
pressure/hPa
0.01
0.10
1.00
10.00
100.00
1000.00
−80
−70
−60
−50
−40
−30
−20
latitude/°
pressure/hPa
latitude/°

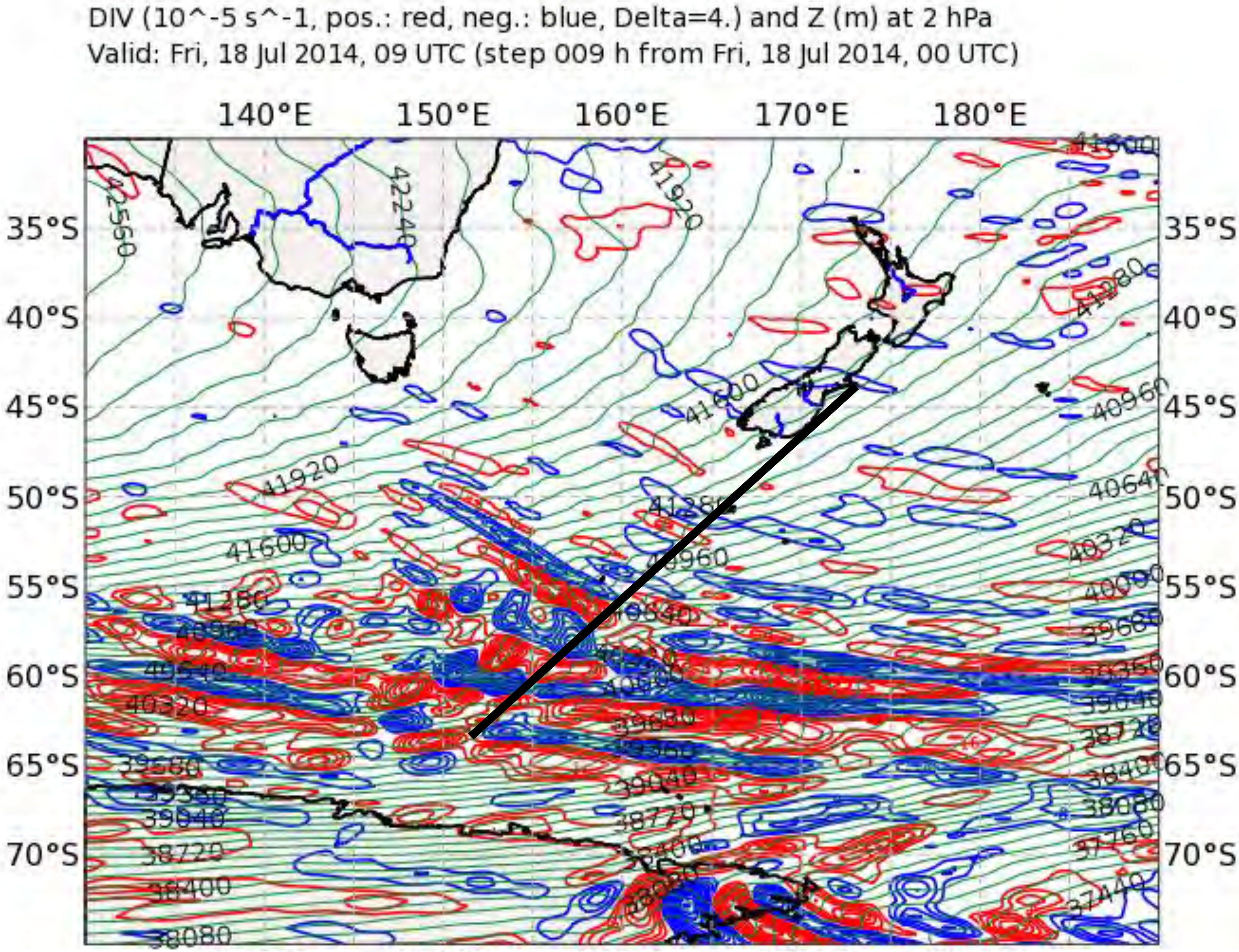
DIV (10^-5 s^-1, pos.: red, neg.: blue, Delta=4.) and Z (m) at 2 hPa
Valid: Fri, 18 Jul 2014, 09 UTC (step 009 h from Fri, 18 Jul 2014, 00 UTC)
140°E
150°E
160°E
170°E
180°E
35°S
40°S
45°S
50°S
55°S
60°S
65°S
70°S

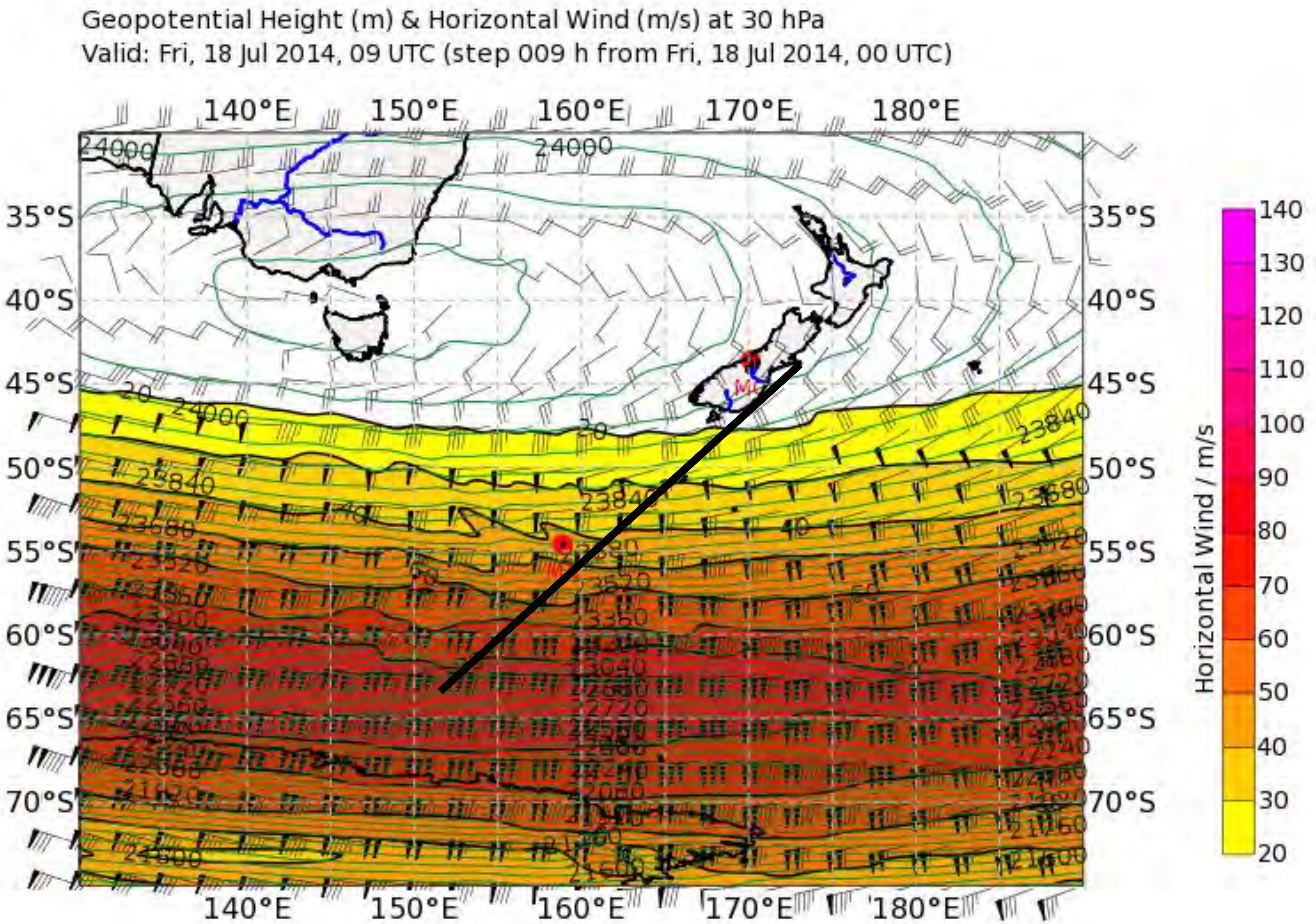
Geopotential Height (m) & Horizontal Wind (m/s) at 30 hPa
Valid: Fri, 18 Jul 2014, 09 UTC (step 009 h from Fri, 18 Jul 2014, 00 UTC)
140°E
150°E
160°E
170°E
180°E
35°S
40°S
45°S
50°S
55°S
60°S
65°S
70°S
24000
23840
23680
Horizontal Wind / m/s
140
130
120
110
100
90
80
70
60
50
40
30
20

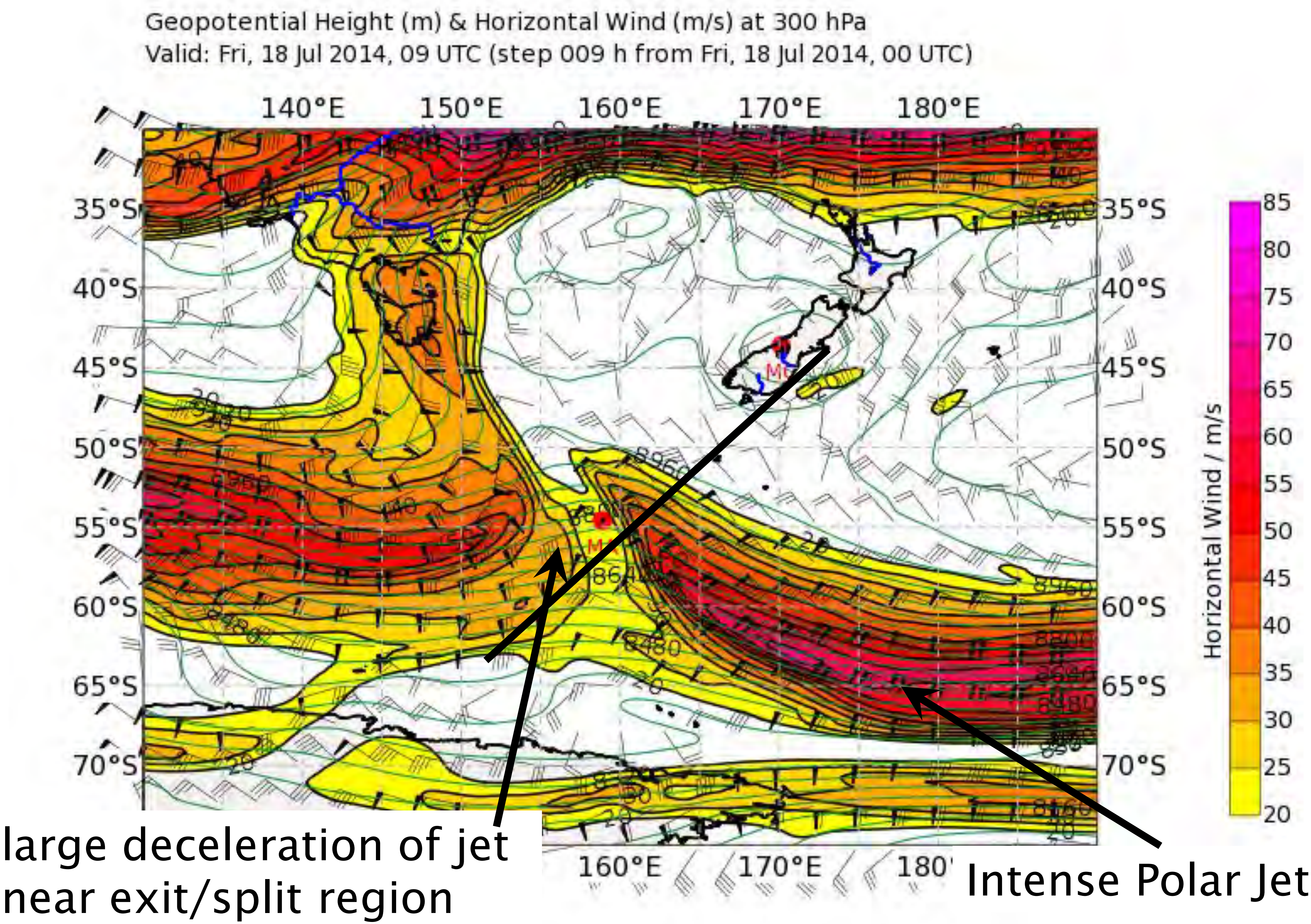
Geopotential Height (m) & Horizontal Wind (m/s) at 300 hPa
Valid: Fri, 18 Jul 2014, 09 UTC (step 009 h from Fri, 18 Jul 2014, 00 UTC)
140°E
150°E
160°E
170°E
180°E
35°S
40°S
45°S
50°S
55°S
60°S
65°S
70°S
Horizontal Wind / m/s
85
80
75
70
65
60
55
50
45
40
35
30
25
20
large deceleration of jet
near exit/split region
Intense Polar Jet

Thank you!
Especially, ECMWF staff for excellent organization of the Annual Seminar 2015!

Flower ducks, Insel Mainau, July 2015, Sonja Gisinger

Polar Stratospheric Clouds Above Scandinavia

PSCs above Finland as seen from DLR Falcon, 26 Jan 2000

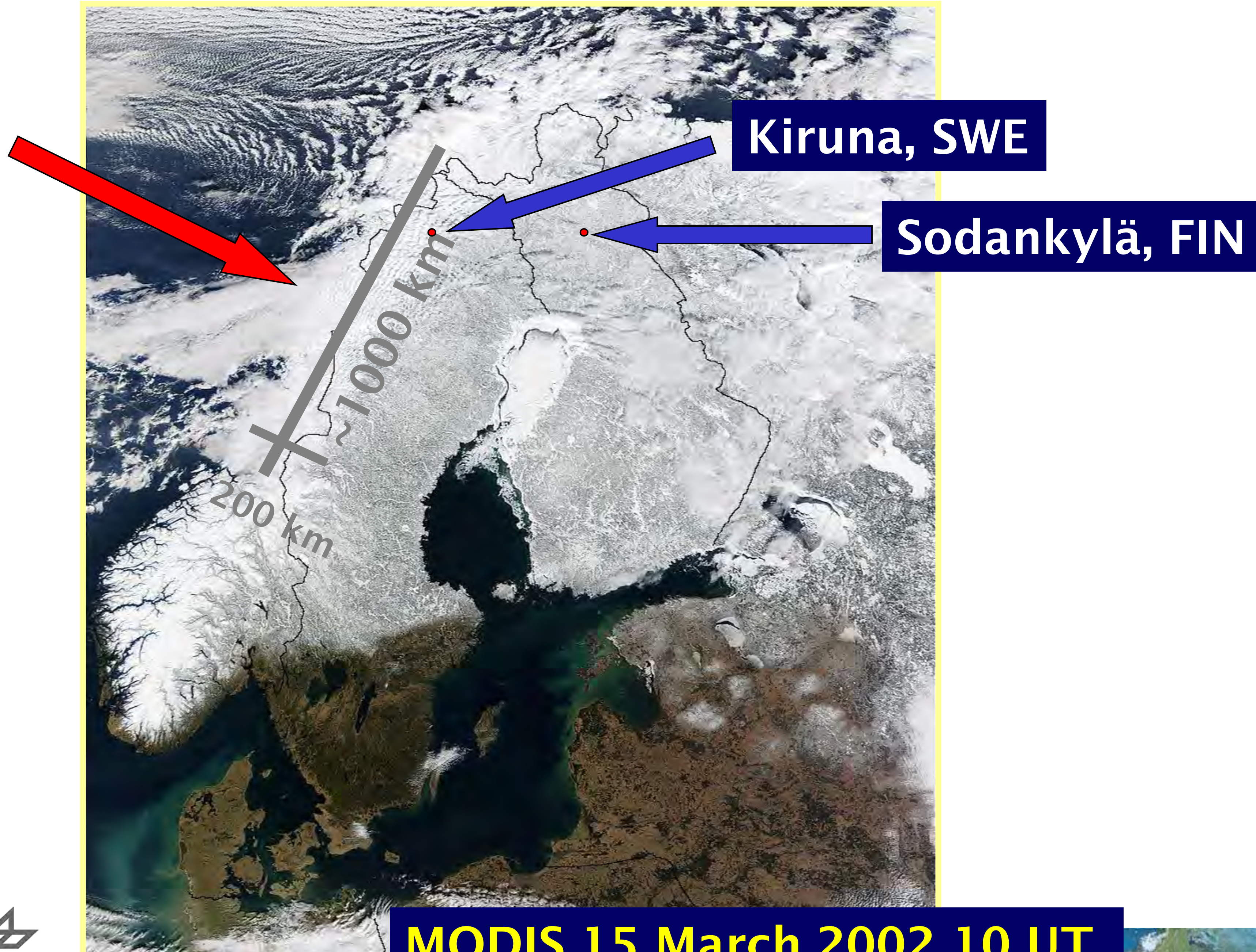

MODIS 15 March 2002 10 UT

Lidar Backscatter Ratio at 1064 nm

Θ from MM5 hindcast

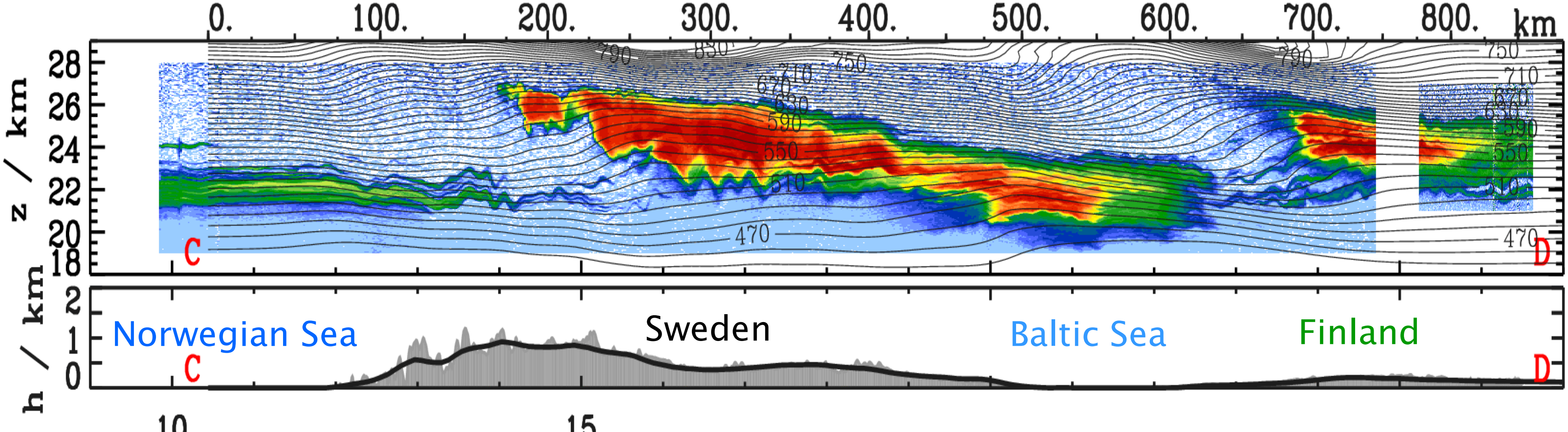

26 Jan 2000 14UT

lon /deg

$Ro = U/fL \approx 15 ms^{-1}/(10^{-4} s^{-1} 250 km) = 0.6$

Mesoscale T-anomalies generated by hydrostatic mountain waves

$\lambda_{hor} \sim 20 \ldots 500km$

$\delta_{MAX} \sim 2000$ m

$\Delta T_{\infty} \sim 6 \ldots 14$ K, $T_{MIN} \sim 175K\ (-98^{o}C)$

$dT/dt < -50$ K/h, $t_{proc} \sim 5.5$ h

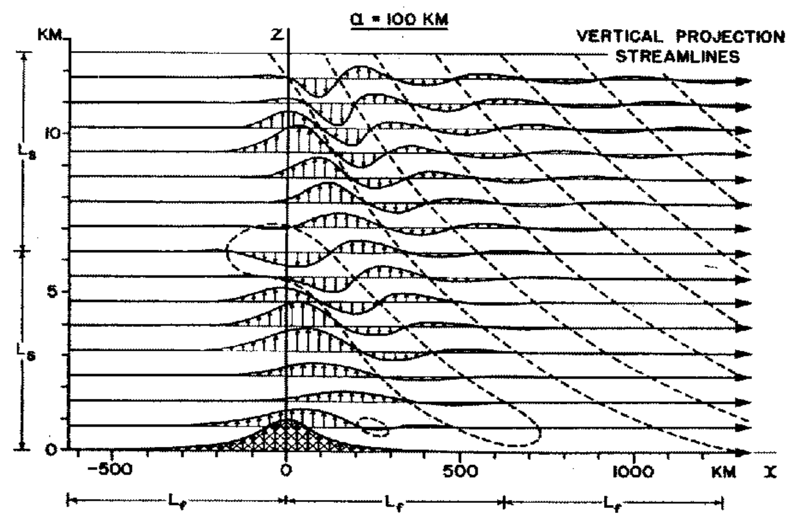

Queney, 1948

DLR

DLR Falcon 25 Jan 2001 - SOLVE/THESEO 2001

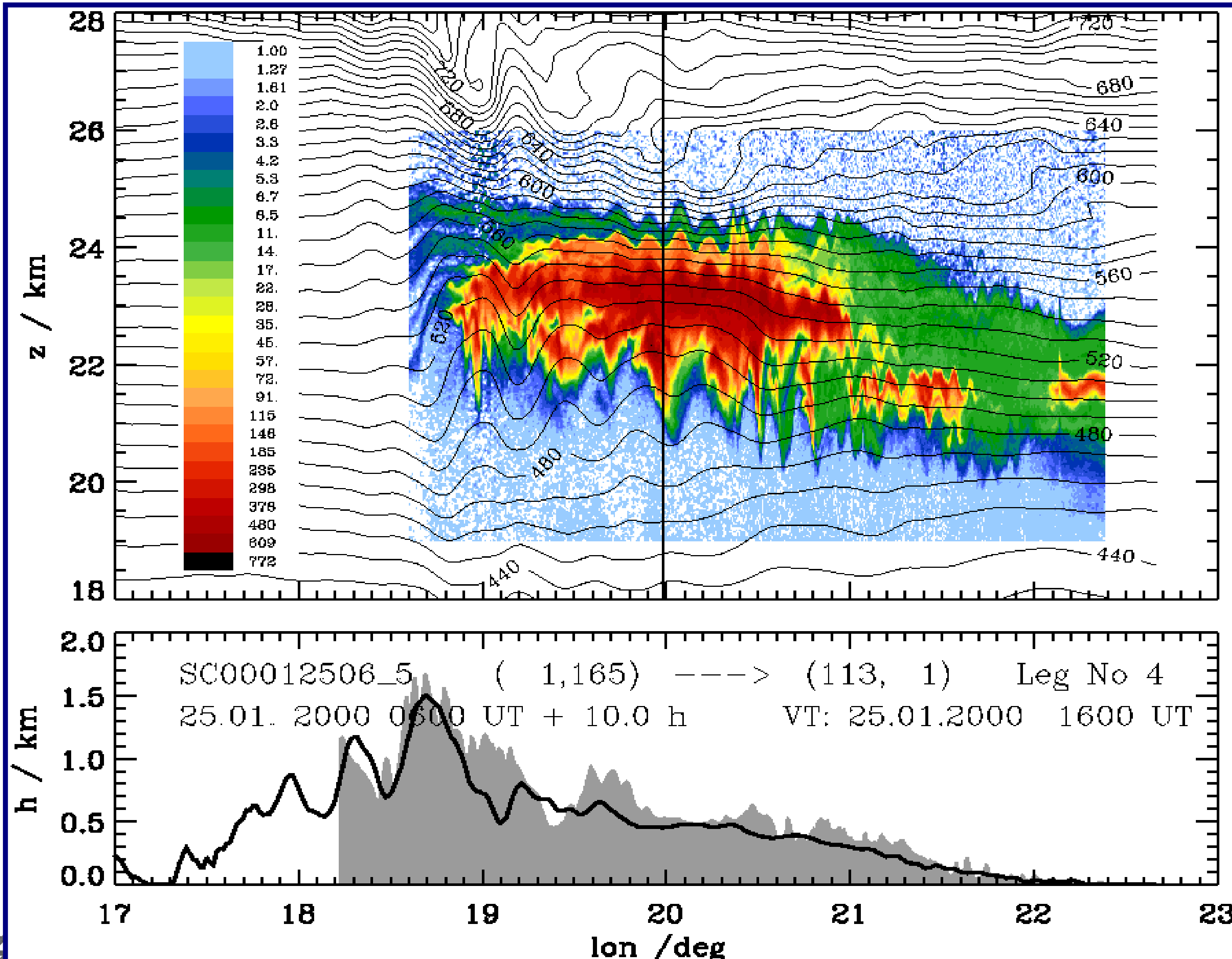

DLR Falcon 25 Jan 2001 - SOLVE/THESEO 2001